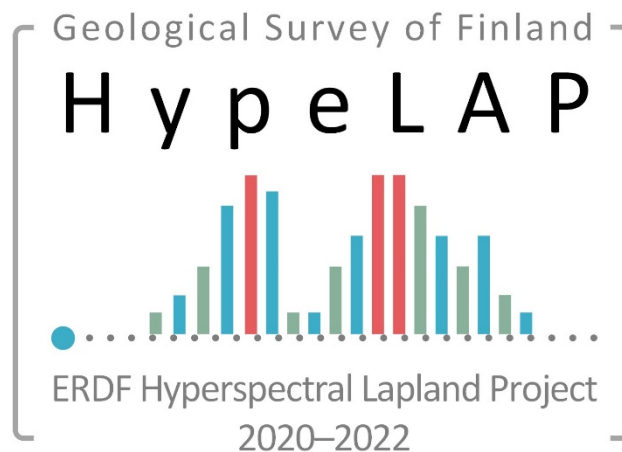


# Hyperspectral Lapland (HypeLAP) – project report



Markku Korhonen, Kati Laakso, Johanna Torppa, Juha Köykkä, Tuomo Törmänen, Virve Heilimo, Maarit Middleton, Alireza Hamedianfar, Kristian Tuusjärvi, Sakari Hautala, Akseli Torppa, Jarmo Rauhala, Samuli Haavikko, Ester Muñoz Jolis, Sari Lukkari, Juho Laitala and Vesa Nykänen



European Union  
European Regional  
Development Fund

Leverage from  
the EU  
2014–2020

December 8, 2022

**GEOLOGICAL SURVEY OF FINLAND****DOCUMENTATION PAGE**

December 8, 2022

<p>Authors</p> <p>Markku Korhonen, Kati Laakso, Johanna Torppa, Juha Köykkä, Tuomo Törmänen, Virve Heilimo, Maarit Middleton, Alireza Hamedianfar, Kristian Tuusjärvi, Sakari Hautala, Akseli Torppa, Jarmo Rauhala, Samuli Haavikko, Ester Muñoz Jolis, Sari Lukkari, Juho Laitala, Vesa Nykänen</p>	<p>Type of report</p> <p>Open File Work Report</p>
	<p>Commission by</p> <p>Business Finland, Geological Survey of Finland</p>
<p>Title of report</p> <p>Hyperspectral Lapland (HypeLAP) – project report</p>	
<p>Abstract</p> <p>Hyperspectral Lapland (HypeLAP) project studied practical solutions for mineral exploration by taking an advantage of the state-of-the-art hyperspectral measurement instrumentation. In this study, the geological research sites were located within the Central Lapland Greenstone Belt. New know-how gained from the hyperspectral technology can, for example, improve the quality and consistency in drill core logging.</p> <p>The project was financed from the European Regional Development Fund in the Sustainable Growth and Jobs 2014-2020 -programme. It was implemented in a period between June 2020 and November 2022 by the Geological Survey of Finland (GTK).</p> <p>In addition to the geological research, the project promoted the hyperspectral imaging-based digitalization of the GTK's National Drill Core Archive from the perspective of a data distribution demo. This demo was set up in an online environment to showcase a digital service intended for the presentation of specific data series produced by hyperspectral imaging.</p> <p>The project also explored the possibilities of establishing a new service around hyperspectral imaging, which would initially be targeted at mining and mineral exploration companies operating in Lapland. The benefits that can be achieved from the hyperspectral method after the project, and how the service related to hyperspectral imaging could be developed, were assessed from the perspective of GTK and its stakeholders.</p> <p>The project results make their contribution to increase knowledge of hyperspectral method in mineral exploration. Thus, the Hyperspectral Lapland project can enhance the activities of those companies and service providers operating in the industry.</p>	
<p>Keywords</p> <p>Central Lapland Greenstone Belt, hyperspectral imaging, drill core, virtual drill core archive</p>	
<p>Geographical area</p> <p>Finland, Lapland, Sodankylä, Kittilä</p>	
<p>Map sheet</p> <p>U424, U442, V433, V511</p>	

December 8, 2022

Other information <b>EURA2014 project code: A76209</b>			
Report serial <b>GTK Open File Work Report</b>		Archive code <b>49/2022</b>	
Total pages <b>71 + 3 appendixes</b>	Language <b>English</b>	Price <b>-</b>	Confidentiality <b>Public</b>
Unit <b>Information Solutions</b>		Project code <b>50403-30147</b>	
Signature/name  <b>Vesa Nykänen</b> <b>Accountable Project Leader</b>		Signature/name  <b>Markku Korhonen</b> <b>Project Manager</b>	

## Contents

### Documentation page

<b>1</b>	<b>Introduction</b>	<b>1</b>
<b>2</b>	<b>Project organisation</b>	<b>3</b>
<b>3</b>	<b>Geology of the study area and description of the sites</b>	<b>4</b>
3.1	Orogenic Au deposits	9
3.1.1	Hirvilavanmaa	9
3.1.2	Kirakka-aapa	13
3.1.3	Ruosselkä	15
3.2	VMS deposits	20
3.2.1	Pahtavuoma	20
<b>4</b>	<b>WP1: Project coordination and management</b>	<b>24</b>
4.1	Description	24
4.2	Implementation	24
4.2.1	Recruitment	24
4.2.2	Equipment purchases	24
4.2.3	Applying for an extension period	24
4.2.4	Reporting	25
<b>5</b>	<b>WP2: Arctic virtual drill core archive</b>	<b>26</b>
5.1	Description	26
5.2	Implementation	26
5.2.1	Requirements specification	26
5.2.2	Technical setup	26
5.2.3	Development testing	27
5.2.4	User testing	27
5.3	Result	27
5.3.1	Technical platform	27
5.3.2	Data storage	27
5.3.3	Functions and content	27
5.3.4	User feedback	33
5.4	Conclusions	33
5.4.1	Work principle	33
5.4.2	Technical platform	33

December 8, 2022

5.4.3	Data	34
5.4.4	Follow-up development	34
<b>6</b>	<b>WP3: Data Acquisition</b>	<b>35</b>
6.1	Description	35
6.2	Implementation	35
6.2.1	Selection of samples	35
6.2.2	Preparation of samples	36
6.2.3	Instrumentation and drill core measurements	37
6.2.4	Polished thin sections	39
6.2.5	Content changes	39
6.2.6	Extended data collection	39
6.3	Results	42
<b>7</b>	<b>WP4: Data Analysis</b>	<b>43</b>
7.1	Description	43
7.2	Image co-registration	43
7.2.1	Co-registration of HS images and micro-XRF data	43
7.2.2	Co-registration of HS images and SEM-EDX/INCA data	44
7.3	The mineralogy and mineral chemistry of the Ruosselkä study area	45
7.3.1	Methods	45
7.3.2	Results	47
7.4	Machine learning aided drill-core mineralogy for a test case from Hirvilavanmaa	50
7.4.1	Data preprocessing	51
7.4.2	Mineralogy based on expert knowledge	52
7.4.3	Mineralogy based on data only	53
7.4.4	Results	54
<b>8</b>	<b>WP5: Preliminary review for hyperspectral imaging service and concept building</b>	<b>58</b>
8.1	Description	58
8.2	Implementation	58
8.3	Summary of the interviews	58
8.3.1	Background of the companies	58
8.3.2	Previous experiences	59
8.3.3	Suitability for the Finnish bedrock	59
8.3.4	Measuring equipment	60
8.3.5	Usability and quality of data	60

December 8, 2022

8.3.6	Companies' own plans	60
8.3.7	Hopes concerning the general development direction	60
8.3.8	Conclusions	61
<b>9</b>	<b>Benefits of the spectral method after the project</b>	<b>62</b>
9.1	Acquisition of new data	62
9.2	Data processing and interpretation	62
9.3	Data distribution solution	62
9.3.1	Operating principle	62
9.3.2	Derived interpretations	63
9.3.3	Service level	63
9.3.4	Conclusions	63
9.4	Development of service related to measurements	64
<b>10</b>	<b>Publication of results</b>	<b>65</b>
<b>11</b>	<b>References</b>	<b>66</b>

December 8, 2022

## 1 INTRODUCTION

Various geological data sources are used in mineral exploration to find new mineral deposits. One of the most important and expensive sources is diamond drilling, from which long, cone-shaped bedrock samples, or drill cores, are obtained from the subsurface. Information on the composition and structure of drill cores is a key element in target-oriented mineral exploration. Drill core reporting (logging) means the systematic recording of this information.

When logging drill cores, a geologist traditionally writes a description of the entire drill core, after which part of the core samples is selected for a detailed laboratory analysis. At that point, the element composition of the sample is determined. This geochemical laboratory analysis is accurate, though it is at the same time a time-consuming and expensive research method. Therefore, not all core samples should be analyzed in laboratory conditions, which emphasizes the importance of drill core logging in research. Consistent drill core logging requires skill and accuracy, as well as practical experience.

Hyperspectral imaging and hyperspectral point measurements represent a spectroscopic research method that can be used to identify different materials and measure their properties. The method is based on the utilization of specific wavelengths from the electromagnetic spectrum. In theory, different materials and compounds reflect or emit radiation in different ways, so they can be distinguished from each other based on their characteristic spectra.

Modern spectral measuring devices such as large scanners and portable analyzers commonly utilize the visible and near infrared (NIR, 350–1100 nm), short-wave infrared (SWIR, 1100–2500 nm) and long-wave infrared (LWIR, 8–12  $\mu\text{m}$ ) ranges of the electromagnetic radiation. The latest technology is represented by devices that use the mid-wave infrared wavelength range (MWIR, 2.5–8  $\mu\text{m}$ ).

In geological research, spectral technology can be used to produce measurable mineralogical data on drill cores. This makes hyperspectral spectroscopy an especially useful method for assisting in drill core logging. In the best case, the technology could make it possible to identify almost all the most commonly occurring minerals from the spectral data. In turn, this would help reveal the origin of the rocks, creating a basis for understanding geological units – including those with mineral deposits.

The Hyperspectral Lapland (HypeLAP) project aims at increasing the practical benefit of hyperspectral measurements in mineral exploration by applying the latest technology to the study of drill cores. The purpose of the project is to especially serve mineral exploration and mining companies whose operations focus on Northern Finland. In this study, the geological research sites are located within the Central Lapland Greenstone Belt.

In addition to the geological research, the project aims to promote the hyperspectral imaging-based digitalization of the GTK's National Drill Core Archive from the perspective of a data distribution solution. The project also explores the possibilities of establishing a new service around hyperspectral imaging, which would initially be targeted at mining and mineral exploration companies operating in Lapland.

December 8, 2022

The project was implemented with funding (90% share) received from the European Regional Development Fund (ERDF), granted by the Business Finland, in the Sustainable Growth and Jobs 2014–2020 -programme. The second funder of the project was the Geological Survey of Finland (10% share). The project was implemented by the Geological Survey of Finland (GTK).

The HypeLAP project started on 1 June 2020 and ended on 30 November 2022. This final report explains the measures taken in the project during the period and the results obtained from them.

The HypeLAP project was divided into five work packages. The results obtained in the project are also arranged in this report according to the work packages. The benefits that can be achieved from the spectral method after the project, and how the service related to hyperspectral measurements could be developed, are assessed from the perspective of GTK and its stakeholders at the end of the report.

The spectroscopic method discussed in the final report is divided into hyperspectral point measurements and hyperspectral imaging.<sup>1</sup> The former produces point-like spectral data, and the latter planar continuous data on the object being studied. They also differ in terms of research equipment and the amount of data generated. Hyperspectral point measurements and hyperspectral imaging are referred in this report as the hyperspectral method or briefer the spectral method.

---

<sup>1</sup> Instead of the expression 'hyperspectral imaging', the form 'hyperspectral scanning' may appear later in the text.

December 8, 2022

## 2 PROJECT ORGANISATION

The accountable project leader was Vesa Nykänen, and the project manager was Markku Korhonen. The leaders of the work packages (WP) were Markku Korhonen (WP1), Markku Korhonen (WP2), Juha Köykkä (WP3), Maarit Middleton (WP4) and Virve Heilimo (WP5). In addition, the project team included Kati Laakso, Johanna Torppa, Tuomo Törmänen, Juho Laitala, Alireza Hamedianfar, Kristian Tuusjärvi, Sakari Hautala, Jarmo Rauhala and Samuli Haavikko. The SEM study was conducted at GTK Outokumpu office under Akseli Torppa. Ester Muñoz Jolis and Sari Lukkari conducted the micro-XRF analysis in GTK Espoo office. Many people from GTK's Rovaniemi, Kuopio and Espoo offices were also involved in assisting or advising positions in the research carried out in the project.

A steering group was established to direct and monitor the project, with representatives from mineral exploration and mining companies operating in Northern Finland, as well as private service providers. The steering group consisted of the following companies: AA Sakatti Mining Oy (Janne Siikaluoma); Agnico Eagle Finland Oy (Jari Ylinen); Aurion Resources Oy (Juhani Ojala); Boliden FinnEx Oy (Markku Montonen, 2020); Boliden (Markku Montonen, 2021; Tobias Hermansson, 2021–2022); Ab Scandinavian GeoPool Ltd (Mathias Forss); Geovisor Oy (Pekka Kantia); Magnus Minerals Oy (Mikko Nenonen); Mawson Oy (Janne Kinnunen); Palsatech Oy (Hannu Ahola); and Rupert Finland Oy (Charlie Seabrook). From GTK, Niina Ahtonen (2020–2021) and Eija Hyvönen (2021–2022) worked in the steering group. Ritva Heikkinen and Maarit Kokko participated in the steering group meetings as representatives of Business Finland.

December 8, 2022

### 3 GEOLOGY OF THE STUDY AREA AND DESCRIPTION OF THE SITES

The research areas of this project in the municipalities of Kittilä and Sodankylä in Central Lapland are known for large mineral deposits, which constitute a key target area for the current studies of exploration companies (Fig. 1). The bedrock of Central Lapland, i.e. the Central Lapland belt (Central Lapland Greenstone Belt), consists mainly of an Archean basement complex (3.5–2.5 Ga) and younger Paleoproterozoic supracrustal rocks (2.5–1.9 Ga), intruded by 2.44–2.05 Ga ultramafic-mafic intrusive rocks, 1.92–1.88 Ga (felsic) porphyritic/lamprophyritic rocks, and 1.88 Ga synorogenic and 1.80 Ga post-orogenic granitoids (Fig. 1). The approx. 5–10 km thick Paleoproterozoic volcanic-sedimentary succession is mainly bordered by the granitoid complex of Central Lapland and several different Archaean basement complexes (Fig. 1).

Köykkä et al. (2019) proposed five different tectonic basin development stages for the Central Lapland belt based on geochemistry, sedimentology and structures: the rifting stage 2.5–2.1 Ga, including (I) initial rifting/early syn-rift, (II) actual syn-rift and (III) syn-rift to early post-rift, (IV) passive margin stage 2.1–1.94/1.92 Ga and (V) foreland basin system 1.94/1.92–1.88 Ga. The overall tectonic development stage represents almost approx. 600 Ma of tectono-sedimentary evolution from the Paleoproterozoic Era (Köykkä et al., 2019). The bedrock has been deformed multiple times, forming separate allochthons bordered by thrust surfaces, i.e. tectonostratigraphic units (Luukas & Kohonen, 2021). The metamorphic degree of the areas varies from greenschist facies to amphibolite facies (Hölttä & Heilimo, 2017).

The Paleoproterozoic evolution of the Central Lapland belt begins with the eruption of komatiitic and rhyolitic lavas associated with the mantle plume onto the Archaean craton c. 2.51–2.44 Ga ago. This stage also includes the formation of large mafic layered intrusions, followed by the deposition of thick sedimentary successions and varying mafic volcanism (Hanski & Huhma, 2005; Köykkä et al., 2019). Supracrustal rock type succession ended with the evolution of the tectonic thrust belt and synorogenic felsic plutonism 1.88 Ga ago (Hanski & Huhma, 2005; Köykkä et al., 2019; Köykkä & Luukas, 2021).

The Salla group (2.51–2.44 Ga) occurs mostly northeast and east of the Sodankylä area, comprising a volcanic unit of variable thickness, consisting mainly of acidic and intermediate volcanic rocks (andesites, dacites and rhyolites) (Manninen, 1991; Köykkä et al., 2022; Figs. 1 & 2). Räsänen & Huhma (2001) determined the age of the Sakamaa dacite as  $2.438 \pm 11$  Ma, and Manninen et al. (2001) the age of felsic tuff from Rookkiaapa as  $2.438 \pm 14$  Ma. It has therefore been thought that the uppermost parts of the Salla group and the 2.44 Ga mafic layered intrusions of Koillismaa and Central Lapland represent contemporaneous magmatism (see Huhma et al., 2018). Stratigraphically, the overlying Kuusamo group (2.43–2.40 Ga) covers a wide area that extends from Kuusamo to Salla and towards Sodankylä and Kittilä, consisting mainly of mafic volcanic rocks from subaerial and subaqueous eruptions (Köykkä et al., 2019, 2022; Figs. 1 & 2). The maximum depositional age of the Kuusamo group  $2.428 \pm 3$  Ma is obtained from porphyritic basal conglomerate clasts, and the minimum depositional age of  $2.403 \pm 3$  Ma from the Onkamonlehto dike cutting the volcanic rocks (Huhma et al. 2018; Köykkä et al., 2022).

December 8, 2022

The Sodankylä group (2.35–2.15 Ga) comprises large areas containing several different metasedimentary formations and small amounts of mafic volcanic rocks (Figs. 1 & 2). The lower part and middle stages of the Sodankylä group are intruded by 2.2 Ga Haaskalehto-type differentiated sills (Hanski, 1987), but it is unlikely that they extend to the upper parts of the group (Köykkä & Luukas, 2021). The metasedimentary rocks of the Sodankylä group consist mainly of conglomerates, quartzites, mudstones and carbonate rocks, characterized by strong albitization in places. The younger Savukoski group (2.15–2.05 Ga) occurs on top of the Sodankylä group, containing mainly graphite-rich black schists and greywacke deposits in the lower parts of the unit and ultramafic volcanic rocks and mafic tuffites in the upper parts of the unit (Figs. 1 & 2). The minimum age of the Savukoski group has been obtained from the 2.05 Ga diabase dikes cutting it. The 2.05 Ga layered intrusion of Keivitsa (Mutanen, 1997) and the 2.13 Ga Rantavaara gabbro have also been formed in the black schists of the lower part of the Savukoski group (Tyrväinen, 1983).

The Kumpu group (<1.88 Ga) and the partly correlated Kuontasjärvi and Kangosselkä represent the uppermost units of the Central Lapland belt, which consists mainly of conglomerate-quartzite associations and syngenetic felsic volcanic rocks (Köykkä et al., 2019; Figs. 1 & 2). In addition, several different lithodemic quartzite and paragneiss units/assemblages occur in the Central Lapland area, the age relations of which are difficult to determine in some places (Köykkä et al., 2019; Köykkä & Luukas, 2021; Figs. 1 & 2). The Kittilä Assemblage (<2.0 Ga) represents one of the largest volcanic deposits in the Fennoscandian shield, with a combined vertical thickness of the current volcanic deposits being up to approx. 9 km (Niiranen et al. 2014) (Figs. 1 & 2). The assemblage is cut by several 2.01 Ga and 1.92 Ga granodiorite rocks (Huhma et al. 2018). To the north of Kittilä, the wide and relatively flat and weakly deformed volcanic complex becomes an increasingly thin and eastward-dipping tectonic zone.

The tectono-sedimentary-volcanic development of the Central Lapland belt has been studied in recent years mainly by Köykkä et al., 2019, Köykkä & Luukas, 2021, and Köykkä et al., 2022. The rifting phase approx. 2.5–2.1 Ga corresponds to the global breakup of the Kenorland supercontinent (Strand & Köykkä, 2012). This early rifting stage comprises the volcanism of the Salla and Kuusamo groups, of which especially the Salla volcanism is related to the global mantle plume event and the massive lava eruption events approx. 2.51–2.49 and 2.45–2.44 Ga (LIP = Large Igneous Province) (see Köykkä et al., 2022). The depositional systems mainly comprised subaerial and subaqueous bimodal volcanic eruptions, as well as continental alluvial and shallow marine clastic sedimentation (Köykkä et al., 2019). The subsequent rifting stages comprise volcanism and sedimentation, which are mostly represented by the units of the Sodankylä group (Köykkä et al., 2019; Köykkä & Luukas, 2021).

The passive continental margin stage approx. 2.1–1.92 Ga comprises sedimentary-volcanic deposits from the Savukoski group and the Kittilä Assemblage in the Central Lapland belt (Köykkä et al., 2019). The overall stage includes the formation of ‘aulacogenes’ and the deepening of the basin, characterized by deeper water sandstone deposits (greywackes) and associated underwater volcanism and hemiplegic sedimentation. Abundant hemiplegic sedimentation is associated with global mantle superplume events, which produced large amounts of carbon dioxide into the atmosphere-ocean system during the Rhyacian Period c. 2.1–2.0 Ga ago (see

December 8, 2022

Köykkä et al., 2019). The siliciclastic sedimentation of the depositional basin increased before the tectonic compression-collision stage (Svecofennian orogeny), which started ca. 1.94 Ga, and this is characterized in the Central Lapland belt by the collision of the Kittilä Assemblage (arc) from the west. This was followed by the actual compression stage approx. 1.92–1.88 Ga and the development of the foreland basin (Lahtinen et al., 2015, Köykkä et al., 2019). According to Köykkä et al., (2019), the foreland basin system is characterized by syn- and postorogenic depositional systems, i.e. the ‘underfilled’ stage and the later ‘overfilled’ stage. The overfilled stage in Central Lapland is characterized especially by the alluvial sedimentation of the Kumpu group, which is controlled by strike-slip faults within the basin (Köykkä et al., 2019).

December 8, 2022

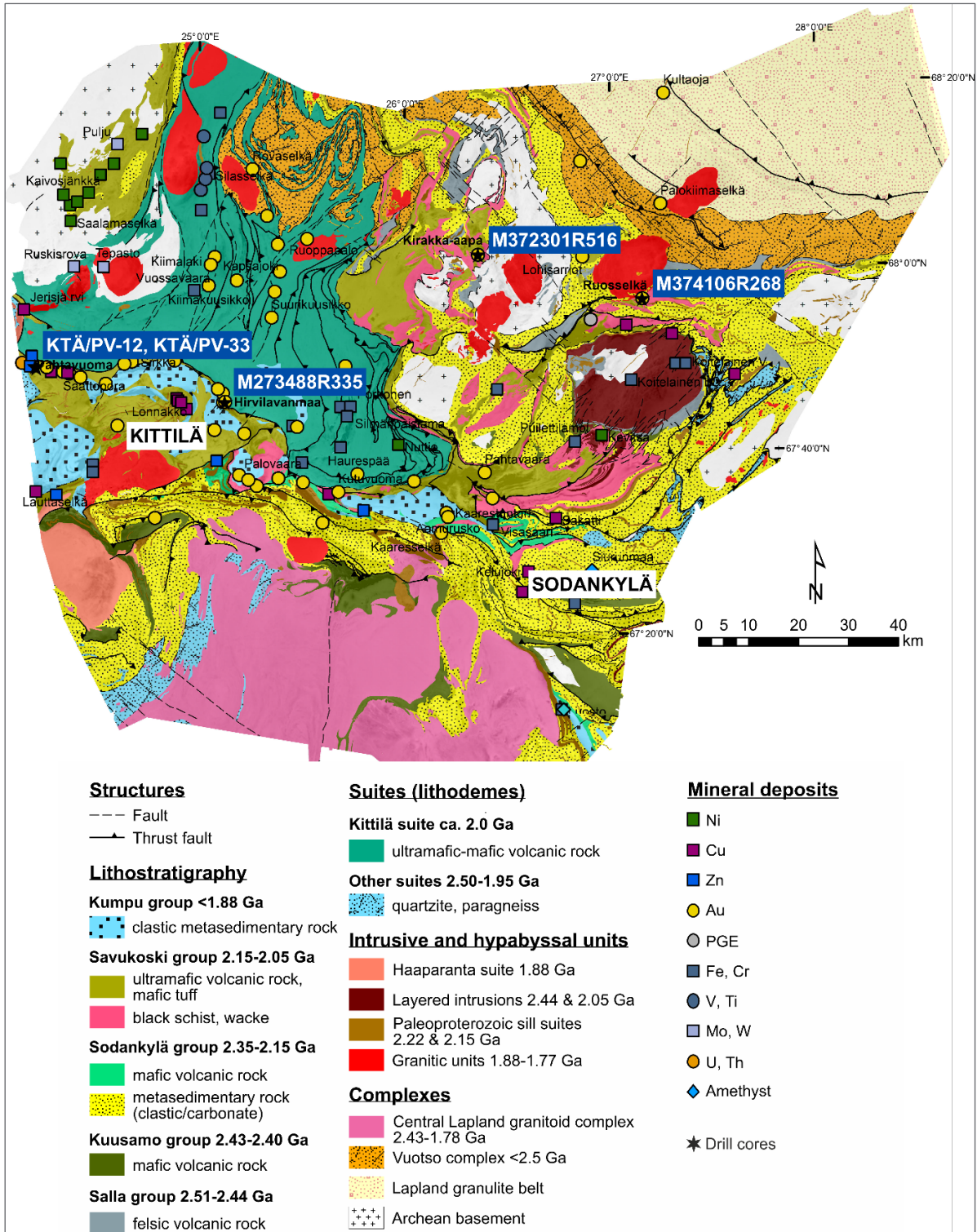


Fig. 1. Bedrock map of the study area in the areas of Kittilä and Sodankylä municipalities (Bedrock of Finland – DigiKP; Köykkä et al., 2019; Köykkä & Luukas, 2021), as well as the location of the drill cores used in the study (black stars) and known mineral deposits (Mineral Deposits and Exploration – MDaE).

December 8, 2022

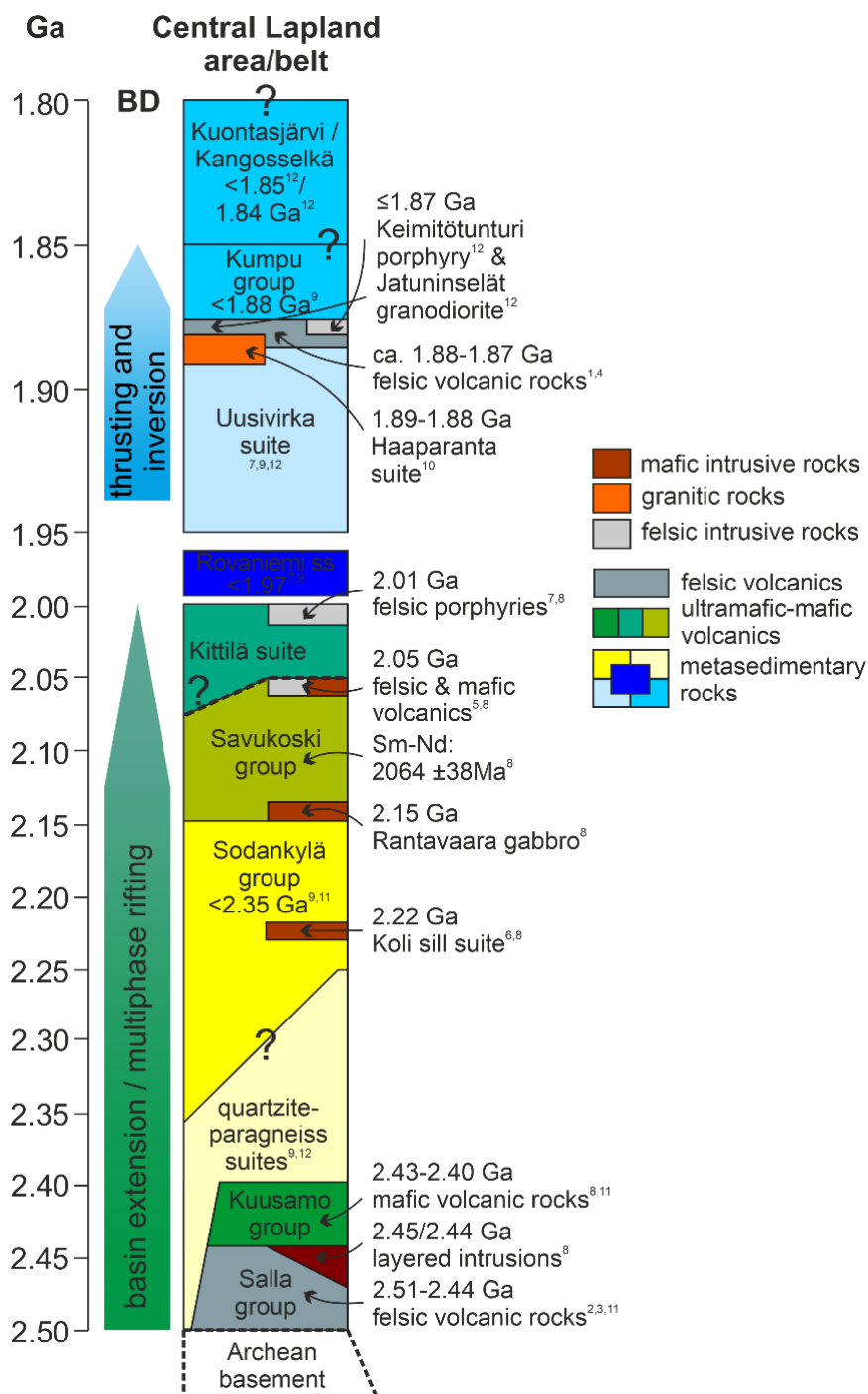


Fig. 2. Simplified stratigraphy of the Central Lapland area/belt (modified from Köykkä et al., 2019; Köykkä & Luukas, 2021; Lahtinen et al., submitted). The drill cores of this study represent the Savukoski group. BD = basin dynamics; ss = super suite. <sup>1</sup>Lehtonen, 1984; <sup>2</sup>Manninen and Huhma, 2001; <sup>3</sup>Manninen et al., 2001; <sup>4</sup>Rastas et al., 2001; <sup>5</sup>Hanski and Huhma, 2005; <sup>6</sup>Hanski et al., 2010; <sup>7</sup>Lahtinen et al., 2015; <sup>8</sup>Huhma et al., 2018; <sup>9</sup>Köykkä et al., 2019; <sup>10</sup>Bergman and Weihed, 2020 and references therein; <sup>11</sup>Köykkä et al., 2022. <sup>12</sup>Lahtinen et al., submitted.

December 8, 2022

### 3.1 Orogenic Au deposits

As their name suggests, orogenic Au deposits are related to orogens, i.e. the collision zones of tectonic plates and especially the large-scale structures that occur in them, such as faults and shear zones (Goldfarb et al., 2001). Extensive crustal metamorphism in collision zones generates metamorphic fluids that are typically CO<sub>2</sub>-rich, slightly saline (2–10% NaCl) and with a near neutral pH, and in which Au migrates as sulphur complexes. The precipitation of Au from the fluid is affected by many factors such as a decrease in pressure and/or temperature or a change in the oxidation-reduction conditions of the fluid. A very common cause of mineralization is the reaction of the sulphur contained in the fluid with the iron in the host rock, e.g. in mafic volcanic rock, causing the solubility of Au to fall sharply and the Au to precipitate. A typical feature of orogenic Au deposits is the alteration zones that occur around them, the width of which typically varies from meters to a few dozen meters. Alteration is usually strongest in the mineralization itself (proximal zone) and weakens further from the mineralization (distal zone). Typical minerals in the proximal zone are quartz, carbonates (especially Fe-Mg carbonates), sericite and sulphides (especially pyrite), and in some deposits e.g. tourmaline and arsenopyrite. Further away from the mineralization, the intensity of alteration weakens, and common alteration minerals are e.g. albite, chlorite, Ca carbonate (calcite) and hematite. The main metal in orogenic Au deposits is gold, in addition to which small amounts of e.g. bismuth and tellurium, in some cases also base metals such as Cu (Saattopora's closed Au-Cu mine in Kittilä) or cobalt (many of the Kuusamo deposits and Rajapalot on the border between Rovaniemi and Yli-Tornio), may occur.

#### 3.1.1 Hirvilavanmaa

The Hirvilavanmaa Au deposit is located approx. 15 km northeast of Kittilä (Figs. 3 & 4). The lithology of the area consists mainly of 2.15–2.05 Ga ultramafic komatiitic rocks of the Sattasvaara formation belonging to the Savukoski group, which have erupted underwater (Figs. 3 & 4) but which, due to hydrothermal alteration, today occur mainly as talc-rich schists, albite-carbonate-sericite rocks and carbonate rocks (Hulkki & Keinänen, 2007). This northwest-southeast oriented peridotitic komatiite zone is surrounded mainly by mafic volcanic rocks of the 2.05–2.01 Ga Kittilä suite in the east, which were created in an island arc environment, and <1.88 Ga Kumpu group clastic alluvial sedimentary rocks and the graphite schist-dolomite rocks of the Pittarova formation in the west (Fig. 3). Ultramafic komatiites, which can be clearly distinguished on a geophysical aeromagnetic map, are Mg-rich and contain graphite schist as intermediate layers and lenses in places. The geological structure of the area is further characterized by the northwest-southeast oriented Sirkka shear zone and the 2.05 Ga albite-rich sills intruding the supracrustal package of the whole Savukoski group (Fig. 4).

Hulkki & Keinänen (2007) distinguished a north-northeast oriented alteration zone approx. 270 m long and 90 m wide, which they divided into distal outer proximal and inner proximal parts. The deepest interceptions are at a depth of approx. 100 m, and the known mineral resources are 0.11 Mt with 2.9 g/t Au (Scan Mining Press Release 9 September 2002). The more distal part comprises talc-chlorite-amphibolite schist, while the more proximal part consists of albite-carbonate-chlorite schist, which also represents the most strongly altered part in the Hirvilavanmaa area (Hulkki & Keinänen, 2007). In turn, the contacts between the alteration zones

December 8, 2022

are characterized by north–south-oriented quartz breccias and dikes around which pyrite and hematite occur, as well as quartz dikes of a younger stage (Figs. 5 & 6). Younger quartz dikes are in some places Au-rich (up to 30 g/t), forming narrow lenticular zones. Massive carbonate rocks and fuchsite-rich green chromium marble also occur in places. Pyrite and to a lesser extent, chalcopyrite and pyrrhotite, and tourmaline are commonly found in the mineralized zone. In mineral chemistry, a change from Ca-rich carbonate in non-mineralized komatiite to Mg and Fe-Mg carbonate in Au mineralization can be seen. Weak K<sub>2</sub>O alteration (biotite/phlogopite) can be seen in the komatiite on the hanging wall of the mineralization. The altered rocks in the area are also cut by pyroclastic komatiitic volcanic rocks, which contain small amounts of Au mineralization. Overall, the transition from the distal part to the altered proximal part is gradual, which is characterized by a significant decrease in talc, chlorite, and chromium and iron oxides and correspondingly, an increase in albite, carbonate and pyrite. The highest individual Au concentrations (1 m) are 10–35 ppm, though the majority are in the range of 0.5–2 ppm. In hole R335, Au concentrations vary between 0.3 and 2.4 ppm in the mineralized zone. The presence of sulphides (pyrite and pyrrhotite) is reflected by elevated but varying S concentrations (<0.002–4.3%).

December 8, 2022

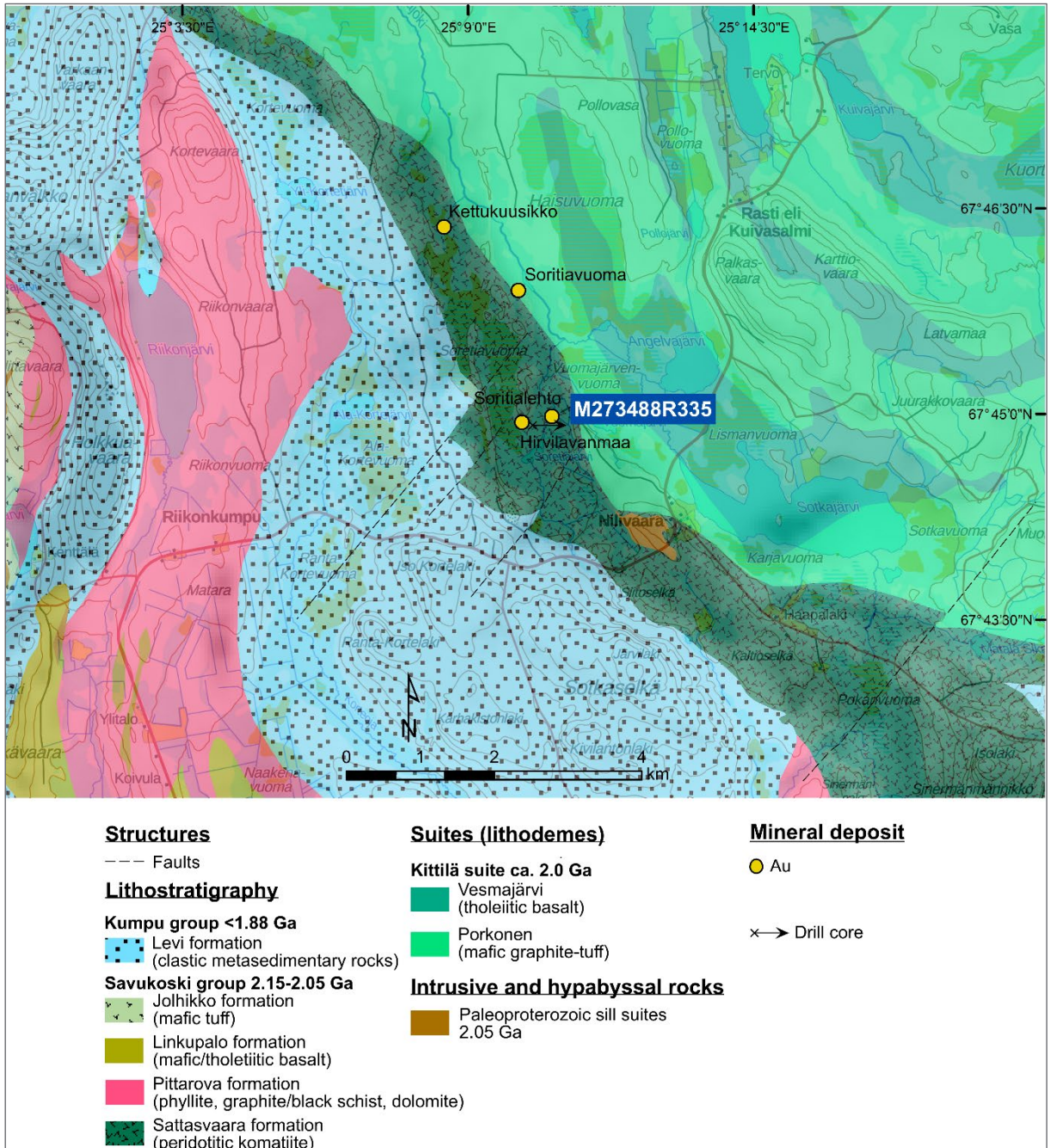


Fig. 3. Bedrock map of Hirvilavanmaa area (Bedrock of Finland – DigiKP) and the location and drilling direction of the drill core M273488R335 used in this study. Background topography © National Land Survey of Finland.

December 8, 2022

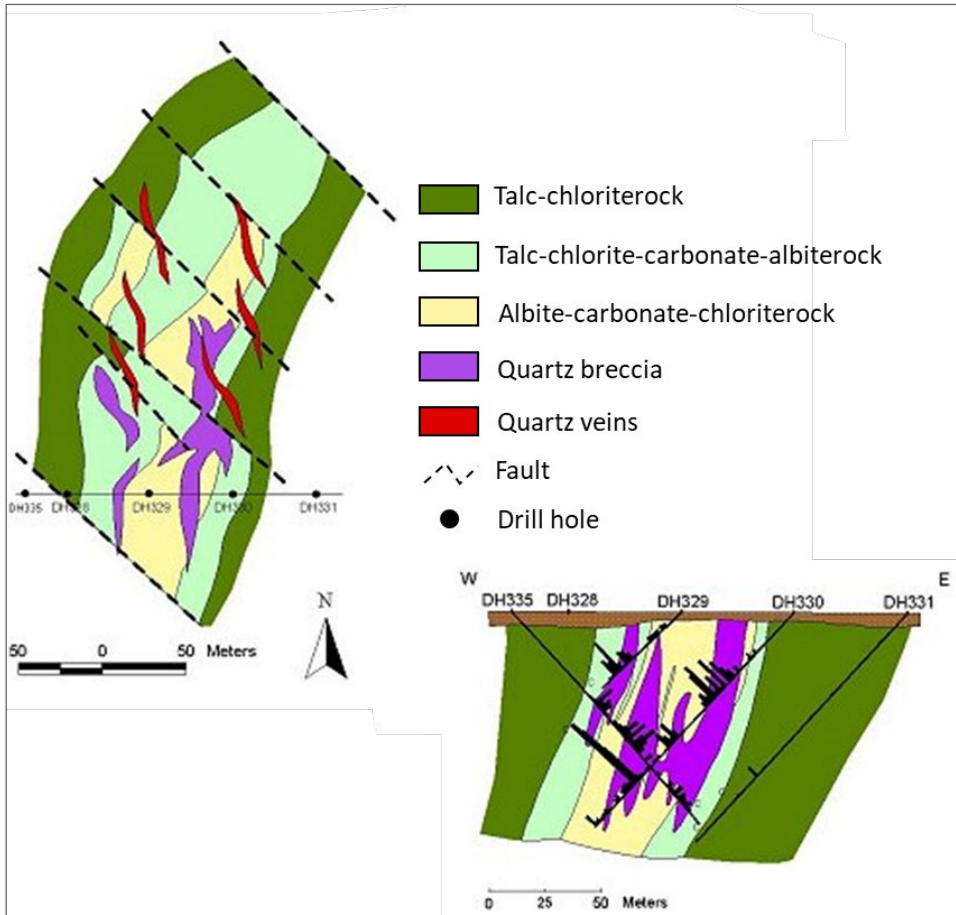


Fig. 4. Geological mineralization map of Hirvilavanmaa and cross-section with alteration zones (modified from Hulkki & Keinänen, 2007).



Fig. 5. Non-mineralized talc-chlorite schist with narrow quartz-carbonate veins (M273488R335).

December 8, 2022



Fig. 6. Mineralized talc-carbonate-albite rock with abundant quartz-carbonate-albite veins (M273488R335).

### 3.1.2 Kirakka-aapa

Kirakka-Aapa is located approx. 70 km north of Sodankylä on the western side of the Porttipahta reservoir (Fig. 7). The bedrock of the area mainly consists of 2.1–2.05 Ga peridotitic komatiites of the Savukoski group (Sattasvaara formation), mafic volcanic rocks, and mica and graphite schists (Fig. 7). Clear cumulate structures can be observed in the ultramafic komatiites of the Sattasvaara formation in places, which appear as sill-like concordant lenses (see Pulkkinen et al., 2007; Lehtonen et al., 1998). They are layered in structure, alternating between coarse and fine-grained parts, and having spinifex textures in places. The komatiites of the southern part of the area also contain olivine-phyric parts, where the glassy groundmass also has a microspinifex texture (Pulkkinen et al., 2007; Lehtonen et al., 1998). Pillow-like structures and hyaloclastic breccias are quite abundant in the central parts, where they alternate in places with volcanoclastites in successions several kilometers long and hundreds of meters thick. In addition, there are amygdaloidal lavas on the deformed northern edge of the area, which stand out as partly weathered (corroded) chlorite or serpentine-chlorite spots.

Mafic amygdaloidal lavas of the area are fine-grained and, in some places, contain pipe amygdules filled with epidote and epidote chlorite larger than 2 cm. In places, pillow structures and hyaloclastic breccias containing 1–5 mm epidote, plagioclase and plagioclase chlorite amygdules also occur in the lavas. In connection with pillow lavas and breccias, redeposited, variably sorted volcanoclastic deposits are also commonly found. In summary, the komatiites of the area and the associated mafic volcanic rocks occur as variably altered chlorite-amphibole-talc rocks and as talc-carbonate rocks in places. Mica schists are sericite-biotite mica schists and locally are chlorite-rich. They contain narrow chlorite-biotite-amphibole+carbonate parts that represent strongly altered mafic-ultramafic volcanic rocks.

Between 2001 and 2005, the Geological Survey of Finland conducted bedrock and ore studies in the area, and elevated Cu(-Au) and Cu-Ni concentrations were observed in places. According to Pulkkinen et al., (2007), the metasediments of the area are characterized by a strong alteration which is cut by a set of pyritized violarite carbonate dikes in which Au mineralization has been observed. The highest Au concentrations were found in hole R516, which consists mainly of mica

December 8, 2022

schists with narrow altered mafic parts. There is a weathered violarite-rich sulphide dike between 29.45 m and 29.85 m, with 3.12 ppm Au, 0.26% Ni and 21.1% S, followed by 1.6 m with 4.96 ppm Au and 1.07% S though the with low base metal contents. Occasional elevated Cu-Au concentrations have been found mainly also in the contact zones of komatiite and the surrounding mica schist (0.1–0.4% Cu, 0.1–0.9 ppm Au) (Pulkkinen et al., 2007). Hydrothermal alteration associated with mineralization is minor; minor albitization and variation in K<sub>2</sub>O concentration occur in places at R516, which, however, do not seem to be related to mineralization.

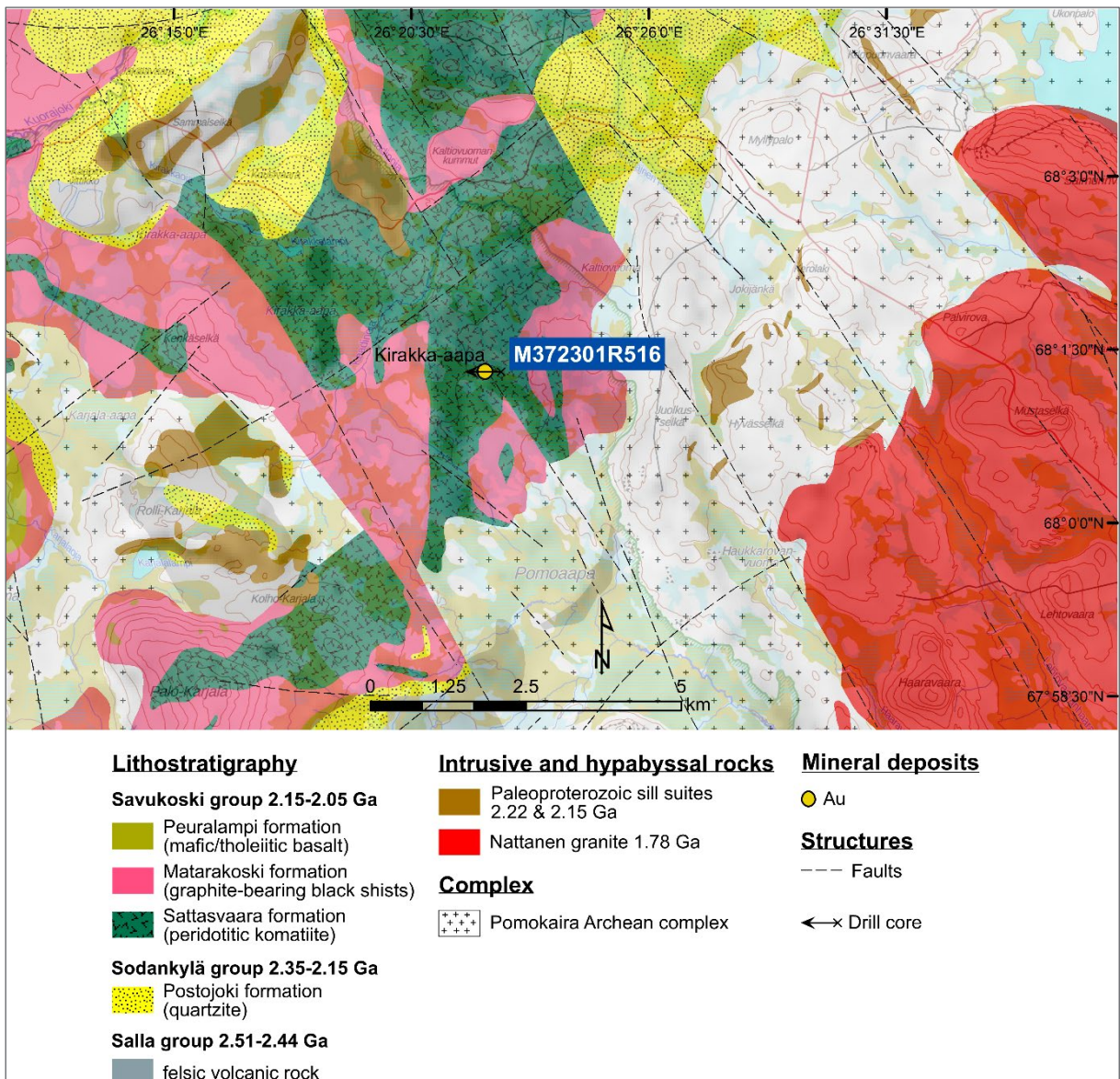


Fig. 7. Bedrock map of the Kirakka-aapa (Bedrock of Finland – DigiKP), as well as the location and drilling direction of the drill core M372301R516 used in this study. Background topography © National Land Survey of Finland.

December 8, 2022

### 3.1.3 Ruossekä

The Ruossekä area is located approx. 70 km northeast of Sodankylä, where GTK discovered the Sakiatieva Au deposit after geochemical and geophysical studies and drilling conducted in 1999–2006 (Figs. 8 & 9; Keinänen et al., 2007). The bedrock of the area consists mainly of supracrustal rocks of the Salla (2.51–2.44 Ga), Sodankylä (2.35–2.15 Ga) and Savukoski (2.15–2.05 Ga) groups, which are intruded by sills of varying ages, as well as post-orogenic Nattanen granite (1.78 Ga) (Fig. 8).

All in all, the bedrock in the area is poorly exposed and very strongly deformed, which can be seen as multiphase folding and abundant fault and shear structures (Räsänen, 2005; Keinänen et al., 2007). The bedrock structures mainly originate from the west–east compression of the early D1 stage, which began approx. 1.94–1.92 Ga ago (see Köykkä et al., 2019), and from the younger north–south compression of the D2 stage (see Lahtinen et al., 2015; Lahtinen et al., submitted). Lithologic contacts between different units are characterized by abundant shearing, which is especially noticeable in the drill cores of the area (see Räsänen, 2005; Keinänen et al., 2007).

In Ruossekä, stratigraphically the lowest part, i.e. the rocks of the Sodankylä group, is mainly characterized by mica-rich (arkose) quartzites of the Postojoki formation, which feature strong schistosity in places (Fig. 8). Sedimentologically, the Postojoki formation is considered to have been deposited in a shallow marine environment (Köykkä et al., 2019). The Savukoski group, which occurs on top of the Sodankylä group, starts with the massive or in places amygdaloidal mafic lava deposits of the Peurasuvanto formation and tuffites in which gabbroic cumulates occur in places. According to Räsänen (2005) and Keinänen et al. (2007), the entire volcanic rock association has a thickness of about 200 m, where especially the amphibolite-like rocks contain mineralized parts. Geochemically, volcanic rocks can be classified as Fe and Mg basalts and komatiites (Keinänen et al., 2007).

The Matarakoski formation, which belongs to the Savukoski group, in turn consists of graphite-rich black schist, in which interlayers of layered greywacke and quartzite and possibly volcanogenic quartz-feldspar schist occur in places (Räsänen, 2005; Keinänen et al., 2007; Figs. 8 & 9). This can be considered a typical deposit of the Matarakoski formation, which can also be found in the nearby Moskuvaara area to the north-northeast of Sodankylä, where albitized rocks are cut by gabbroic/komatiitic dykes in places (Köykkä et al., 2019). Massive ultramafic/mafic volcanic rocks consisting of pillow lavas, in which pillow breccia and hyaloclastic tuffs with peridotite-gabbro cumulates occur in places were intersected in the drillings (see Keinänen et al., 2007). These volcanic rocks also belong to the Savukoski group and have been considered part of the Sattasvaara formation in Central Lapland (see Bedrock of Finland – DigiKP; Köykkä et al., 2019). The cumulates are also typically strongly deformed, as well as serpentized and carbonated. According to Keinänen et al. (2007), a typical cumulate contains a peridotitic bottom part, on top of which there are pyroxenite and peridotite-pyroxenite layers of varying thickness, while the upper part of the cumulate consists exclusively of gabbro. A typical mineralization associated with this occurs as disseminated Fe sulphide, and in some places as Ni-Cu sulphides. Some of the layers are also enriched with PGE group minerals (Keinänen et al., 2017). Based on geochemistry, it can be assumed that the Sakiatieva intrusion and volcanic rocks of Matarakoski

December 8, 2022

are of the same magmatic origin (Keinänen et al., 2007). The contact metamorphism of the area is indicated by the transformation of carbonate-rich layers into tremolite and diopside skarn in places, which occurs especially at the contact of granitic dikes and volcanic-sedimentary deposits.

The Ruoselkä Au mineralization is associated with a northeast–southwest fracture zone and often occurs in the contact zone of mafic volcanic rocks and mica schists (Fig. 9). The mineralization is approx. 10 m wide and 200 m long, and the associated alteration zone is approx. 50–200 m wide and 400 m long (Figs. 9 & 10; Keinänen et al., 2007). Typically, the most strongly mineralized zones are 1–5 m wide and contain 1–3 ppm of Au. Au-anomalous (>0.1 ppm) zones can be up to 20 m wide. In addition to Au, mineralized zones contain anomalous Cu concentrations, typically 0.1–0.2%. Strong bleaching of the rocks, caused by quartz-albite+sericite alteration, can be seen in the Au-mineralized zones, as well as an increase in the sulphide amount ( $S = 1–5\%$ ) (Fig. 10). In addition, quartz-carbonate-sulphide veins, calc-silicate alteration (hornblende-tremolite-diopside) and epidotization can occur. In the proximal zone, the alteration is similar, but less intense, and biotite-alteration also occurs (Fig. 10). Distal alteration is visible as weak biotite-quartz-albite alteration.

December 8, 2022

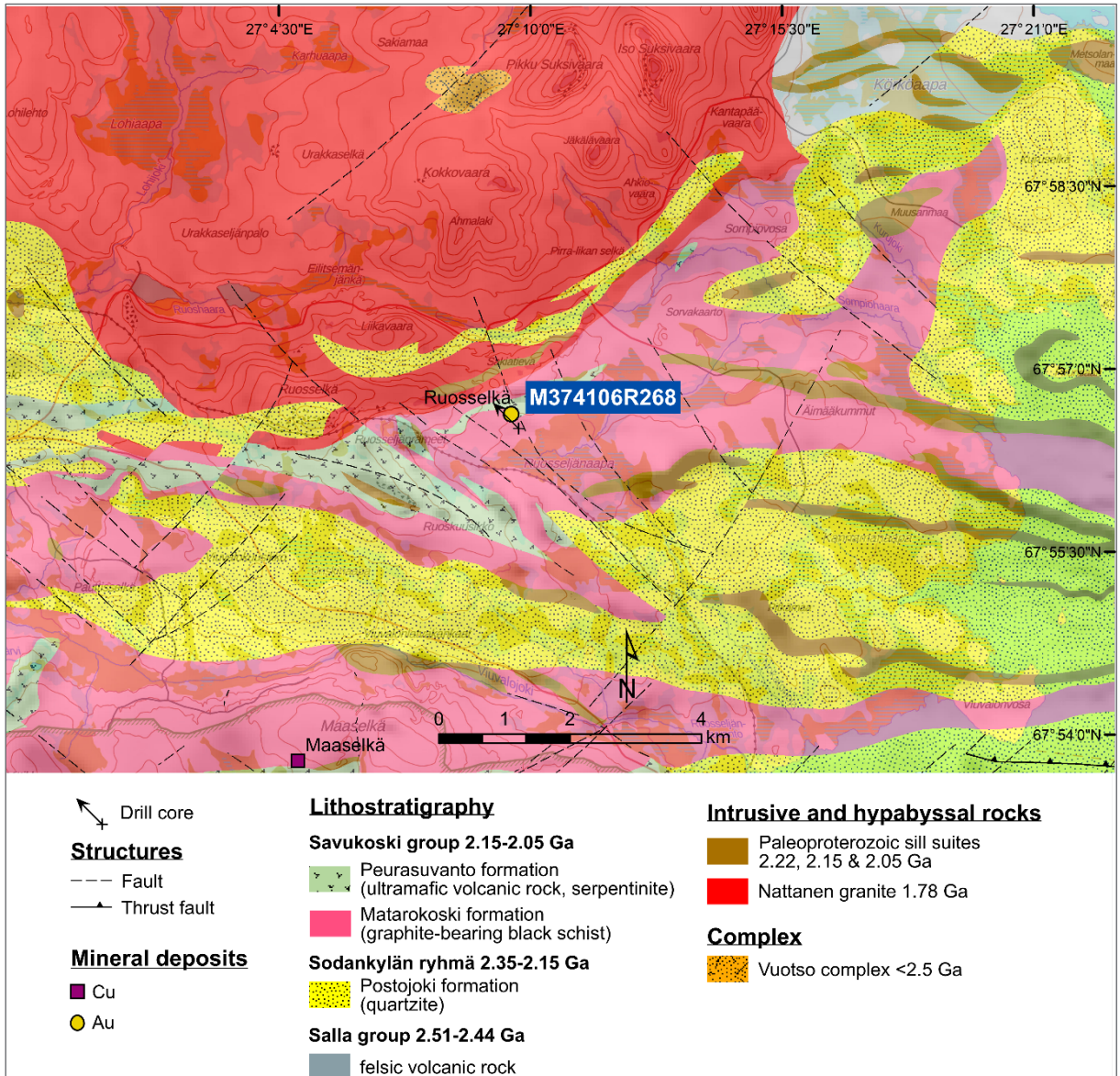


Fig. 8. Bedrock map of Ruosselkä area (Bedrock of Finland – DigiKP), as well as the location and drilling direction of the drill core M374106R268 used in this study. Background topography © National Land Survey of Finland.

December 8, 2022

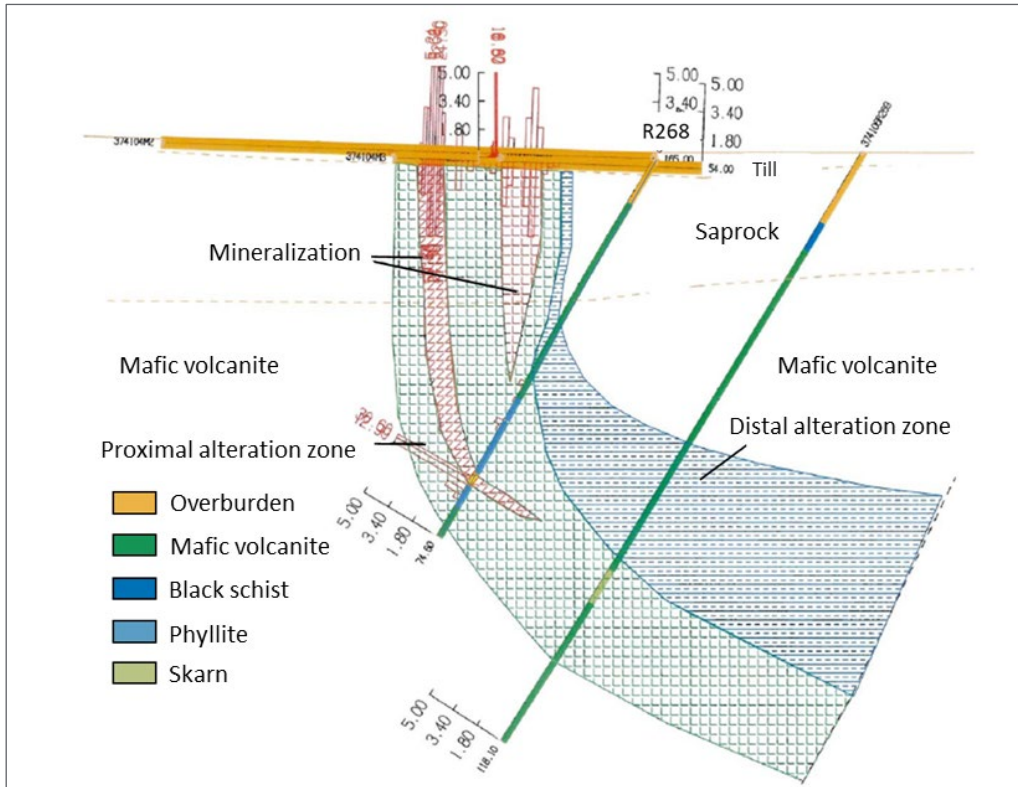


Fig. 9. Cross-section of Ruosselkä Au mineralization and alteration zones (modified from Keinänen et al. 2007).

December 8, 2022



Fig. 10. Drill core tray images (M374106R268) showing the transition from the less mineralized dark biotite-sericite altered mica schist to the highly Au-mineralized quartz-albite-rich rock. Also note the sharp contact of mineralization and alteration with mafic volcanic rock on the foot wall.

December 8, 2022

## 3.2 VMS deposits

Volcanogenic Cu-Zn-Pb sulphide ores are formed by precipitation from hot fluids erupting onto the ocean floor. In principle, VMS-type sulphide ores can form anywhere on the ocean floor where there is 1) a suitable heat source such as a magma chamber that maintains fluid circulation, 2) structures such as faults, along which cold seawater can penetrate the (oceanic) crust and 3) sufficient water depth, so that the fluids cannot boil before erupting onto the ocean floor. Most of the deposits are related to rift zones on the ocean floor, such as mid-ocean ridges or island arc systems. The deposits vary in shape from lenticular to plate-like, sometimes pipe-shaped, and usually consist of massive sulphide formations, under which there may be stringer ore) (Shanks & Thurston, 2012). VMS deposits are characterized by rock alteration of varying intensity on the foot wall, which can appear as pipe-shaped, zonal alteration or a stratiform plate-like alteration zone. Pipe-shaped alteration zones usually consist of a highly altered inner/proximal quartz-chlorite-sulphide zone surrounded by a chlorite-sericite-sulphide zone, which in turn transitions into an outermost sericite (+chlorite+sulphide) zone (Gibson et al., 2007).

The known VMS deposits in Finland are concentrated in the Raahe-Laatokka zone, the Outokumpu area and the Orijärvi-Aijala zone in Southern Finland. The best-known VMS deposit in Lapland is Pahtavuoma Cu-Zn deposit. In addition, Cu-Saattopora and Riikonkoski Cu deposits are possibly also VMS-type deposits.

### 3.2.1 Pahtavuoma

The Pahtavuoma area is located west of Kittilä, where it is bordered by the 2.0 Ga tholeiitic volcanic rocks of the Kittilä Assemblage in the north and <1.94 Ga Uusivirta group and the 1.88 Ga metasediments of the Kumpu group in the west (Figs. 11 & 12). The Pahtavuoma deposit was discovered by Outokumpu in the 1970s based on stream sediment studies, in connection with which several outcrops containing chalcopyrite were found. The Pahtavuoma Cu deposit was an open-pit mine when in operation and underground mining was conducted mainly in years 1974–1976, and in 1993, when up to 261,000 tonnes of Cu were extracted from it. The total extraction of the mine was approximately 0.6 Mt, of which ore accounted for 0.3 Mt (Korkalo, 2006). Geologically, the Pahtavuoma area belongs to the Matarakoski formation of the 2.00 Ga Savukoski group (Fig. 11) and comprises numerous east–west oriented graphite-rich black schist, greywacke and tuffite zones, as well as smaller amounts of altered albite schists, skarn and carbonate rocks (Inkinen, 1979; Korkalo, 2006). The area's mafic volcanic rocks and albite diabbases occur around the aforementioned rocks.

The area comprises four distinct Cu deposits, which occur as separate lenses (Fig. 12). Deposit A, the largest of these, is about 450 m long, 20 m wide and up to 400 m deep, and follows the east–west structures of the area along its length, dipping 70 degrees to the north. The separate Cu mineralization in Pahtavuoma is related to the contacts of metasediments and mafic volcanic rocks in the area, where the host rock mainly consists of graphite-rich phyllitic black schists that are cut by narrow quartz carbonate and sulphide-rich fissure veins (Fig. 13; Korkalo, 2006). The sulphide-rich zone is characterized by the presence of abundant scapolite, amphibolite and garnet porphyroblasts. Magnetite also occurs in connection with scapolite, especially in narrow

December 8, 2022

Cu-rich skarn zones, which can be considered an exception in the Cu-Au deposits of Central Lapland (Korkalo, 2006).

Pahtavuoma's Cu content increases strongly in the foot wall contact, typically being 1–2% (Korkalo, 2006). The deposits are relatively poor in sulphides, with a sulphur content of approximately 2.4%. The most important ore minerals in the deposit are chalcopyrite and pyrrhotite, along with various other sulphide minerals, e.g. pyrite, sphalerite, galena and arsenopyrite. Magnetite occurs especially in the skarn zones of the area and chalcopyrite as breccia-like gouges with calcite and quartz, as well as disseminated on layer surfaces, suggesting a strata-bound origin (see Inkinen, 1979; Korkalo, 2006).

The highest Cu concentrations (15–20%) have been observed in the area's narrow stratiform dike, which is 0.3 m in thickness and consists exclusively of chalcopyrite and pyrrhotite. This has been thought to represent either a mobilized sulphide precipitate or a massive sulphide deposit occurring in the proximal parts of the volcanic system (see Korkalo, 2006). The average Au concentrations in Pahtavuoma are below 0.01 g/t, while the highest concentration (0.16 g/t) was measured in connection with a chalcopyrite-pyrrhotite vein. In addition, Pahtavuoma comprises numerous zinc-rich zones that occur in connection with Cu deposits on the hanging wall and parallel to metasediment deposits.

December 8, 2022

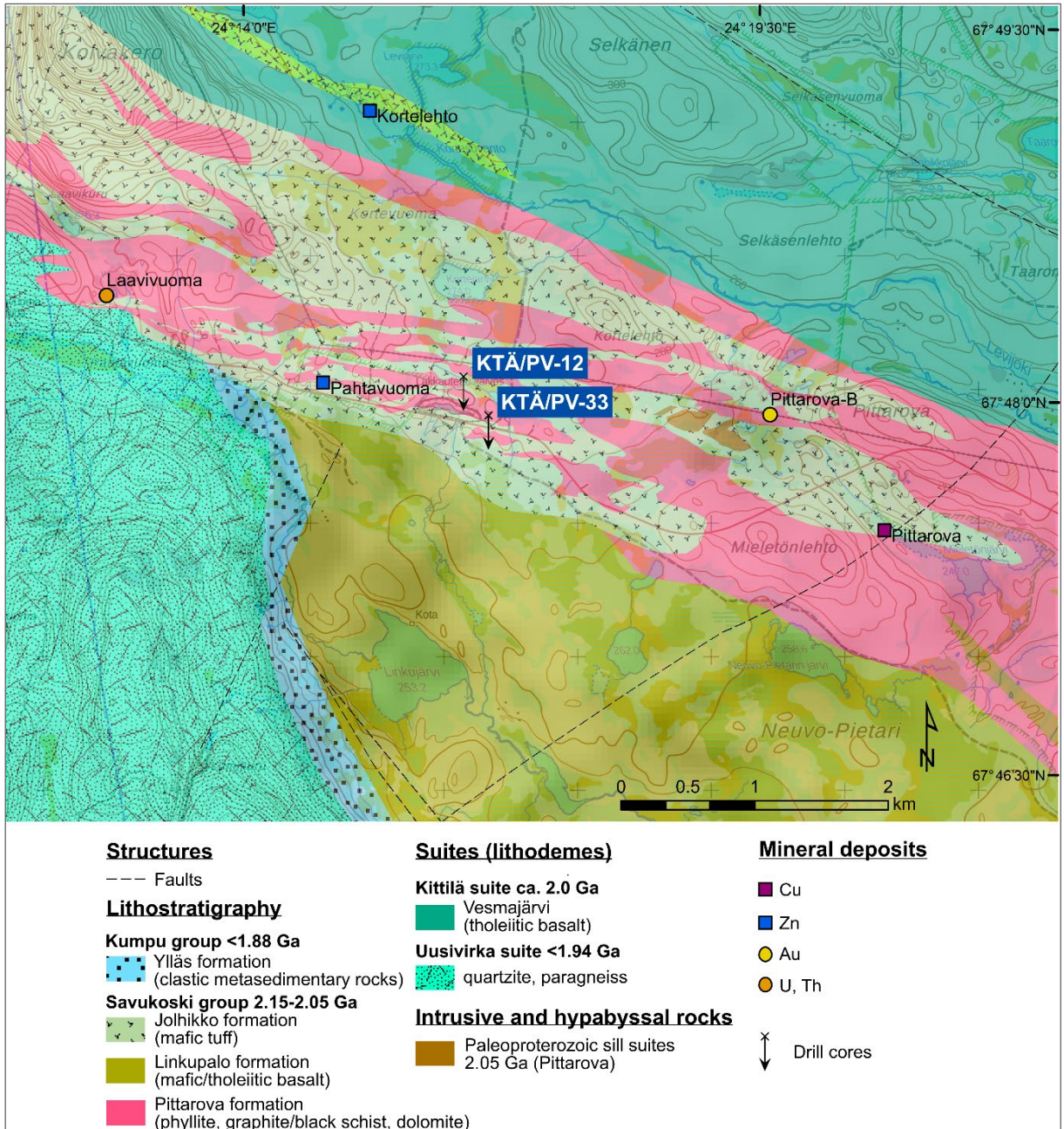


Fig. 11. Bedrock map of Pahtavuoma (Bedrock of Finland – DigiKP), as well as the location and drilling direction of the drill cores KTÄ/PV-12 and KTÄ/PV-33 used in this study. Background topography © National Land Survey of Finland.

December 8, 2022

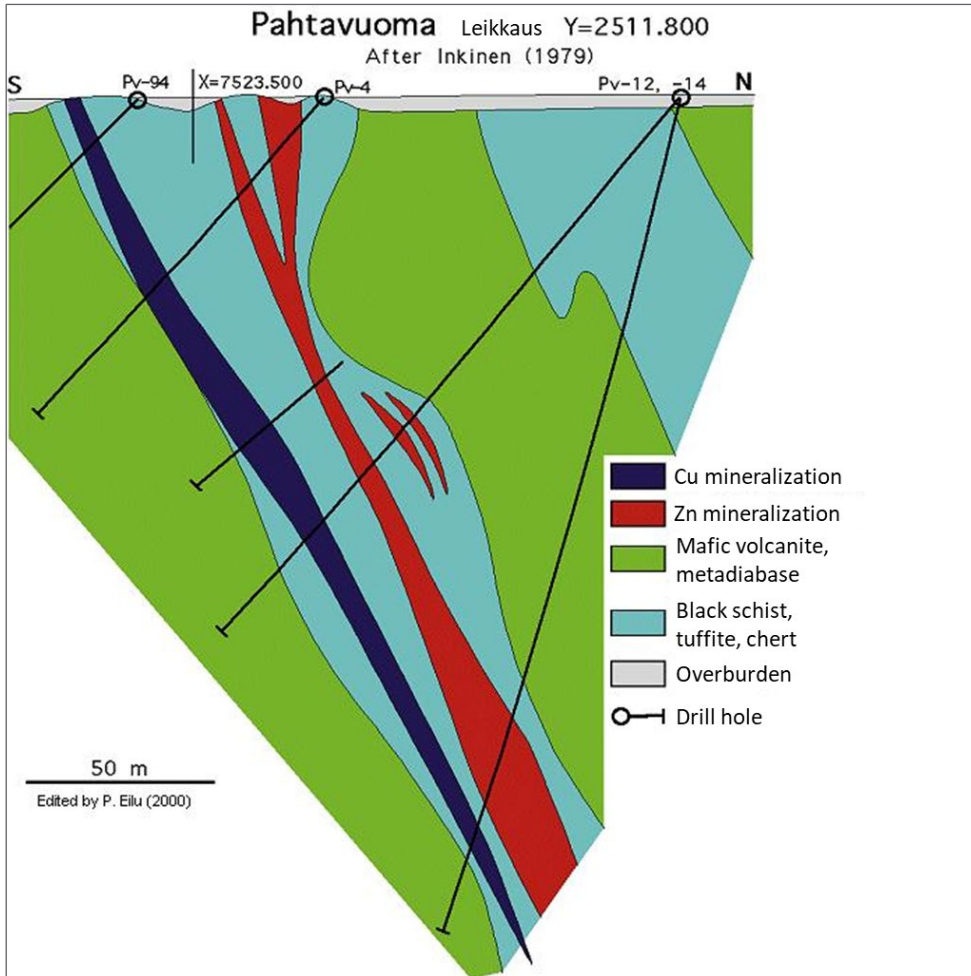


Fig. 12. Section of Pahtavuoma showing the location of Cu and Zn lenses (modified from Inkinen, 1979).



Fig. 13. Drill core tray image (PV-12), showing mineralized phyllite with narrow sulphide-carbonate-quartz dikes.

December 8, 2022

## **4 WP1: PROJECT COORDINATION AND MANAGEMENT**

### **4.1 Description**

The tasks of work package 1 consisted of project coordination and management. The accountable project leader supervised the project and acted as the coordinator of the scientific research. The project manager was responsible for project implementation and reporting. The project manager also acted as the secretary of the steering group.

### **4.2 Implementation**

#### **4.2.1 Recruitment**

The project plan included the hiring of a temporary employee for the project. This software engineer position, connected with work package 2, was put up as an open application in November 2020. The application period ended in December 2020. All the planned job interviews were conducted in January 2021. According to the overall assessment, none of the applicants interviewed met the requirements of the application notice to the extent that there would have been grounds to select any of them. It was therefore decided that the temporary position in question would be left unfilled. The coding expertise needed in work package 2 was arranged through GTK's internal resources. The replacement resource was able to start in the project in May 2021.

#### **4.2.2 Equipment purchases**

A significant part of the data collection included in work package 3 was implemented using two portable spectrometers (see chapter 6). One spectrometer was acquired for GTK as a new device. A market survey was a mandatory part of the procurement process for this portable FTIR analyzer (spectrometer). According to the survey conducted in August 2020, the Agilent 4300 Handheld FTIR was the only commercially available FTIR spectrometer that met the requirements. No sensible alternatives or replacement solutions were then available, as it was desired that the device to be purchased should function as a handheld model.

An order for the Agilent 4300 Handheld FTIR analyzer was placed in September 2020, when GTK's internal procurement procedure had been completed. Based on the market survey, the device was ordered from Agilent Technologies Inc. The actual device order was made through Agilent's representative in Finland (Agilent Technologies Finland Oy).

The purchase of the analyzer included equipment training provided by the supplier, which was organized remotely using MS Teams. The instructor in the training was product specialist Donald Inglis (Agilent Technologies). A total of 22 people from GTK, including the HypeLAP development team, participated in the training.

#### **4.2.3 Applying for an extension period**

At the beginning of 2020, the global Covid-19 pandemic spread to Finland, also causing considerable restrictions in workplaces in the form of remote work practices, for example. The HypeLAP project faced a lack of resources in its operation during 2021, due to the secondary

December 8, 2022

impacts of Covid-19. This meant some of the researchers assigned to the HypeLAP project were preoccupied longer than expected with a previously launched project to which they had been assigned. While the schedule of this second EU-funded project was extended from the original, the impacts also cumulated to cause delays the progress of the HypeLAP project, as the researchers' working time was unavailable to the project as planned.

In addition, GTK's expertise in the interpretation of spectral data gained more scope during the project when a new researcher specializing in spectral geology was recruited to the organization in December 2021. The researcher in question was assigned to the HypeLAP project to supplement the interpretation expertise it required.

Due to the strengthened researcher resources and the overlapping personnel assignments of 2021, the HypeLAP project applied for a six-month extension period. The intention with the new schedule was to ensure that the project would be able to fulfil the goals more comprehensively, so that the benefits to be achieved would also be more thoroughly available to the stakeholders.

Business Finland granted the requested extension period, which was supported by the steering group. The actual project work therefore ended in November 2022 in accordance with the new schedule.

#### 4.2.4 Reporting

The project's first technical interim report was submitted with cost statements to Business Finland in January 2021, and the second corresponding interim report in January 2022.

The project steering group was informed of the progress of the project at the steering group meetings, which were organized on 4 September 2020, 15 January 2021, 21 May 2021, 17 September 2021, 19 January 2022, and 18 May 2022. Short project status reviews were also organized at the request of the steering group on 27 November 2020 and 25 March 2021.

December 8, 2022

## 5 WP2: ARCTIC VIRTUAL DRILL CORE ARCHIVE

### 5.1 Description

An online demo service (Arctic Virtual Drill Core Archive), which is intended for the presentation and distribution of diamond drilling data owned by GTK, was set up in work package 2. The demo service presents selected images produced in hyperspectral drill-core imaging campaign at GTK in 2018 (Ojala & Vuollo, 2019). Also, tabulated collar, lithology and assay data related to these drill cores are included in the demo. The online service is a prototype, which can be utilized in upcoming development projects which aim at using a corresponding service for production.

The demo service was used to test how the above-mentioned specific geological data can be presented visually in an online environment in such a way that it was also systematically cataloged and could be browsed easily. During the project, selected users evaluated the usability of the created demo service.

The development work aimed to create a starting point for a virtual research platform and its further development. This means that in possible production use, the service itself could be used for studying drill core data.

The purpose of work package 2 was also to contribute to the digitization of the National Drill Core Archive managed by GTK, whose implementation is based on hyperspectral imaging. Efforts were made to facilitate digitization through the above-mentioned data distribution service.

### 5.2 Implementation

#### 5.2.1 Requirements specification

The creation of the demo service started with requirements specification, which was prepared by the work package staff. The specification focused on the description of the demo service environment, the data content to be presented, and the user interface. Another important part of this preparatory phase was familiarization with the literature on the hyperspectral imaging method and other background material.

The requirement specification was based on a review of different types of publicly available online services and the practices used in them. The practices that were considered best suited for the prototype were selected to be used in the created graphical user interface (GUI). In the design of the GUI, the nature of the offered service was considered, with emphasis on geological data content and its presentation, as well as tool functionality related to the service.

#### 5.2.2 Technical setup

The demo service was set up in Esri Inc.'s cloud-based (Software as a Service) ArcGIS Online system. The ArcGIS Experience Builder platform and the widgets included in it were used in the coding work. Wireframe images were prepared to illustrate the planned service. The images served also as coding guidelines.

December 8, 2022

### 5.2.3 Development testing

The first draft version of the online service to be piloted was completed for the work package's internal development testing in August 2021. In this work phase, the development team ensured that the implemented online service complied with the requirements set for it, and that it worked flawlessly. All detected errors were corrected before proceeding to the next phase. The testing was based on the requirement specifications. The development of the draft version was then continued among the software experts of the work package so that the service could be handed over to an external test group for evaluation.

### 5.2.4 User testing

After the development testing, the online service to be piloted was released to a test group consisting of the actual end users. The test group consisted of members of the project steering group and the companies they represented. At the same time in February 2022, the online service was also released to GTK's experts outside the project team for a trial. The testing period ended in April 2022. The test group had an opportunity to give coordinated feedback on the usability of the online service and the usefulness of its contents.

## 5.3 Result

### 5.3.1 Technical platform

The demo service was set up in Esri Inc.'s cloud-based (Software as a Service) ArcGIS Online system. In other words, Esri Inc. provided the technical environment in which GTK set up the demo service and customized it to suit its needs.

### 5.3.2 Data storage

The demo service reads the data it presents from separate copies. All the service's data are extracted from the GTK's databases into these copies, which are stored in the ArcGIS Online system and Azure Blob Storage cloud service.

### 5.3.3 Functions and content

The demo service was offered to users in the form of a website. Users did not need to install or download anything on their own computers.

GTK's data produced in diamond drilling or related to drilling are shared through the demo service. A key element in the shared data is the images captured from the drill cores with hyperspectral imaging. These images form three different groups in the service:

- RGB images;
- False color images in the VSWIR (350–2500 nm) wavelength range; and
- False color images in the LWIR wavelength range

December 8, 2022

Selection for the false color images is as follows:

- SWIR wavelength range, red: 1940 nm, green: 2200 nm, blue: 2340 nm
- LWIR wavelength range, red: 8600 nm, green: 10000 nm, blue: 11800 nm

In addition, the service contains tabular data from diamond drilling in the following sub-areas: drill hole identification and location data (collar data); lithological description of the drill cores (lithology data); and whole rock chemical analyses of the drill core samples (assay data). All material distributed through the demo service represent data that is situated within Central Lapland area.

The frame of user interface is a browsable map view, through which the user can search for drilling data of interest based on geographical location (see Fig. 14). This means the drilling data are listed in the user interface according to their locations. In practice, each diamond drilling location (drill hole collar) is displayed as a point placed on the base map.

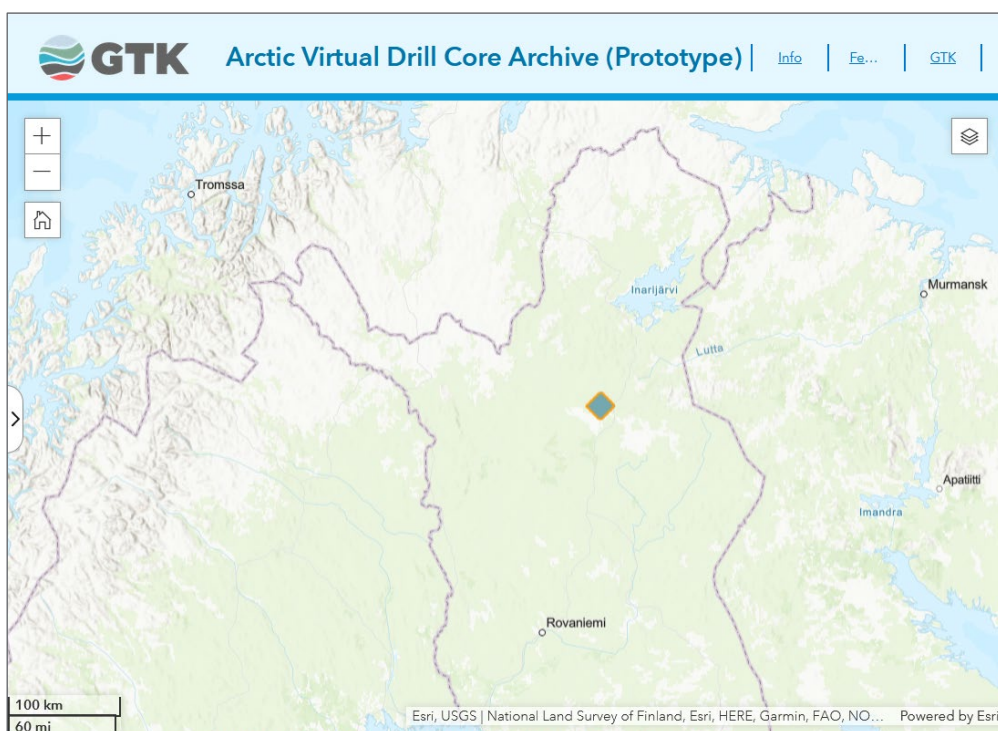


Fig. 14. Browsable map view of the demo service. The map view forms the frame for the user interface.

December 8, 2022

In the map user interface, searches are made for the data libraries, the primary search condition being the ground location of a single drill hole. The data content corresponding to the searches is presented in the user interface either as tables (see Figs. 15–17) or as images (see Figs. 18–20).

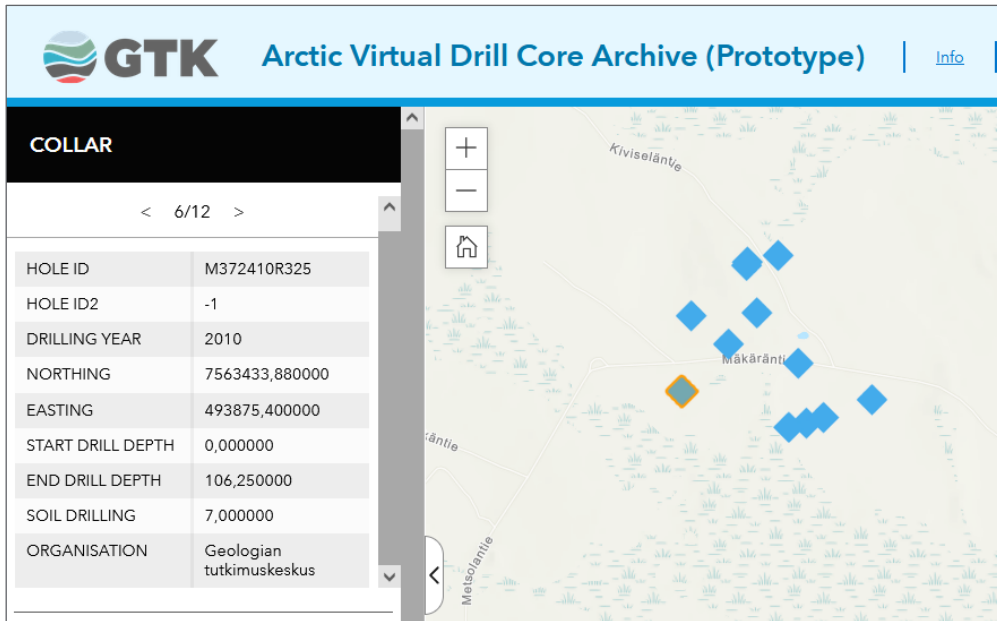


Fig. 15. Identification and location data (collar) of the drill core M372410R325 tabulated. An excerpt from the content of the demo service.

December 8, 2022

Lithology			
HOLE_ID	START_DEPTH	END_DEPTH	FIELD_NAME
M372410R325	0	7	MAATA
M372410R325	7	27,8	RAPAKALLIO
M372410R325	27,8	32	AMFIBOLIITTI
M372410R325	32	40	ARKOSIITTI
M372410R325	40	41,5	AMFIBOLIITTI
M372410R325	41,5	49,2	RAPAKALLIO
M372410R325	49,2	60,5	AMFIBOLIITTI
M372410R325	60,5	63,6	TONALIITTI
M372410R325	63,6	63,85	ARKOSIITTIJUONI
M372410R325	63,85	65	AMFIBOLIITTI
M372410R325	65	66	ARKOOSIKIVI
M372410R325	66	78,3	FELSINENKIVI
M372410R325	78,3	85	TONALIITTIGNEISSI
M372410R325	85	106,25	TONALIITTIA

Fig. 16. Lithological description of the drill core M372410R325 at a depth range of 0–106.25 m tabulated. An excerpt from the content of the demo service.

Assay				
SAMPLE_ID	START...	END...	ELEMENT	CONTENT
M372410R325 7.00-...	7	8,1	Al	95 600
M372410R325 7.00-...	7	8,1	Al	98 900
M372410R325 7.00-...	7	8,1	As	100
M372410R325 7.00-...	7	8,1	As	100
M372410R325 7.00-...	7	8,1	Au	2 530
M372410R325 7.00-...	7	8,1	B	100
M372410R325 7.00-...	7	8,1	B	100
M372410R325 7.00-...	7	8,1	Ba	355
M372410R325 7.00-...	7	8,1	Ba	321
M372410R325 7.00-...	7	8,1	Be	10
M372410R325 7.00-...	7	8,1	Be	10
M372410R325 7.00-...	7	8,1	Bi	5

Fig. 17. Chemical analyses (assay) of the drill core M372410R325 tabulated. An excerpt from the content of the demo service.

December 8, 2022

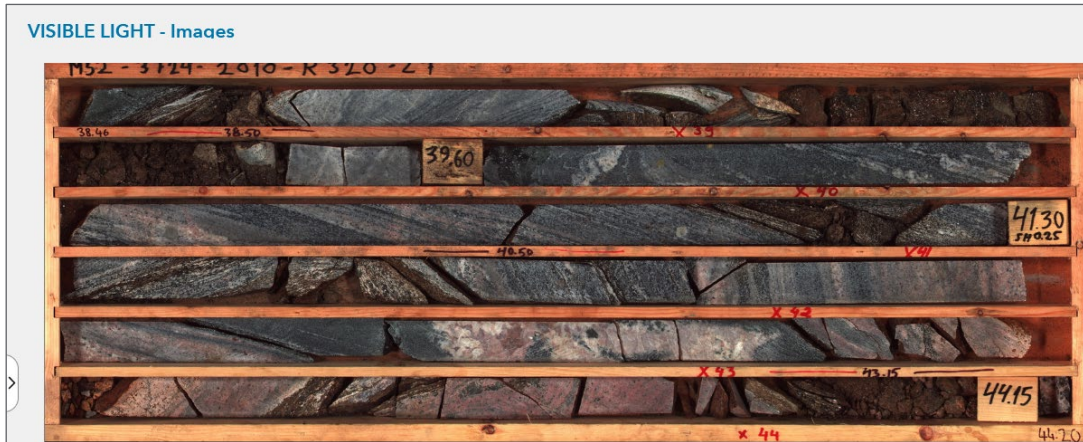


Fig. 18. RGB image of the drill core M372410R320 at a depth range of 38.46–44.2 m. An excerpt from the content of the demo service.

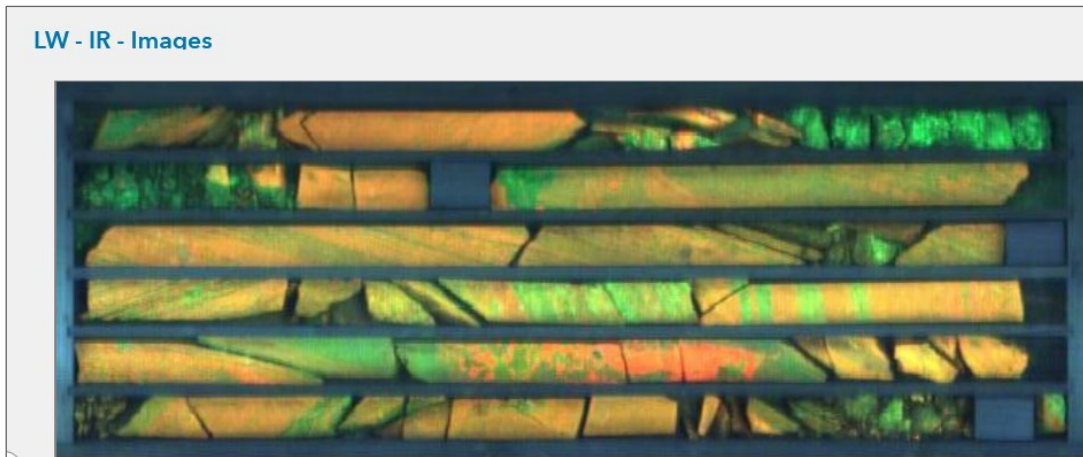


Fig. 19. False color image (LWIR wavelength range) of the drill core M372410R320 at a depth range of 38.46–44.2 m. An excerpt from the content of the demo service.

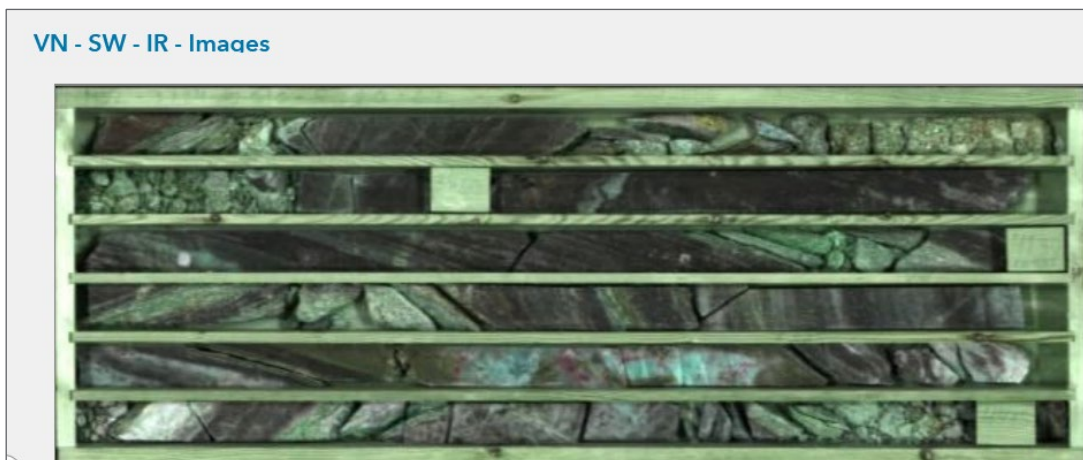


Fig. 20. False color image (VSWIR wavelength range) of the drill core M372410R320 at a depth range of 38.46–44.2 m. An excerpt from the content of the demo service.

December 8, 2022

Table 1 composes a description of the geological data content included the demo service. In the same context, the importance of each dataset is evaluated.

Table 1. Compilation of the geological data content included the demo service (Arctic Virtual Drill Core Archive).

Data type	Content description	Achievable information	Role in the service
Drilled hole location map layer	Shows the location of the diamond drill holes as points on the base map.	The locations of the diamond drilled holes can be seen on a browsable map.	Acts as a directory for the datasets included the service.
Collar data table	Shows the drill hole identification and location data in tabular form.	Displays the identification and location data of a selected drill hole.	Serves as a primary/auxiliary dataset.
Lithology data table	Presents a tabulated lithological description of drill core samples.	Contains a lithological description of a selected drill core at specified depth intervals.	Serves as a primary/auxiliary dataset.
Assay data table	Presents the results of the chemical analyses of the drill core samples in tabular form.	Shows the chemical analysis results of a selected drill core at specified depth intervals.	Serves as a primary/auxiliary dataset.
RGB image of a drill core	RGB photograph of a single drill core tray. Each drill core forms a set of images covering its entire length. The images are zoomable based on their resolution. The images have a pixel resolution of 0.15 mm.	When zoomed out, it is possible to get a good overall picture of the appearance of the drill cores from the images. With full resolution, the images reveal countless details of the drill cores. The data content of the images is comparable with traditional research conducted in physical core storage facilities and based on visual observations made from the drill cores.	Forms the frame of the datasets included the service.
False color image of a drill core (VSWIR)	False color image of a single drill core tray produced from hyperspectral VSWIR / LWIR data. Each drill core forms a set of images covering its entire length. The images have pixel resolution of 1.5 mm.	The false color images highlight the structures of the drill cores and illustrate the relative amounts of minerals and rock types.	Serves as an auxiliary dataset for the RGB images of the drill cores.
False color image of a drill core (LWIR)			

December 8, 2022

#### 5.3.4 User feedback

The feedback received during the user testing phase mostly concerned the visual aspects of the data presented in the demo service. According to the test users, the current map user interface, the RGB images and false color images create a good basis for the visual examination of the data.

In addition, in the feedback, it was hoped it would be possible to display the data of the elemental concentrations of the drill cores and the wavelengths of the spectral measurements as line graphs. When several line graphs are placed side by side, aligned with each other in terms of depth, the human eye can observe possible deviations or trends.

In turn, tabular data are considered to bring out details about different variables. The users also hoped that if a production version of the service was published later, the option to purchase the data should be added.

### 5.4 Conclusions

#### 5.4.1 Work principle

In a way, the development work carried out in work package 2 followed the principle of experimentation. The purpose of the work package was to provide a prototype product for testing by end users, and for collecting user feedback. The experts involved in the project defined the content and functionalities of the prototype based on their research work.

The prototype development work could also have been carried out so that the requirements of the demo service would have been clarified in the planning phase with the aid of preliminary surveys and interviews targeted at mining and mineral exploration companies. However, recording the requirements received from outside the project team, for a service described only verbally, was considered too theoretical. It is often difficult for end users to explain or even know what they desire if no examples of possible services or products are provided. Therefore, achieving an outcome that could have been used successfully in the actual implementation was considered unlikely.

To put effort into implementing the basic features of the demo service, some of the functionalities included in similar online services, such as user authorization management, were left out deliberately. This way it was possible to develop the demo service within the frame of this project. Auxiliary features and improved usability will be the subject of upcoming projects.

#### 5.4.2 Technical platform

As the ArcGIS Online platform is already part of GTK's information technology system, it was therefore decided to use it in this project as well. However, in terms of the possible further development of the demo service constructed in the project, it must be ensured that ArcGIS Online can be used for commercial purposes if one wishes to add a paywall to the final service. Otherwise, it must be replaced with an alternative technical solution.

December 8, 2022

### 5.4.3 Data

In the project plan, the intention was to store a considerable amount of hyperspectral imaging data in the demo service. However, the implementation deviated from the plan in that only a minor part of these datasets was included in the service. This is because of a free demo service, through which the intention is not to share materials that may be productized later. In any case, the nature and functionalities of the demo service could be presented even with a significantly smaller amount of data.

### 5.4.4 Follow-up development

When the fundamental aspects of the demo service have now been implemented in a high-quality manner, it will be easy to start adding more advanced functions to the service after the HypeLAP project. In follow-up development, it is also possible to benefit from the experiences and new knowledge gained in this project. The justification for such multiphase cross-project development work is the awareness of the complexity involved in creating new information systems, in which it is challenging to consider all the dependences or variables in advance.

In terms of possible follow-up development, it is important that the received user feedback is considered in the implementation. The developers can thus react to the requirements of the environment and deliver a result that better meets the users' needs.

The demo service created in this project is an example of what a digital sample archive complying with the previously described theme could be like in the production phase. However, this example does not prevent the making of significant functional or content changes to the service's next development version if the end users consider them necessary. The final analysis and recommendation about which direction to take with further development at GTK and with what kind of contribution, should be made after the HypeLAP project. However, this issue has already been discussed in the final part of the report (see chapter 9).

December 8, 2022

## 6 WP3: DATA ACQUISITION

### 6.1 Description

The analytical work conducted in work package 3 was done with portable handheld instruments which only require a short technical training. The emphasis was on spectroscopic techniques which are based on illumination of the samples artificially and measuring the reflected portion of the radiation at visible and infrared portions of the electromagnetic radiation. The spectral data produced with the spectrometers were utilized for characterization the mineralogy of the rocks, specifically the alteration minerals related to Au mineralization. The goal was to recognize the alteration zoning around Au mineralization and identify the minerals and mineral chemistry related to alteration from the drill core samples.

There was no new field work conducted but the work was based on existing drill core stored in the GTK drill core archive. The drill core sections were selected to fulfill the criteria set by the HypeLAP project.

The handheld spectrometer used in the project measure the spectra across the entire electromagnetic spectral portion of the visible and near infrared radiation. The visible, near infrared, and short-wave infrared portions were covered with TerraSpec Halo (Analytical Spectral Devices ASD, Malvern PanAnalytical) and the mid wave infrared and long wave infrared portions with 4300 handheld FTIR (Agilent). The later 4300 FTIR device was acquired by the HypeLAP project. The purchasing process is described in section 4.2.2.

### 6.2 Implementation

#### 6.2.1 Selection of samples

GTK personnel studied the GTK sample archives to find relevant rock samples to present a variety of alteration types related to Au mineralization for the use of the HypeLAP project. The focus was on Au prospects from Lapland. Firstly, the possibility of utilizing a hand specimen sample set from the GTK Lapland Volcanite Project (LVP, 1984-1989, Lehtonen et al. 1998) was researched. However, in contradiction to prior information received these bedrock samples were chosen to represent primary unaltered rocks. Thus, the sample set was rejected for the purpose of the HypeLAP project.

Secondly, possible drill cores related to Au prospects were searched from the GTK drill core database. Drill cores from several small Au prospects were found in the Central Lapland Green stone belt. These drill cores, according to the reports, cross Au or Cu-Zn mineralized zones and related alteration halo is reported to be detected. According to these criteria five drill core sets were selected. The total length of the core was 608.4 meters. The drill core basic information is presented in Table 2, and the locations of the cores are showed in Fig. 1. Geological descriptions representing the drill core sites from Hirvilavanmaa, Kirakka-Aapa, Ruoselkä and Pahtavuoma are explained in chapter 3.

December 8, 2022

*Table 2. Basic information of the drill cores selected for the study.*

Drill hole identifier	Samples	Area	Mineralization	Drill hole depth (m)	Drilling year
M273488R335	6	Hirvilavanmaa	Au	153.3	1988
M372301R516	8	Kirakka-Aapa	Au	72.5	2001
M374106R268	8	Ruosselkä	Au	74.6	2006
KTÄ_PV-012	4	Pahtavuoma	Cu-Zn	188.83	1971
KTÄ_PV-033	4	Pahtavuoma	Cu-Zn	108.18	1971

### 6.2.2 Preparation of samples

The selected drill cores were located in the GTK sample storage at Loppi. They were transported to the drill core facility in Rovaniemi for inspection and measurements. Core trays were prepared for the research by lifting them on the roller tables in the order of the drill depth (see Fig. 21). In addition, length intervals were measured and marked. The samples were vacuum free of dust and debris because the penetration of the used electromagnetic wavelengths is very shallow, at 50 µm at maximum. Every drill core tray was also photographed with an RGB camera.

December 8, 2022



Fig. 21. One set of drill cores lifted onto the roller table for examination. Photo: J. Köykkä.

### 6.2.3 Instrumentation and drill core measurements

The drill core measurements were conducted with four different instruments: <sup>1)</sup> TerraSpec HALO (Fig. 22a, Malvern Panalytical, 2022) and <sup>2)</sup> Agilent handheld FTIR 4300 spectrometers (Fig. 22b, Agilent Technologies, 2022) for mineral identification, <sup>3)</sup> Vanta XRF (Olympus, 2022) for whole rock chemistry and <sup>4)</sup> KT-6 Kappameter (SatisGeo 2022) for magnetic susceptibility. The Agilent handheld FTIR 4300 spectrometer was purchased by the HypeLAP project to complement the spectral range of the TerraSpec HALO (see table 3).

December 8, 2022

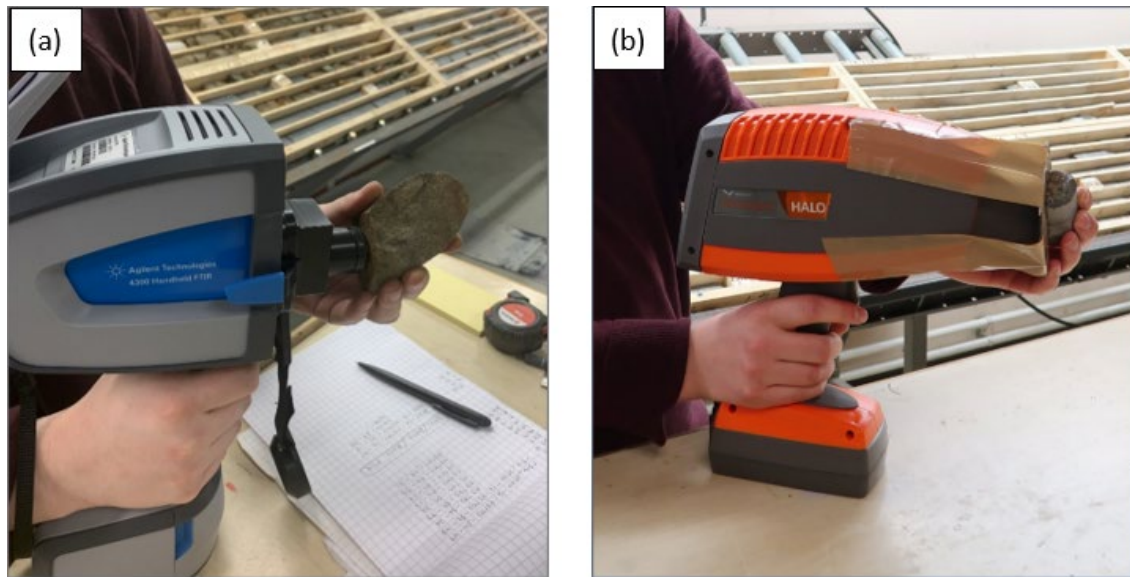


Fig. 22. Measuring drill core samples with the handheld spectrometers a) TerraSpec HALO and b) Agilent FTIR 4300. Photos: J. Köykkä.

Table 3. Specifications of the handheld spectrometers used in the study.

Handheld spectrometer	TerraSpec HALO	Agilent FTIR 4300
Spectral wavelength/ wavenumber range	400–2,500 nm	2,222–15,384 nm / 4000–650 cm <sup>-1</sup>
Spectral resolution	Varies according to measured spectral range between 3–9.8 nm	Adjustable 4–16 cm <sup>-1</sup> , used resolution 4 cm <sup>-1</sup>
Measurement field of view	~ 10 mm	~ 7 mm
Instrument weight	2.5 kg	2.2 kg
Measurement time	app. 20 sec	app. 30 sec
Measured spectra to be averaged to represent the measurement	20	64
Used foreoptics	None	Diffuse Reflectance

The measurements were made from the drill cores at one-meter intervals using each of the four instruments. Additional measurement points were selected from the drill cores at specific representative points where a typical mineral related to alteration was clearly visible appearing in large enough crystals to be measured. About 600 measurement points were accumulated on each device, which means a total of approximately 2,400 individual measurements, of which 1,200 were actual spectral measurements. All the measurements were mainly conducted between November and December 2020 and completed in January 2021.

December 8, 2022

#### 6.2.4 Polished thin sections

A total of 30 offcuts (see Table 2) were systematically collected from the measured drill cores for the validation of mineralogical interpretation derived from the spectroscopic data. The thin sections made from these offcuts were studied using optical microscopy. Microscopic examination was preceded by the sample preparation, in which a polished thin section was prepared from each rock sample. The thin sections were made at the laboratory of the Oulu Mining School Research Centre.

The thin sections were examined by the experts of the work package using a polarizing microscope in May 2021. Based on optical properties, it was possible to verify those parts from the mineral composition of the samples that were the most important (alteration minerals). All thin sections were also photographed as whole thin section photography through a microscope in two lighting conditions (polarized/non-polarized light). The offcuts used in preparing the thin sections were also measured using Agilent FTIR, Terraspec HALO and Vanta XRF devices in May 2021, and with SisuRock in August 2021.

#### 6.2.5 Content changes

The implementation of work package 3 differed from the original plan as the project progressed in that a thematic map of the alteration zones in the study area was not prepared according to the sub-goal. Based on the sample data, the thematic map was replaced by more extensive data collection than was intended in the original plan. At the same time, it was decided to focus the work on the data collection, and the data interpretation would be implemented in work package 4 (see chapter 7).

#### 6.2.6 Extended data collection

Extended data collection included three separate entities: <sup>1)</sup> the hyperspectral imaging of the drill core trays and 30 offcuts taken from the drill cores, <sup>2)</sup> the SEM-EDX/MLA analysis of thin sections made from the offcuts, and <sup>3)</sup> the SEM-EDX/INCA and micro-XRF analysis of two and seven, respectively, of the selected offcuts.

**The hyperspectral imaging** was carried out in the Lepikontie core storage facility in Rovaniemi as part of GTK's more extensive drill core scanning campaign, which was fully financed from GTK's budget (see Fig. 23). All five drill cores selected for the HypeLAP project, as well as 30 offcuts taken from them, were imaged on a hyperspectral core imaging system.

The scanning work was outsourced so that a private operator (TerraCore) and its subcontractor (Geopool Oy) were responsible for the measurements. The scanning was conducted using a SisuROCK Gen2 core imaging system by Specim (Spectral Imaging Ltd., Oulu, Finland) that had three cameras: <sup>1)</sup> an RGB camera, <sup>2)</sup> a FENIX hyperspectral camera and <sup>3)</sup> and OWL camera. These cameras span a wavelength range from the visible (400–700 nm) to the near-infrared (700–1,300 nm), short-wave infrared (1,300–2,500 nm) and long-wave infrared (7,700–12,300 nm). The main data acquisition parameters are given in Table 4. GTK's personnel organized the logistics and the necessary preparation related to the samples to be examined. All drill cores of the HypeLAP

December 8, 2022

project were scanned in September 2021. The operator handed over the collected data to the project team in November 2021.

Table 4. The data acquisition parameters of the imaging data (TerraCore, 2021).

Camera	Wavelength range	Spectral resolution	Image dimensions	Spectral bands	Pixel size
RGB	not applicable	not applicable	4000 pixels	3	0.15 mm
FENIX	380–970 nm, 970–2,500 nm	3.5 nm (VNIR), 12 nm (SWIR)	384 pixels	174 (VNIR), 274 (SWIR)	1.5 mm
OWL	7,700–12,000 nm	100 nm	384 pixels	96	1.5 mm



Fig. 23. The hyperspectral imaging equipment used in the study (SisuROCK Gen 2, Specim, Oulu, Finland). Photo: J. Rauhala.

December 8, 2022

Thirty thin sections made from offcuts taken from the drill cores were analyzed with a scanning electron microscope (SEM) equipped with an energy dispersive X-ray spectrometer (EDX) and Mineral Liberation Analyzer© software (MLA), which operates the instruments and conducts automated collection and processing of mineral data. In the following we refer to this instrumentation as **SEM-EDX/MLA**. The SEM-EDX/MLA instrument used in this work is a FEI Quanta 600 that contains two EDAX EDX detectors. The MLA analyses are based on automated segmentation of polished sections to separate mineral phases using grey-scale images produced by back scatter electrons (BSE), and collection of EDX data for mineral identifications by comparison to spectral libraries.

There are several MLA operation modes, which allow for quantification of various mineral and particle properties such as size distribution, shape characteristics, liberation, and association. In this work, the XMOD\_STD mode was used, which is similar to point-counting by optical petrographic microscope. XMOD uses the BSE images to discriminate minerals from the background and collects one X-ray spectrum at each counting point from the minerals only. The STD extension enables simultaneous data collection and analysis of the collected X-ray spectrum, so that spectra that do not have match in the spectral library are automatically added to the database for later identification. For the MLA analyses in the HypeLAP project, 123 000 – 202 000 measurement points were collected from each specimen over the entire areas of studied polished thin-sections. The instrument and measurement parameters were as follows: acceleration voltage 25 kV, spot size ~6.5 µm, chamber pressure <math>6 \times 10^{-5}</math> mbar.

The SEM-EDX/MLA analysis of the thin sections was carried out at GTK's Outokumpu office in August 2021 (see Fig. 24). The received data (appendix A and B) were handed over to the project team in September 2021.



Fig. 24. GTK's process mineralogy laboratory has two pieces of SEM MLA equipment at its disposal (Torppa, 2021): FEI Quanta 650 FEG-SEM (on the right) and the FEI Quanta 600 SEM used in this study (on the left). Photo: A. Torppa.

December 8, 2022

In the HypeLAP project, the purpose of the SEM-EDX/MLA analysis was to systematically determine the mineral compositions of all prepared thin sections. The intention was to use the resulting analysis as an aid in the interpretation of the spectral data measured from the drill cores.

Seven of the drill-core offcuts (#33, #35, #41, #44, #46, #47 and #49) from three study areas (Hirvilavanmaa, Ruossekä, Pahtavuoma) were furthermore analyzed to acquire training and validation data for machine learning classification analyses. All seven were analyzed with a micro-XRF instrument and two of them with a SEM-EDX instrument. The latter analysis was conducted using the INCA Feature phase detection software, and we refer to this system as **SEM-EDX/INCA**. Mineral concentrations were analyzed using a Scanning Electron Microscope (SEM), model Hitachi SU3900 equipped by an Oxford Instruments EDX-spectrometer X-Max 20 mm<sup>2</sup> (SDD). The run conditions were: 20 kV acceleration voltages and 1 nA probe current.

INCA Feature phase detection and classification software has been used to characterize the mineralogical composition of the samples. The INCA Feature grid software divides the measured area into fields and from each field (1.25·10<sup>6</sup> μm<sup>2</sup>) 80 points with 112 μm frequency have been analyzed and classified by EDX. The total number of analyzed points per sample were over 50,000. The quality of the data is semiquantitative and the results are normalized to 100%. Identification of mineral phases is based on numerical elemental compositions converted from the EDX spectra that is compared against GTK's internal database. SEM-EDX/INCA analysis was carried out at GTK's Espoo office in June-July 2022.

The third reference dataset, the **micro-XRF** data, were acquired by GTK Espoo staff in June-July 2022. Data were acquired from seven drill core offcut samples.

The results of the micro-XRF analysis were delivered to the project team in July 2022 (Appendix C). The system has an Rh X-ray 30-Watt Rh anode target, two simultaneously operating 30mm<sup>2</sup> XFlash®.

### 6.3 Results

In the implementation phase, it was agreed among the project team that work package 3 would focus on producing new data, and that the data would be interpreted in work package 4. Applicable parts of the data collected in work package 3 were thus interpreted in work package 4 (see chapter 7).

December 8, 2022

## 7 WP4: DATA ANALYSIS

### 7.1 Description

As the project progressed, the project team gained a better understanding of what data would be required in WP4, so that the needs of this work package would be met as well as possible. Therefore, it was decided to expand the data analysis from the original plan as described in section 6.2.6. At the same time, it was agreed that WP3 is dedicated to data collection, and data interpretation is implemented in WP4.

Data analysis was performed for both the hyperspectral imaging and point spectral data. It aimed at modelling both the mineralogy and mineral chemistry of the samples.

### 7.2 Image co-registration

As the training data for machine learning, we used SEM-EDS derived minerals for the SOM based data analysis and micro-XRF derived minerals for supervised machine learning. Since data from multiple measurement devices was integrated, co-registration of data was required to bring all the data into the same coordinate system. Thus, both, the SEM-EDS and micro-XRF data had to be co-registered with the hyperspectral imaging data. Due to the differences in the coverage of and complementary information available for the SEM-EDS and micro-XRF data, we used different techniques to co-register the hyperspectral images with these two sources of training data. Common to both cases is that the low resolution of the HS image allows co-registration only based on the outline of the offcut.

#### 7.2.1 Co-registration of HS images and micro-XRF data

Image-to-image registration tool in ENVI software was used to create a spatial alignment between hyperspectral and mineral class images generated from the micro-XRF derived minerals. The hyperspectral image was used as a base image and micro-XRF was considered as a warp (target) image. A case example is provided below for sample 33. First, the hyperspectral image for sample 33 was clipped from the image containing all existing offcut samples. As the micro-XRF mineral data was available only as an RGB image, the RGB triplets were first transformed into a set of unique conditions, represented as integer values 1...n, to facilitate the creation of regions of interest (ROIs), discussed later. The co-registration process was employed to adjust the micro-XRF image to the closest pixel alignment based on the hyperspectral image and was then resampled to the micro-XRF image's pixel size. The co-registration was conducted by matching 4 tie points at the corner of hyperspectral image with their corresponding location in the micro-XRF image. Finally, warping process was performed using Nearest Neighbor resampling to produce the co-registered micro-XRF image by taking the nearest pixel into account without performing any interpolation. After the co-registration was complete, ROIs were created for each relevant mineral class, later to be used in machine learning classification. Here, relevant mineral classes comprise minerals that have one or several spectral features either in the SWIR or LWIR wavelength region, or both. Hence, the ROIs vary per wavelength region because some minerals that are LWIR-active can be featureless in the SWIR (for instance: quartz), although minerals can be active in both wavelengths (for instance: the carbonate minerals). The samples did not have

December 8, 2022

significant amounts of minerals that are only active in the VNIR (e.g. iron oxides), and hence the said wavelength region was irrelevant in our study.

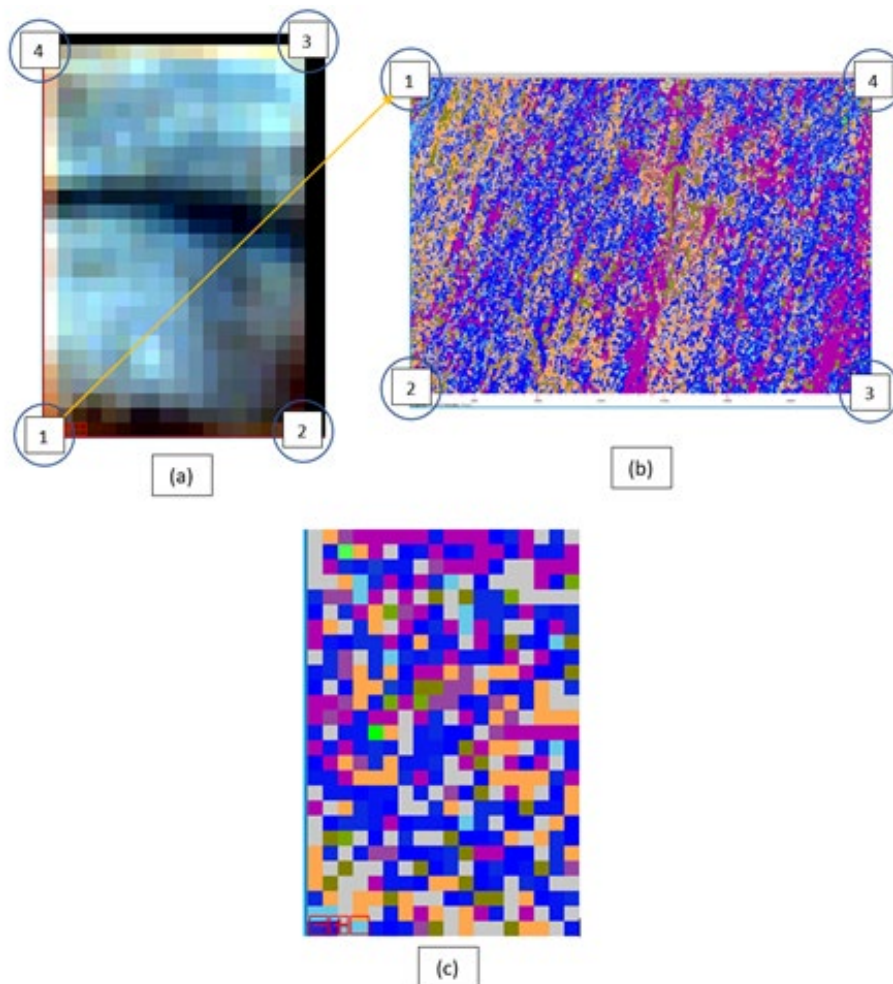


Fig. 25. Example of image-to-image registration for sample 33 by choosing the tie points at the corner of images. (a) is the hyperspectral image, (b) is the corresponding micro-XRF image, and (c) is the co-registered micro-XRF image.

### 7.2.2 Co-registration of HS images and SEM-EDX/INCA data

As neither the SEM-EDX/INCA data nor the RGB image with SEM-EDX/INCA reference points covered the entire offcut area, it was not possible to directly co-register the HS offcut images with SEM-EDX/INCA data using the outline of the offcut. Thus, co-registration was carried out in three stages using a script written in Matlab:

1. The SisuRock RGB image of the offcut was co-registered with the HS image of the offcut based on the outline. All the four corner points were used for co-registration.
2. The offcut RGB image, with SEM-EDX reference points marked, was co-registered with the co-registered SisuRock RGB image based on several identifiable features in the offcut's area.

December 8, 2022

3. Transformation of SEM-EDX/INCA data to HS image coordinate system was done using the reference point coordinates on the registered offcut RGB image (manually pointed on the image), and the reference point coordinates in the SEM-EDX measurement system, provided along with the SEM-EDX/INCA mineral data. As only two reference points were given, only rotation, scaling and shift could be accounted for, and possible mirroring had to be done manually before registration.



Fig. 26. Co-registration workflow of offcut HS images to RGB image with SEM-EDX/INCA reference points.

### 7.3 The mineralogy and mineral chemistry of the Ruosselkä study area

In this section, we are reporting the mineralogy and mineral chemistry of drill core M374106R268 of the Ruosselkä study area, extracted from point and image spectral data. The study area was selected to act as a representative of the full set of results due to its variable mineralogy and mineral chemistry.

#### 7.3.1 Methods

##### *Point spectral data analysis*

The point spectral data collected in work package 3 were used to determine the mineralogical and mineral chemical composition of the drill cores. First, the mineralogy was determined using the TSG™ (“The Spectral Geologist v 8.1.0.5”, CSIRO, Perth, Australia) software, which uses linear spectral unmixing to find the combination of mineral reference spectra that best match an unknown spectrum (Schodlok et al., 2016). The thus obtained mineralogy was visually checked by a geologist and corrections were made where necessary. This work was guided by the MLA results and conducted separately for the VSWIR and LWIR wavelength regions because different minerals are active (have identifiable spectral features) in different wavelength regions.

The mineral chemistry of the drill cores was estimated using a selected set of TSG™ scalars listed in Table 5. These scalars take the band position of a spectral feature from a radius around a centre wavelength, after which a “continuum removal” is conducted to that wavelength range. Continuum removal is done to account for the effects of the grain size variation and the presence of water and minerals that do not have unique spectral features in the wavelength range (Laukamp et al., 2021). Continuum removal is conducted by dividing the reflectance value of each band by the corresponding continuum (Laukamp et al., 2021), i.e. an imaginary line above the spectral feature. The radii and wavelength ranges used by the scalars are listed in Table 5. Scalars

December 8, 2022

which use a three-band polynomial fit around the reflectance minimum were used to reduce potential effects of noise in the spectra. It should be noted that in the LWIR range, absorbance spectra were given as input for the TSG, instead of reflectance spectra. The LWIR range is characterized by strong “peaks”, instead of absorptions that are characteristic of the VSWIR wavelength ranges, and by using the LWIR absorbance spectral data (instead of the reflectance data), the same software logic can be applied to the VSWIR and LWIR wavelength ranges.

TSG scalars target specific minerals groups, also listed in Table 5. For instance, scalar 2200W is used to determine the band position of white micas and other Al-bearing sheet silicates, such as specific clay group minerals. The band position of white micas varies as a function of ionic exchange processes, e.g. the Tschermak substitution or the simple Fe-Mg substitution. This causes changes in the O-H vibrational frequencies of white micas, which can be detected in the SWIR wavelength region (Duke, 1994). Because alteration zones where these changes can be observed are commonly several times the size of the associated ore deposits, their presence and composition can act as exploration vectors, leading to mineralization.

The scalars used in the project were selected based on the known mineralogy of the drill cores, as determined by the MLA results. Moreover, specific scalars were only applied to the drill cores where the target mineral (e.g. white micas) was present in significant quantities. The scalars were only calculated for point spectral measurements where the minerals of interest were present, for instance, the 11300W scalar was applied exclusively to those LWIR data where carbonate minerals were abundantly present.

Table 5. The spectral scalars used to determine the mineral chemical composition of the drill core samples. Scalar descriptions: Laukamp et al. (2021). Gr.=group, PS=point spectral (data), IM=image (data).

Scalar	Spectral feature	Target minerals	Radius (nm)	Start wavelength (nm)	End wavelength (nm)	Drill core identification	PS	IM
2200W	Al-OH	white micas	63	2,120	2,246	M374106R268	X	X
2250W	Al(Fe,Mg)-OH	chlorite gr. (biotite gr.)	25	2,230	2,280	KTÄ_PV-012	X	
						KTÄ_PV-033	X	X
						M273488R335	X	
						M374106R268	X	
9800W	Si(Al,Fe)O <sub>4</sub>	chlorite gr.	200	9,600	10,000	KTÄ_PV-012	X	
						KTÄ_PV-033	X	X
						M273488R335	X	X
11300W	CO <sub>3</sub>	carbonate gr.	450	10,900	11,800	M273488R335	X	X

### Image data analysis

The point spectral results, discussed above, were used to guide the analysis of the imaging spectral data. The mineral chemistry of the hyperspectral image drill core data was calculated following the methodology described in section 7.3.1 (point spectral data analysis). However, due

December 8, 2022

to the lack of off-the-shelf software for conducting such analysis on image data, algorithms were developed by the project team to get the reflectance minima and maxima for the SWIR- and LWIR-data, correspondingly. Furthermore, if point spectral data did not show apparent mineral chemical changes in the chosen wavelengths, no analysis was conducted using the image data. The analyzed spectral features and sites are shown in Table 5. Contrary to the point spectral data analysis, with the image data, only the statistically highest abundances of minerals, indicated by the depths or heights of the spectral features (depending on the wavelength), were considered. This was done to reduce the influence of data points where the chosen minerals are not present, i.e. “false positives”. Unlike with the point spectral data, the project team did not have mineral classification results for entire drill cores at the time of report writing.

### 7.3.2 Results

The mineralogy of the analyzed drill core, extracted from point spectral data, shows abundant white micas throughout the sample set (Fig. 27a). Of the common alteration minerals, there is also some chlorite and epidote, but their distribution is patchy and does not cover the whole drill core (Fig. 27a-b). Therefore, their chemistry was not analyzed in the study area. The Al(Fe,Mg)-OH absorption of chlorite is commonly used for exploration vectoring in hyperspectral studies (see e.g. Neal et al., 2018), the spectral features of the epidote group minerals less commonly so (for an example, see e.g. Roache et al., 2011). Orogenic Au deposits, such as Ruoselkä, are typified by quartz-dominant vein systems with sulphide and carbonate minerals (Groves et al., 1998). Due to the close link between Au and these vein systems, special attention was paid to the presence of quartz and carbonate minerals. In the sample drill core, the carbonate minerals are present only at a few depths. Quartz appears to become more abundant close to the mineralization at 50–70 m depth (Figs. 27b-c), but also occurs in more distal areas. It should be noted that the carbonate minerals are predominantly calcite, based on the VSWIR data and MLA data (for the MLA results, see Appendix A). No effort was made to use the LWIR range to classify different types of carbonate minerals, and hence they are only labeled using their mineral group name (“carbonate minerals”). Example spectra of different minerals in the drill core are shown in Fig. 28.

The white mica chemistry, extracted from point spectral data (Fig. 27d) and image data (Fig. 27e), suggests that white micas may show some chemical variation within the drill core. In the point spectral data, the Al-OH band positions range between 2195 nm and 2209 nm, which is close to the range detected in the image data (2195–2212 nm). In the image data, an apparent outlier at 2184 nm was removed from further analysis. It should be noted that any disagreements between the point spectral and image data must be caused either by differences in instrument properties (e.g. the spectral resolution and sampling), data processing, or both. In image data, a large number of observations are averaged, instead of the point spectral data that are collected every one meter. Also, due to the lack of mineral classification results for the image data, the pixels with white micas were selected based on the depths or heights of the spectral features, wavelength depending, contrary to the point spectral data that were filtered based on the observed mineralogy. Absorption depths and spectral peak heights are related to the abundance of minerals, and only pixels with the statistically highest abundance values were selected for further processing.

December 8, 2022

Any band position shifts, even if detectable in both point spectral and image data (Figs. 27d-e, 29), are slight, as demonstrated by three example spectra in Fig. 29. Therefore, the results need to be validated by electron probe microanalysis (EPMA) to ensure that the observed spectral shifts are truly caused by mineral chemical changes in white micas and not by any other factors. At the time of report writing, no such data were available, and hence the results should be considered tentative until validated.

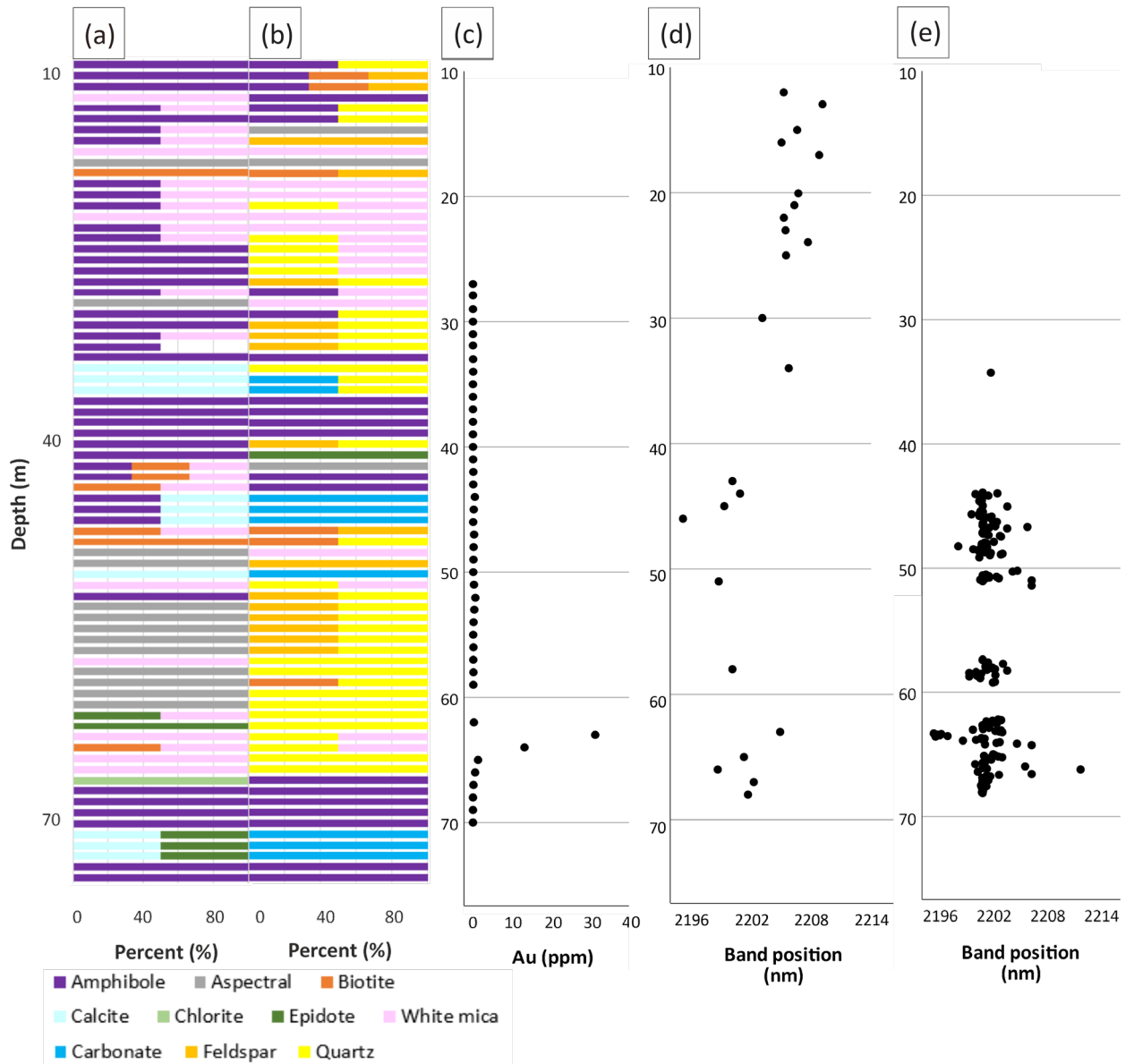


Fig. 27. (a) The mineralogy of drill core M374106R268 from the Ruusselkä study area in the VSWIR wavelength region (point spectral data) and (b) LWIR wavelength region (point spectral data); (c) geochemical assay results of Au; (d) the band positions of the Al-OH absorption of white micas in the SWIR wavelength region (point spectral data) and (e) image data. In the image data, the results are averaged for every 6.5 cm.

December 8, 2022

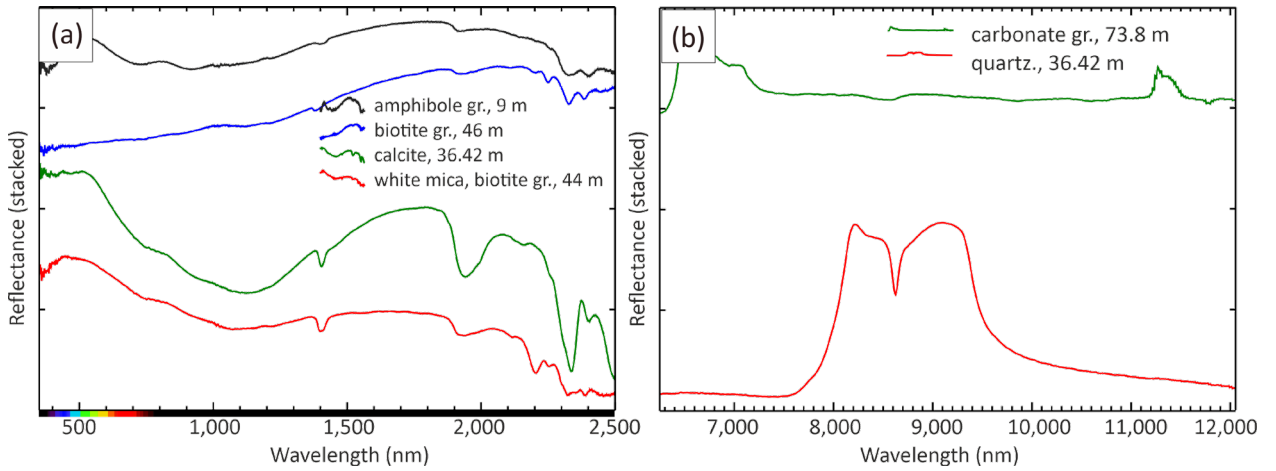


Fig. 28. Example spectra from different depths of drill core M374106R268; (a) spectra obtained in the VSWIR and (b) LWIR. gr.=group. The spectra are offset for clarity.

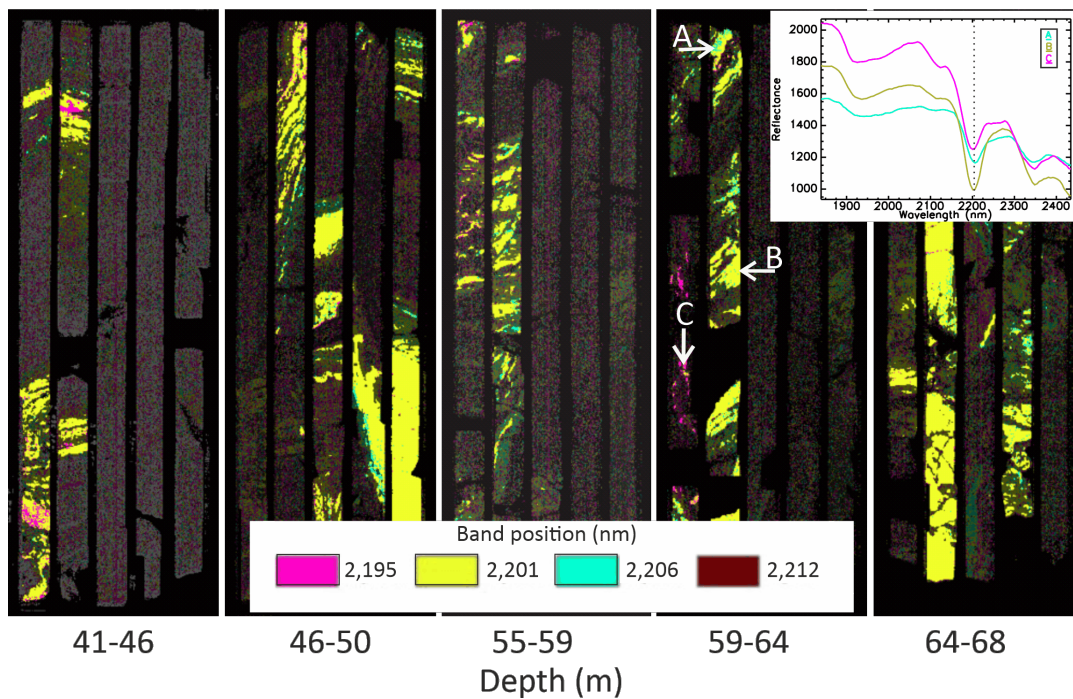


Fig. 29. The Al-OH band positions (2,195–2,212 nm) of white micas of drill trays #7 (41–46 m), #8 (46–50 m), #10 (55–59 m), #11 (59–64 m) and #12 (64–68 m) of drill core M374106R268. Letters A–C point to the locations of the spectra in the subfigure.

December 8, 2022

#### 7.4 Machine learning aided drill-core mineralogy for a test case from Hirvilavanmaa

Machine learning based mineral identification methods using hyperspectral imaging data face challenges caused by ambiguities in the relation of the reflectance to the mineralogy. Because each image pixel usually represents a mixed spectrum of several minerals with varying compositions, the spectra show a continuous range of values, and the data cannot be uniquely divided into mineral classes. In addition, the spectral features of minerals can vary due to variation in their elemental composition (for instance, solid solution series in chlorite group minerals), which makes spectroscopy-based mineral identification more challenging. To investigate the quality and significance of uncertainties caused by these ambiguity issues, we used unsupervised machine learning methods to restructure the hyperspectral imaging data, after which we applied complementary data and expert knowledge to retrieve the mineralogy.

We used self-organizing maps (SOM) and k-means clustering methods to study the structure of the data, to find the number of clusters in the data and evaluate the quality of the clusters. This way it was possible to find out how many different types of spectra there are in the dataset in the first place and how well can the different types of spectra be divided into mineral classes. The actual mineralogy was derived using both expert knowledge and additional training data obtained with SEM-EDX/INCA measurements of drill core offcuts taken from the drill core.

The SOM and k-means computations were carried out on VSWIR data using the GisSOM software (<https://github.com/gtkfi/GisSOM>). As the amount of data in the entire drill core was too large for GisSOM, we concentrated on performing the clustering for one drill core tray at a time. Even this dataset consists of 213 data points with 416 variables. The idea was to retain information from all the spectral channels in relevant wavelength ranges and, thus, no dimension reduction such as PCA or similar was performed. We tested two different approaches for retrieving the mineralogy for the drill core tray. In the first approach, we clustered the drill core tray hyperspectral dataset with SOM and k-means methods and let an expert interpret the mineralogy represented by each cluster. In the second approach, clustering was performed for the hyperspectral dataset from a drill core offcut, taken from this particular drill core tray, and the clusters were classified using mineralogy derived from the SEM-EDX/INCA measurements. Mineralogy for the drill core tray was obtained by applying the SOM and mineral composition classes of the drill core offcut to the drill core tray dataset. Before data analysis, preprocessing was carried out to include only relevant parts of the image and the spectrum, and to make all the spectra comparable.

December 8, 2022

### 7.4.1 Data preprocessing

#### *Removal of the drill core tray*

First, the pixels of the wooden core tray were removed. This is a simple procedure in the VSWIR wavelength range as, in the visual wavelengths, the wood has a distinct increase in reflectance towards red color (Fig. 30).

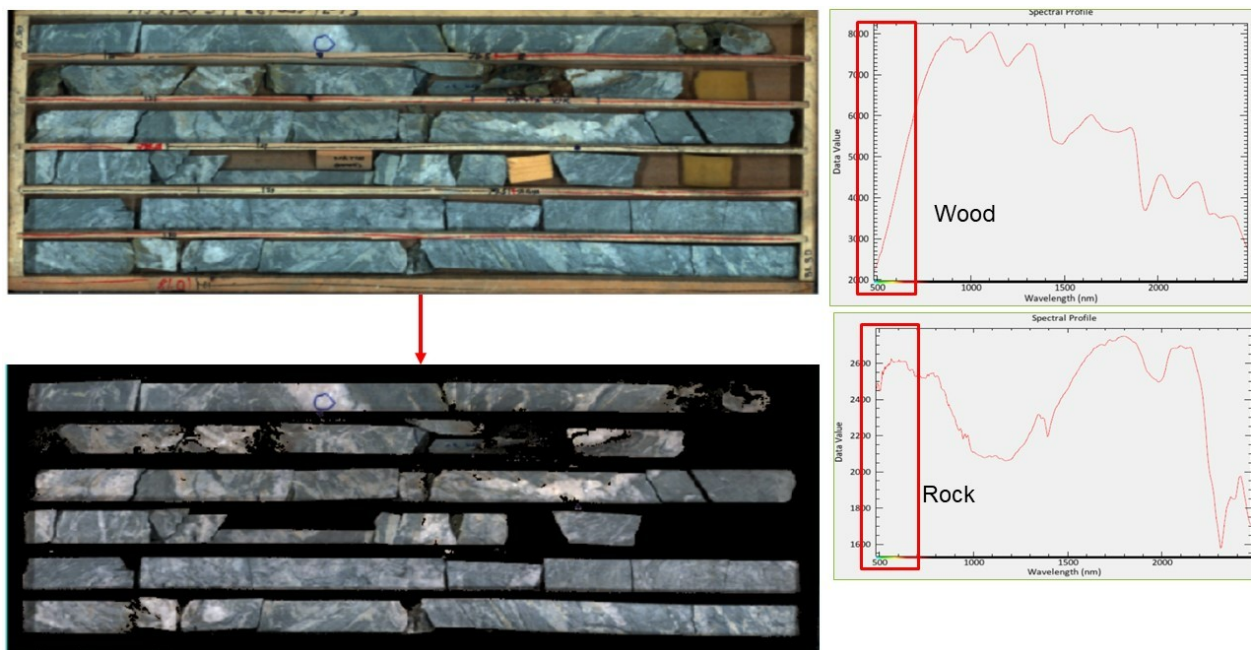


Fig. 30. Spectra: Typical VSWIR spectra of wood and rock in the visual wavelengths. Drill core trays: Top tray is the RGB image showing wooden parts and bottom tray represents the hyperspectral data with wooden parts removed.

#### *Processing the reflectance data*

Second, based on expert knowledge, we selected spectral subsets of the hyperspectral data for the analysis. More specifically, subranges 1300–1500 nm and 2040–2400 nm were selected to take advantage of the spectral features of the minerals of interest in the Hirvilavanmaa study area. Talc, chlorite and carbonate minerals have their spectral features in the chosen wavelength range and thus, using the said wavelength range in data allows their identification. For instance, the carbonate minerals have diagnostic spectral features around 2300–2400 nm, induced by the overtones and combination tones of the internal vibrations of the  $\text{CO}_3$  radical (Hunt and Salisbury, 1971). Also, the sparsely sampled full range [400,2500] nm was used with every twentieth wavelength band included to describe the overall shape of the spectrum. In the third step of preprocessing, continuum removal was performed for each wavelength range separately, and all the preprocessed bands were then combined to one single dataset. An example of the original spectrum and the continuum removed subsets are shown in Fig. 31.

December 8, 2022

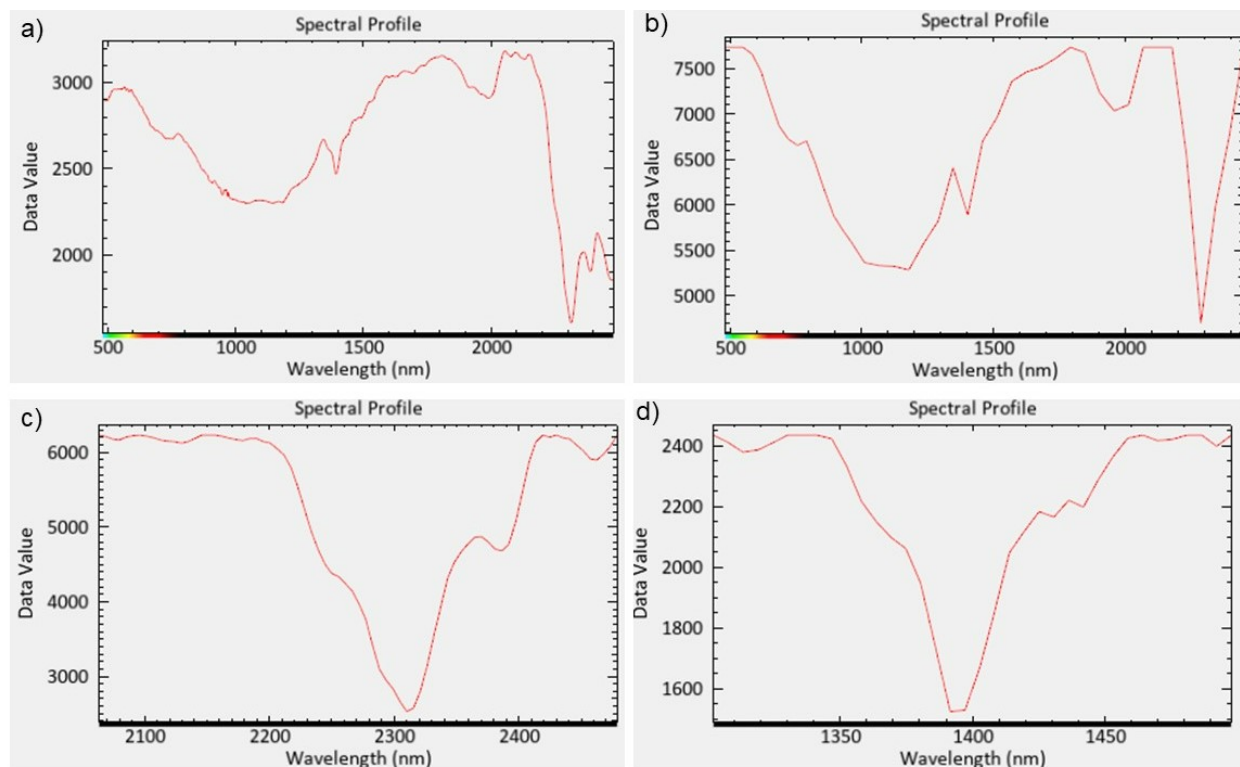


Fig. 31. An example of (a) the original measured VSWIR spectrum with all bands and the continuum removed (b) sparsely sampled spectrum over the entire wavelength range, (c) range [2060,2500] nm and (d) range [1300,1500] nm.

#### 7.4.2 Mineralogy based on expert knowledge

In this hybrid approach we applied machine learning to find the optimal clustering scheme for the dataset and expert knowledge to interpret the mineralogy of the clusters. First, we performed SOM analysis for the drill core data of Hirvilavanmaa tray 10 (Fig. 34). We used the U-matrix to visually inspect the quality of clusters present in the data. U-matrix shows large differences between neighboring node vectors as high values (yellow-red colors), while a neighborhood with similar node vectors is shown as dark blue. If there are dark blue areas, surrounded with yellow or red boundary, this area is a cluster (Fig. 32). If the clusters are not clear, the optimal number of clusters must be determined using some metric, like the Davis-Bouldin index, that measures the intra-cluster spread and inter-cluster differences.

December 8, 2022

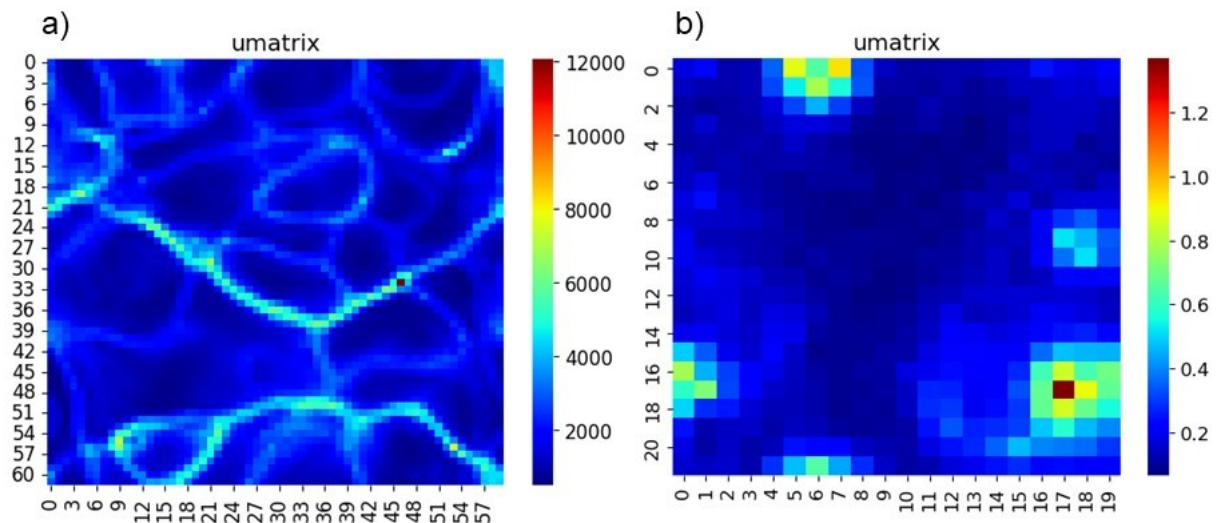


Fig. 32. Examples of a SOM with (a) clear cluster boundaries and (b) no cluster boundaries seen on the U-matrix.

The mineralogy of clusters was determined by expert interpretation using VSWIR spectra of the clusters together with complementary data (Fig. 35). SOM quantization error and deviation of measured spectra from the corresponding k-means clusters (k-means quantization error) was used to qualitatively estimate the goodness of the SOM and the similarity of the spectra within each cluster (Fig. 34d and Fig. 35b). Large quantization error values may refer to bimodal cluster or SOM node structure or a large continuous spread within the cluster or node, while small quantization error indicates small spread within the cluster or SOM node (Fig. 33).

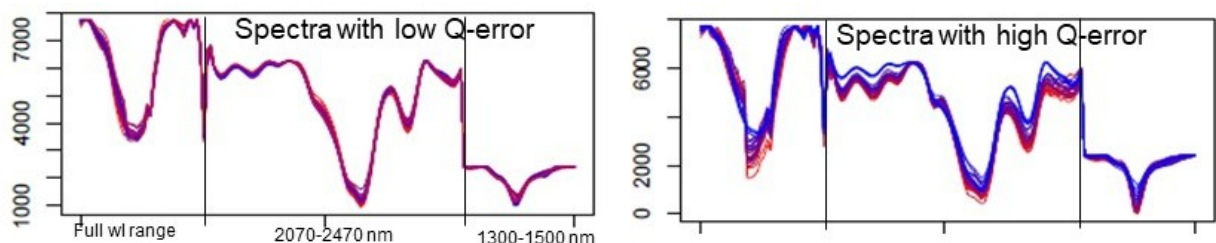


Fig. 33. Examples of spectra in two nodes with low (left) and high (right) quantization error.

### 7.4.3 Mineralogy based on data only

Complementary to the approach utilizing expert knowledge, we also used a purely data driven approach to retrieve the mineralogy of a drill core. However, our intention was not to attempt modeling the complex, at times non-unique relation between the hyperspectral data and mineral composition, but to empirically match clusters with mineralogy obtained from SEM-EDX measurements. The procedure consisted of the following phases:

December 8, 2022

1. Performing SOM analysis to hyperspectral data of a rock chip extracted from a drill core.
2. Co-registering the hyperspectral data with SEM-EDX/INCA measurement data.
3. Classifying the clusters to mineral classes by computing the mineral composition of each cluster from the SEM-EDX/INCA based mineral identifications.
4. Applying the SOM of the drill core offcuts to the actual hyperspectral drill core dataset.
5. Applying the classification scheme of the drill core offcuts to the SOM result of the drill core dataset.

#### 7.4.4 Results

The results from the two different approaches (with and without expert interpretation) yield similar features, but yet cannot be considered as the same result. In the approach taking advantage of expert interpretation, clustering of the drill core tray hyperspectral data yielded nine clusters (using the minimum Davies-Bouldin index) (Fig. 34b and 34c). It can be seen on the U-matrix (Fig. 34a) that there are no clear clusters in the data, which has to be born in mind when interpreting the division of the image into clusters. By comparing the SOM cluster image (Fig. 34b) and the U-matrix, it is obvious that clusters 1, 3 and 5 are quite homogenous (dark blue colors on U-matrix), while clusters 4, 7, 8 are heterogenous, especially cluster 7. Clusters 0, 2 and 6 are somewhat heterogenous. The same phenomenon is observed by comparing the quantization error (Fig. 34d) and clusters (Fig. 34c) on the drill core tray frame: the higher the quantization error, the larger the variation in the corresponding cluster can be expected to be.

December 8, 2022

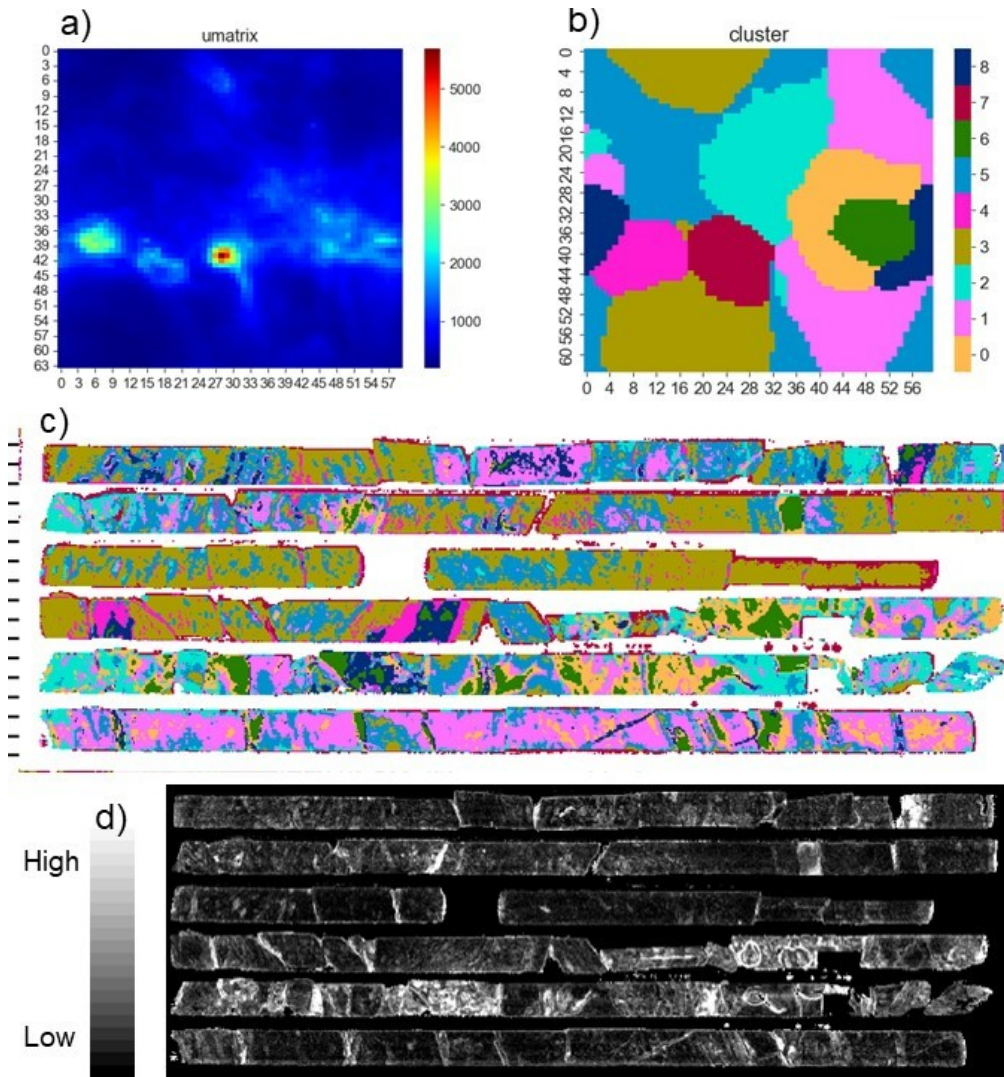


Fig. 34. SOM and k-means clustering result for Hirvilavanmaa tray 10: (a) SOM U-matrix, (b) k-means clusters on SOM, (c) k-means clusters on the drill core tray and (d) SOM quantization error of the measured spectra.

Based on expert interpretation, part of the clusters from the SOM and k-means analysis were combined to one mineral class, finally yielding three mineral composition classes for the drill core tray (Fig. 35). Based on the above consideration of quantization errors and U-matrix structure vs. cluster distribution, clinocllore-talc class is mostly well-clustered, while dolomite-talc and talc classes contain heterogeneity in the hyperspectral data.

December 8, 2022

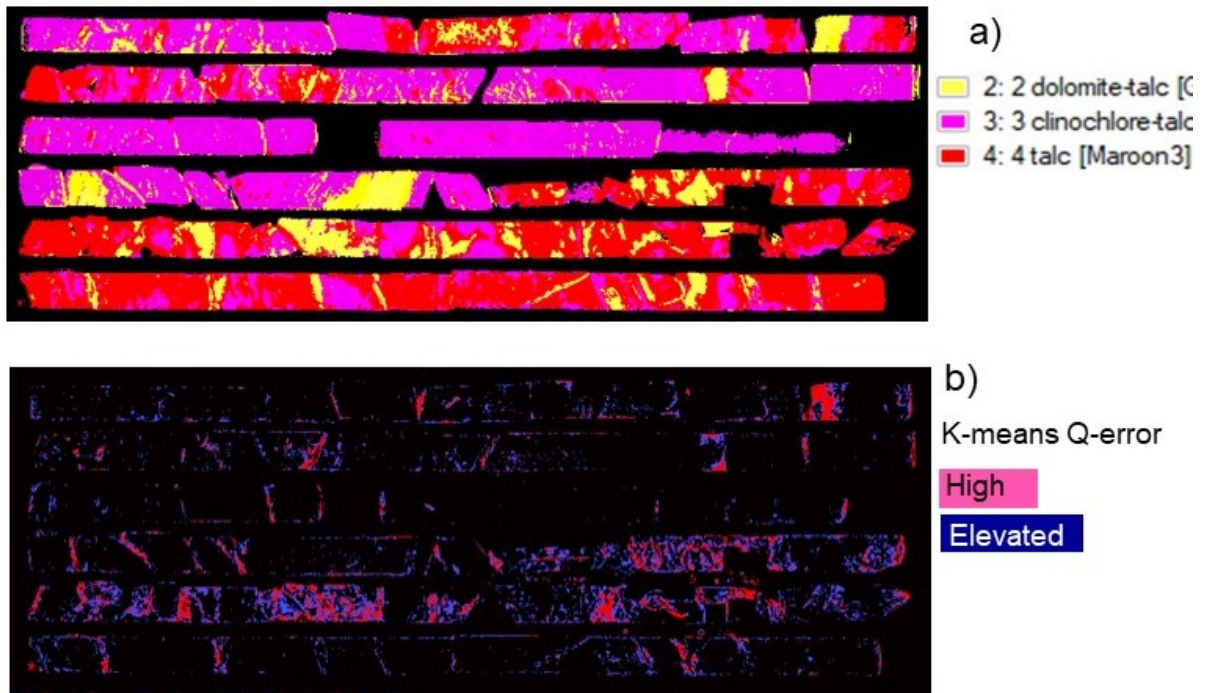


Fig. 35. (a) Mineralogy of the Hirvilavanmaa core tray 10 interpreted by an expert and (b) deviation of measured spectra from the corresponding cluster mean spectra.

In the other approach, that did not allow expert interpretation but solely relied on measurements, the hyperspectral data of a drill core offcut (Fig. 36 a) were analyzed with SOM, yielding in nine clusters (Fig. 36 c). The U-matrix of the offcut SOM (Fig. 36 b) has more clear structure than the SOM from the entire data of the drill core tray. Even though there are clear boundaries, they do not always form closed entities, making unique determination of the number of clusters impossible in this case as well. The Davies-Bouldin index was used to define the optimal number of clusters. In this case clusters 1, 3 and 8 are quite heterogenous, while the rest are more or less homogenous, especially clusters 0, 2, 4 and 5.

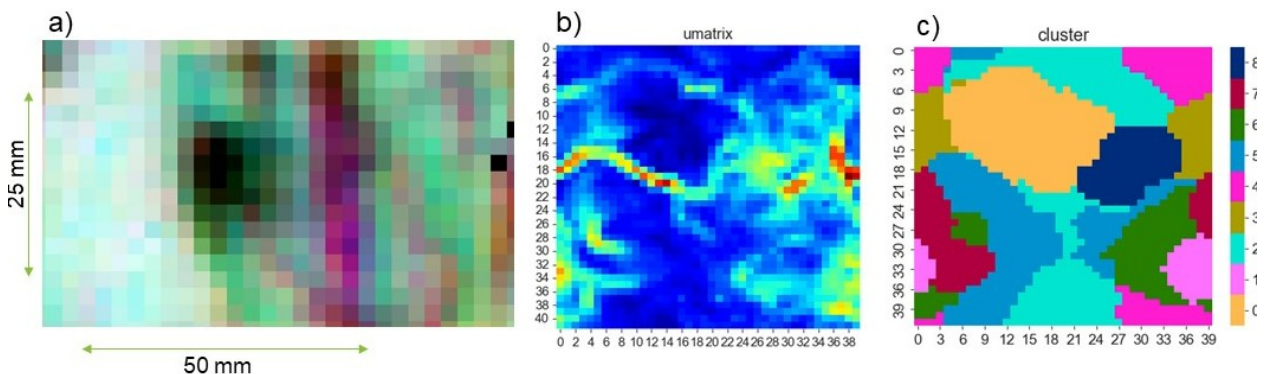


Fig. 36. (a) Drill core offcut hyperspectral image, (b) SOM of the hyperspectral offcut image data and (c) k-means clusters on the SOM of the hyperspectral offcut image data.

December 8, 2022

By matching the SEM-EDX/INCA derived minerals with the clusters obtained for the drill core offcut, the mineral compositions corresponding to each cluster could be defined (Fig. 37). By applying the SOM and the related k-means clustering scheme computed for the offcuts to the hyperspectral data of the entire drill core tray, the mineral classes defined for the offcut could be applied to the drill core tray data (Fig. 38).

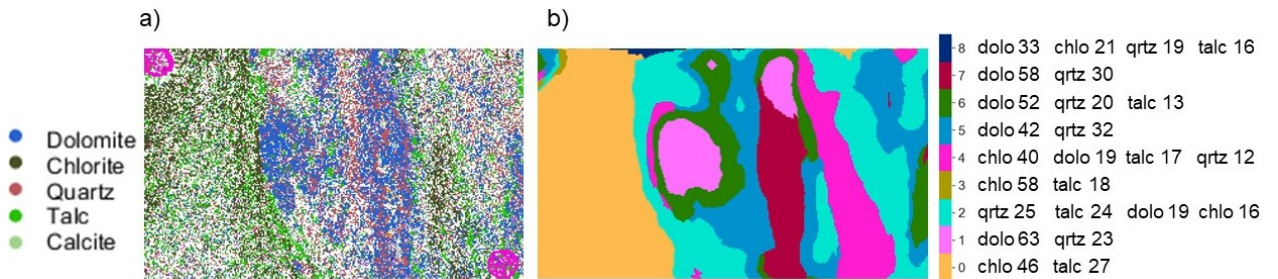


Fig. 37. (a) SEM-EDX/INCA derived minerals on the offcut and (b) SEM-EDX/INCA data based mineral compositions of the offcut clusters.

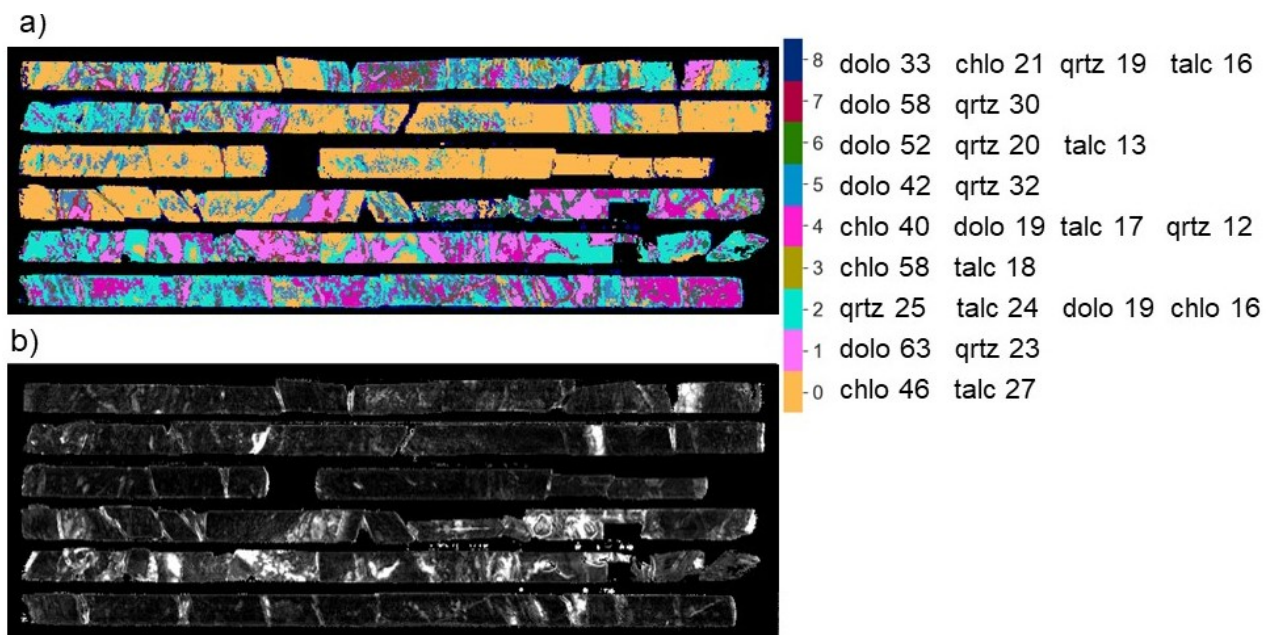


Fig. 38. Mineral compositions of a drill core tray obtained from training SOM and k-means clustering with SEM-EDX/INCA derived minerals.

December 8, 2022

## **8 WP5: PRELIMINARY REVIEW FOR HYPERSPECTRAL IMAGING SERVICE AND CONCEPT BUILDING**

### **8.1 Description**

An interview round was conducted in work package 5 the theme of which was the utilization of the spectral method in mineral exploration. The interviews were conducted with the companies belonging to the project steering group. Interview requests were sent to all seven mineral exploration and mining companies of the steering group. A written summary of the interviews was prepared (see section 8.3).

### **8.2 Implementation**

The project staff prepared a set of questions about the spectral method to be used as a guideline to the interviews. In connection with the interview requests, the companies were asked to think about the interview topics in advance. This was done to ensure the smooth progress of the interviews.

The time allotted for each individual interview was kept to maximum of one hour. Attention was paid to flexibility of the interview times, listening to the companies' wishes.

Four of the seven companies responded affirmatively to the request and participated in the interview. The interviews were conducted as individual interviews with each company separately through the Microsoft Teams platform.

The leader of the work package conducted the interviews in November 2020. A summary of the interviews was jointly prepared by the work package leader and the project manager. The anonymity of the interviewees was taken into consideration in the summary.

The implementation of the work package differed from the project plan only in that the written survey preceding the actual oral interview was omitted. Instead of the survey, the interviews were prepared with a more informal format, as mentioned above, by asking the company representatives to think about the interview topics in advance.

### **8.3 Summary of the interviews**

#### **8.3.1 Background of the companies**

The exploration work carried out by the interviewed companies focused on the most common base metals (Cu, Ni, Zn, As), gold (Au), and platinum group elements (PGE). The companies had operated in Finland for 5–15 years, so they basically know the characteristics of the Finnish bedrock and the conditions for mineral exploration in Finland. They use modern mineral exploration methods on a broad scale, including geological mapping and boulder tracing, till sampling, diamond drilling and geophysical surveys.

December 8, 2022

### 8.3.2 Previous experiences

All the interviewees were previously familiar with the use of spectral technologies. The companies had used the method to examine drill core samples, and some also for examining grab samples. The amount of experience gained varied according to company from early-stage testing to a few years of advanced use. One company had already used the method for several years, establishing it as part of its operations.

The following summarizes the companies' experiences with the spectral method and its suitability for mineral exploration.

Pros:

- produces quantitative data
- allows observations from rock samples that the human eye cannot see
- works well in identifying mineralogical alteration in rocks
- supports drill core logging work by increasing the understanding of the geology of the studied samples

Cons:

- the method is slow: logistics, measurement and interpretation take time
- the interpretation of the data obtained is demanding and often ambiguous
- measuring and scanning devices are expensive

The interviewees believed the relatively limited use of the spectral method in mineral exploration was partly due to ignorance, and that knowledge of the method was not yet part of the geologist's basic skills. Furthermore, spectral research is not considered a straightforward method, but benefiting from it is thought to require extensive processing and interpretation of the data. In addition, the interpretation of the data is often still seen as ambiguous. Some of the interviewees felt more development work was needed for the application of the method, e.g. from the perspective of the required use of time to better highlight the benefits it offered. According to the interviewees, several other alternatives and less laborious analysis methods are available.

### 8.3.3 Suitability for the Finnish bedrock

The spectral method is considered suitable for studying the rocks common in Finland. Some interviewees had experienced that minerals especially in dark-colored rocks could be distinguished better with spectroscopy than visually. Some had opposite experiences, stating that the method had worked well especially with light-colored rocks, but there had been challenges with dark-colored rocks. The companies especially needed to identify alteration minerals and pyrites related to mineralization in their studies.

December 8, 2022

### 8.3.4 Measuring equipment

The interviewed companies did not use their own spectral measurement equipment. In practice, they purchased the necessary measurements, and often their interpretation, from private service providers. Only one company had tried a portable measuring device. However, all the interviewed companies were interested in portable measuring devices. This is also evident from the fact that the companies declared they would be willing to test such devices if they had the opportunity to do so.

### 8.3.5 Usability and quality of data

When evaluating the ease of use of spectral data, it became apparent that the content of the answers depended on the person's duties in the mineral exploration team. Those working in positions focusing on data management felt that integrating data with the company's other datasets was difficult and there were significant challenges in it. Those whose work on geological interpretation and ore models found the data easier to use. Data storage and ensuring long-term availability also prompted discussion among the interviewees.

Spectral data acquired as an outsourced service is considered challenging if it is received from service providers either in report form or should be browsed using a separate online application. In that case, the data cannot be integrated into the companies' own systems but remain detached, making it difficult to use them and obtain the benefits available. In cases where the companies themselves had interpreted spectral data; they sometimes perceived the identification of minerals as difficult due to overlapping data. The companies were generally satisfied with the quality of the data, though the interviewees' answers suggested they had still been unable to utilize all the potential offered by spectral measurements.

### 8.3.6 Companies' own plans

The companies strived to promote the use of the spectral method in their operations by testing portable devices in a grab sample study. In addition, the goal of speeding up spectral measurement workflows was mentioned. Several companies wanted to supplement the data collected from the drill core samples they had examined with data measured using spectral technology. One of the companies was involved in Aalto University's LASO-LIBS development project, which partially dealt with the same topic as the HypeLAP project.

### 8.3.7 Hopes concerning the general development direction

In general, the interviewees saw much potential in the spectral method for mineral exploration. They expected that its use would expand and become commonplace as new publications appeared on the topic. For example, they hoped that a collaborative project between GTK and a private entity with sufficiently large resources would be implemented, the results of which would be public and available to everyone.

Mineral exploration companies traditionally want to focus on target-specific data. According to the companies, GTK could help them create a broader geological picture, e.g. by providing spectrally measured data from the National Drill Core Archive it manages. According to the interviewees, sufficiently representative data series produced from the National Drill Core

December 8, 2022

Archives were particularly suitable for studying regional alteration zones. Some of the companies were very interested in hearing when the systematic digitization of the Loppi archive using the method of continuous hyperspectral imaging began.

In addition, it is noteworthy that in one of the interviews, the possibility of applying the spectral method not only in mineral exploration but also in mines was raised. One of the topics contemplated in the interviews was how concentration processes could be enhanced with the spectral-assisted identification of gangues.

### 8.3.8 Conclusions

An interview round was conducted in work package 5 with the mineral exploration and mining companies belonging to the project steering group, the theme of which was the utilization of the spectral method in mineral exploration. During the interviews, it became apparent that some of the companies were interested in hearing when the systematic digitization of the National Drill Core Archive managed by GTK, i.e. the Loppi archive, using the continuous hyperspectral imaging method would begin.

The companies were interested in the drill cores which geographical location matched the companies' ongoing or future mineral exploration projects. If new research material capable of promoting targeted mineral exploration could be produced from the archived drill cores, it would undoubtedly prompt interest in the companies. The historical drill cores of interest to the companies would thus gain added value through the data generated with hyperspectral imaging.

The minimum benefit that could be obtained from the new data would then be achieved by selling spectral data, e.g. through GTK's current online store directly in the form in which GTK received it from the hyperspectral imaging service provider. In that case, the companies could buy themselves the right to use the datasets and manage the supplied data files themselves using their own resources.

However, selling the data ordered from a contractor as such is not in the interest of GTK or its customers in terms of the institute's expert role. Instead, if GTK produces added value for the spectral data it owned with new interpretations, this would strengthen its role as an expert organization and introduce a completely new product for customers. In the same context, if it was also provided such a high-quality online service intended for examining spectral data that companies would like to use it to outsource their data storage to GTK, the institute's customer operations would be even more comprehensive.

December 8, 2022

## **9 BENEFITS OF THE SPECTRAL METHOD AFTER THE PROJECT**

### **9.1 Acquisition of new data**

Several drill cores were selected from GTK's sample archives in the 2018 pilot project (Ojala & Vuollo, 2019), in which a contractor conducted hyperspectral scanning measuring a total of 28,000 meters of drill core. Encouraged by the experience gained in 2018, GTK implements a self-financed project between 2021 and 2023. The primary goal is to digitize parts of the extensive National Drill Core Archive based on hyperspectral imaging. Over the years, a significant number of samples drilled from the bedrock have been stored in this archive, which is located in Loppi. The hyperspectral imaging campaign focuses on selected drill core samples which represent sites from different parts of Finland that are important in terms of bedrock and ore geology.

The measurement project started in 2021 and continued in 2022. In 2021, a total length of 44,000 meters of drill core was scanned (Terracore, 2021). In 2022, the scanning total was 44,500 meters of drill core (P. Lintinen, personal communication, November 2022). The measurements were carried out by a contractor specializing in hyperspectral imaging. The scanning campaign will be continued with new sample material selected from the Loppi archive in 2023.

### **9.2 Data processing and interpretation**

The processing and interpretation requirements of the raw hyperspectral data must be carefully evaluated at GTK before a decision can be made on the course of action to be followed. However, it is certain that GTK is accumulating a considerable reserve of the raw data generated through scans in the next few years. Considering their massive data content, the raw data must be processed with efficient processing and pre-interpretation methods before usable information begins to emerge.

### **9.3 Data distribution solution**

#### **9.3.1 Operating principle**

GTK's hyperspectral data can be distributed using two principles. It could be done as an online service maintained by GTK, which would act as a directory for the acquired hyperspectral data. These datasets would only be listed in the service. The data would be stored on GTK's internal file servers. The data files would be delivered to customers by mail, copied to external storage media or distributed manually through a reliable cloud service.

Alternatively, the data could be distributed through an online service maintained by GTK which would have both a hyperspectral data directory and the possibility to view the content of the data. In other words, the content would be viewable either in the distribution service itself, or on a separate online platform rented from a partner (e.g. IntelliCore Viewer) and linked to GTK's data directory. In both cases, customers could view the data as images, and see data interpretation directly online (see section 9.3.2). Thus, customers would not necessarily have to order original data files for themselves.

December 8, 2022

It is recommended that the adopted distribution solution should follow the principle of the prototype created in the HypeLAP project, i.e. the online service would not be a file download environment that focused solely on data distribution. Instead, the concept would be that customers could view the data library offered by the service. They could thus use themes of interest directly in the service (virtual research platform). In addition, customers would not need to install or download anything on their own computers. Such an online service would be a research tool for the companies and a viable option to outsource part of their data management.

### 9.3.2 Derived interpretations

It is a good idea to include the interpretation of the raw spectral data obtained in hyperspectral scans in possible follow-up developments. When high-quality interpretations from the raw data is produced, the drill core data offered through the online service can be expanded with data analyses.

However, it is also important that the end user have access to the spectral data on which the mineral interpretation is based. When these datasets have been provided for each drill core, each user can search for new meanings and signals in the data without someone else having previously locked down the interpretation.

### 9.3.3 Service level

From a technical perspective, it would be desirable to make the datasets easily available, without any user-limiting causes or dependencies. When companies or organizations do not have to acquire or install any extra software to view the data content, the attractiveness of the online service for customers would undoubtedly increase. In addition to data coverage, the main needs from the customer's perspective are the usability and visual clarity of the content, as well as the operational reliability of the entire service.

### 9.3.4 Conclusions

The decision of GTK creating a new IntelliCore Viewer type online service must be carefully considered because of the amount of work involved. A less laborious solution for GTK would be to create just a portal (data directory) and request offers from private service providers to a system where all the provided services relate to this portal. The portal directory would thus form a link to the services and interpretations offered by contractors but derived from the spectral data owned by GTK.

GTK's own information systems or data archives should not be tied too strongly to the services of data interpretation suppliers. Instead integration should be based as largely as possible on linking web platforms. If necessary, this will guarantee a technically easy way for GTK to disconnect from the external platforms if one wishes to abandon them later or replace them with another system.

December 8, 2022

#### 9.4 Development of service related to measurements

In the project plan, one goal was to outline a service related to hyperspectral imaging that would serve as a starting point for productization and could eventually lead to the launch of economically profitable activities in the mineral exploration sector. One option for such a service could be to form a coalition between different organizations at GTK's initiative, where the benefit would come to the participating partners through joint procurement.

In practice, the hyperspectral scanning of drill cores requires expensive high-tech equipment and experienced operators. Due to the need for expertise and valuable equipment, investing their own scanning capability is not necessarily justified in mineral exploration and mining companies. Instead, it makes more sense to acquire the scanning work as an outsourced service.

GTK manages a large National Drill Core Archive, in which sample sets obtained through mineral exploration, mining and rock engineering have been recorded over decades. GTK has launched a three-year project in which a tendered contractor is doing hyperspectral imaging of selected sections of this drill core archive (see section 9.1).

If the digitization of the drill cores were implemented as an even longer-term program such that a contractor would scan a set number of drill cores from GTK's archive each year, the companies in the above-mentioned coalition could also take this into account in their own operations over a longer period. This means the hyperspectral scanning programs included in each company's mineral exploration projects which could be combined with GTK's measurement campaigns.

In addition to the collaborative offer process, benefits could be derived from sharing the costs of mobilizing the measuring equipment and its operators, as well as the rental costs involved in necessary premises. Due to their larger size, joint requests for offers made in the name of several organizations would also be more attractive to scanning contractors, who could then be more willing to make better offers to customers.

When performing the scans, sufficient facilities are required for the temporary storage and the sample preparation, as well as for the actual measurements. In addition, logistical expertise and transportation, and an auxiliary workforce would be needed to organize and prepare core samples. All this could be offered to partner companies, thus supplementing the outlined service, from GTK's facilities, personnel and vehicle fleet.

A coalition between different organizations would bring financial benefits to the participating companies through the centralized procurement. It would also create a good foundation for developing economically profitable activities through networking, possible partnerships and specified customer needs following the co-operation.

December 8, 2022

## 10 PUBLICATION OF RESULTS

This public final report about the project has been prepared for GTK's Open File Work Report series. Key results will be presented at the final seminar of the project in December 2022.

The project results were presented at two conferences in September 2022: Earth Resources and Environmental Remote Sensing/GIS Applications XIII (Berlin, Germany, presented by Kati Laakso) and 21st Annual Conference of the International Association for Mathematical Geosciences (Nancy, France, presented by Johanna Torppa). Abstract publications have been prepared for the conferences (Laakso et al., 2022; Torppa et al., 2022).

The project's final report and other key material produced in the project can be downloaded from the project website at <http://projects.gtk.fi/hypelap/>

In addition, there are plans to publish one peer-reviewed publication of the results.

Part of the datasets acquired in the HypeLAP project will be further used for research purposes in one Master's Thesis that started at Aalto University in fall 2022.

December 8, 2022

## 11 REFERENCES

- Agilent Technologies, 2022. Agilent 4300 Handheld FTIR Spectrometer. Available at: [https://www.agilent.com/cs/library/brochures/5991-4067EN\\_LR.pdf](https://www.agilent.com/cs/library/brochures/5991-4067EN_LR.pdf)
- Bedrock of Finland – DigiKP. Digital Map Database [Electronic resource]. Geological Survey of Finland [referred 22.3.2022].
- Bergman, S. & Weihed, P. 2020. Archean (>2.6 Ga) and Paleoproterozoic (2.5–1.8 Ga), pre- and syn-orogenic magmatism, sedimentation and mineralization in the Norrbotten and Överkalix lithotectonic units, Svecokarelian orogen. In: Stephens, M. B. & Bergman Weihed, J. (eds) 2020. Sweden: Lithotectonic Framework, Tectonic Evolution and Mineral Resources. Geological Society, London, Memoirs 50, 27–81. Available at: <http://dx.doi.org/10.1144/M50-2016-29>
- Duke, E.F. 1994. Near infrared spectra of muscovite, Tschermak substitution, and metamorphic reaction progress: Implications for remote sensing. *Geology* 22, 621–624.
- Eilu, P. 1987. Muuttumisilmiöiden keskinäistä vertailua. In: H. Papunen (ed.) Lapin vulkaniittien tutkimusprojekti. Loppuraportti. Department of Geology, University of Turku Report. 165–170. (in Finnish). Available at: [http://tupa.gtk.fi/raportti/arkisto/71\\_2014.pdf](http://tupa.gtk.fi/raportti/arkisto/71_2014.pdf)
- Gibson, H., Allen, R., Riverin, G. & Lane, T. 2007. The VMS model: advances and application to exploration targeting. In: Mikereit, B. (ed.) Proceedings of exploration 07, fifth decennial international conference on mineral exploration, 713–730.
- Goldfarb, R.J., Groves, D.I. & Gardoll, S. 2001. Orogenic gold and geologic time: a global synthesis. *Ore Geology Reviews* 18, 1–75. Available at: [https://doi.org/10.1016/S0169-1368\(01\)00016-6](https://doi.org/10.1016/S0169-1368(01)00016-6)
- Groves, D.I., Goldfarb, R.J., Gebre-Mariam, M., Hagemann, S.G. & Robert, F. 1998. Orogenic gold deposits: A proposed classification in the context of their crustal distribution and relationship to other gold deposit types. *Ore Geology Reviews* 13, 7–27.
- Hanski, E. 1987. Differentioituneet albiittidiabaasit - gabrowehrliittiassoiaatio. Summary: Differentiated albite diabases - gabbro wehrlite association. In: Aro, K. & Laitakari, I. (Eds.) Suomen diabaasit ja muut mafiset juonikivilajit. Geological Survey of Finland, Report of Investigation 76, 35–44.
- Hanski, E. & Huhma, H. 2005. Central Lapland greenstone belt. In: Lehtinen, M., Nurmi, P.A. & Rämö, O.T. (eds) Precambrian Geology of Finland. Key to the Evolution of the Fennoscandian Shield. Elsevier Science B.V., Amsterdam, 139–193.
- Hanski, E., Huhma, H. & Vuollo, J. 2010. SIMS zircon ages and Nd isotope systematics of the 2.2 Ga mafic intrusions in northern and eastern Finland. *Bulletin of the Geological Society of Finland* 82, 31–62. Available at: <http://dx.doi.org/10.17741/bgfsf/82.1.002>

December 8, 2022

Huhma, H., Hanski, E., Kontinen, A., Vuollo, J., Mänttari, I. & Lahaye, Y. 2018. Sm-Nd and U-Pb isotope geochemistry of the Palaeoproterozoic mafic magmatism in eastern and northern Finland. Geological Survey of Finland, Bulletin 405, 150 p. Available at: [https://tupa.gtk.fi/julkaisu/bulletin/bt\\_405.pdf](https://tupa.gtk.fi/julkaisu/bulletin/bt_405.pdf)

Hulkki, H. & Keinänen, V. 2007. The Alteration and Fluid Inclusion Characteristics of the Hirvilavanmaa Gold Deposit, Central Lapland Greenstone Belt, Finland. In: Ojala, V.J. (ed.) Gold in the Central Lapland Greenstone Belt. Geological Survey of Finland, Special Paper 44, 137–153, 10 figures and 2 tables. Available at: [https://tupa.gtk.fi/julkaisu/specialpaper/sp\\_044\\_pages\\_137\\_153.pdf](https://tupa.gtk.fi/julkaisu/specialpaper/sp_044_pages_137_153.pdf)

Hunt, G.R. & Salisbury, J.W. 1971. Visible and near-infrared spectra of minerals and rocks: II. carbonates. *Modern Geology* 2, 23–30.

Hölttä, P. & Heilimo, E. 2017. Metamorphic map of Finland. In: Nironen, M. (ed.) Bedrock of Finland at the scale 1:1 000 000 – Major stratigraphic units. Metamorphism and tectonic evolution. Geological Survey of Finland, Special Paper 60, 77–128. Available at: [http://tupa.gtk.fi/julkaisu/specialpaper/sp\\_060.pdf](http://tupa.gtk.fi/julkaisu/specialpaper/sp_060.pdf)

Inkinen, O. 1979. Copper, zinc, and uranium occurrences at Pahtavuoma in the Kittilä greenstone complex, northern Finland. *Economic Geology* 74 (5), 1153–1165. Available at: <http://dx.doi.org/10.2113/gsecongeo.74.5.1153>

Keinänen, V., Pulkkinen, E., Ojala, V.J., Salmirinne, H., Chernet, T., Räsänen, J., Turunen, P. & Sarapää, O. 2007. Report on the Sakiatieva gold prospect: claims Ruoselkä 8 (Mine Reg. No 7300/1) and Sakiatieva (Mine Reg. No 7392/1), Sodankylä, Finland. Geological Survey of Finland, archive report M06/3741/2007/10/60. 47 p. Available at: [https://tupa.gtk.fi/raportti/valtaus/m06\\_3741\\_2007\\_10\\_60.pdf](https://tupa.gtk.fi/raportti/valtaus/m06_3741_2007_10_60.pdf)

Korkalo, T. 2006. Gold and copper deposits in Central Lapland, northern Finland, with special reference to their exploration and exploitation. *Acta Univ. Oulensis, A Scientiae Rerum Naturalium* 461. 122 p. Available at: <http://jultika.oulu.fi/files/isbn951428108X.pdf>

Köykkä, J., Lahtinen, R. & Huhma, H. 2019. Provenance evolution of the Paleoproterozoic metasedimentary cover sequences in northern Fennoscandia: Age distribution, geochemistry, and zircon morphology. *Precambrian Research* 331, 105364. Available at: <https://doi.org/10.1016/j.precamres.2019.105364>

Köykkä, J. & Luukas, J. 2021. Keski-Lapin litostratigrafia ja paleoproterotsooisen Sodankylän ryhmän kivilajiyksiköiden määrittely. Summary: Lithostratigraphy of the Central Lapland area and definition of the Paleoproterozoic Sodankylä group rock units. Geological Survey of Finland, Open File Research Report 13/2021, 63 p. (In Finnish, with an English abstract). Available at: [https://tupa.gtk.fi/raportti/arkisto/13\\_2021.pdf](https://tupa.gtk.fi/raportti/arkisto/13_2021.pdf)

December 8, 2022

Köykkä, J., Lahtinen, R. & Manninen, T. 2022. Tectonic evolution, volcanic features and geochemistry of the Paleoproterozoic Salla belt, northern Fennoscandia: From 2.52 to 2.40 Ga LIP stages to ca. 1.92–1.90 Ga collision. *Precambrian Research* 371, 106597. Available at: <https://doi.org/10.1016/j.precamres.2022.106597>

Laakso, K., Haavikko, S., Korhonen, M., Köykkä, J., Middleton, M., Nykänen, V., Rauhala, J., Torppa, A., Torppa, J. & Törmänen, T. 2022. Applying self-organizing maps to characterize hyperspectral drill core data from three ore prospects in Northern Finland. *Earth Resources and Environmental Remote Sensing/GIS Applications XIII*. Available at: <https://doi.org/10.1117/12.2635988>

Lahtinen R, Huhma H., Lahaye Y., Jonsson E., Manninen T., Lauri L., Bergman S., Hellström F., Niiranen T. & Nironen M. 2015. New geochronological and Sm-Nd constraints across the Pajala shear zone of northern Fennoscandia: reactivation of a Paleoproterozoic suture. *Precambrian Research* 256, 102–119. Available at: <https://doi.org/10.1016/j.precamres.2014.11.006>

Lahtinen, R., Köykkä, J. & Kurhila, M. submitted. Tectonic evolution of a Paleoproterozoic diffuse cryptic suture zone in northern Fennoscandia and correlation of northern Fennoscandia and southern Greenland. *Journal of Geology*.

Laukamp, C., Rodger, A., LeGras, M., Lampinen, H., Lau, I.C., Pejčić, B., Stromberg, J., Francis, N. & Ramanaidou, E. 2021. Mineral physicochemistry underlying feature-based extraction of mineral abundance and composition from shortwave, mid and thermal infrared reflectance spectra. *Minerals* 11(347). Available at: <https://doi.org/10.3390/min11040347>

Lehtonen, M. I. 1984. Muonion kartta-alueen kallioperä. Summary: Pre-Quaternary rocks of the Muonio map-sheet area. *Geological Map of Finland 1: 100 000, Explanation to the Maps of Pre-Quaternary Rocks, Sheet 2723*. Geological Survey of Finland (In Finnish, with an English abstract and Summary). 71 p. Available at: [http://tupa.gtk.fi/kartta/kallioperakartta100/kps\\_2723.pdf](http://tupa.gtk.fi/kartta/kallioperakartta100/kps_2723.pdf)

Lehtonen, M., Airo, M-L., Eilu, P., Hanski, E., Kortelainen, V., Lanne, E., Manninen, T., Rastas, P., Räsänen, J. & Virransalo, P. 1998. Kittilän vihreäkivalueen geologia. Lapin vulkaniittiprojektin raportti. Summary: The stratigraphy, petrology and geochemistry of the Kittilä greenstone area, northern Finland. A Report of the Lapland Volcanite Project. Geological Survey of Finland. Report of Investigation 140. 144 p. (In Finnish, with an English abstract and Summary). Available at: [https://tupa.gtk.fi/julkaisu/tutkimusraportti/tr\\_140.pdf](https://tupa.gtk.fi/julkaisu/tutkimusraportti/tr_140.pdf)

Luukas, J. & Kohonen, J. 2021. Major thrusts and thrust-bounded geological units in Finland: a tectonostratigraphic approach. In: Kohonen, J., Tarvainen, T. (eds) *Developments in map data management and geological unit nomenclature in Finland* Geological Survey of Finland, Bulletin 412, 81–114. Available at: [https://tupa.gtk.fi/julkaisu/bulletin/bt\\_412.pdf](https://tupa.gtk.fi/julkaisu/bulletin/bt_412.pdf)

Manninen, T. 1991. Sallan alueen vulkaniitit - Volcanic rocks in the Salla area, northeastern Finland. Geological Survey of Finland. Report of Investigation 104. 97 p. (In Finnish, with an English abstract and Summary). Available at: [https://tupa.gtk.fi/julkaisu/tutkimusraportti/tr\\_104.pdf](https://tupa.gtk.fi/julkaisu/tutkimusraportti/tr_104.pdf)

December 8, 2022

Manninen, T. & Huhma, H. 2001. A new U-Pb zircon constraint from the Salla schist belt, northern Finland. In: Vaasjoki, M. (ed.) Radiometric age determinations from Finnish Lapland and their bearing on the timing of Precambrian volcano-sedimentary sequences, Geological Survey of Finland, Special Paper 33, 201–208. Available at: [https://tupa.gtk.fi/julkaisu/specialpaper/sp\\_033\\_pages\\_201\\_208.pdf](https://tupa.gtk.fi/julkaisu/specialpaper/sp_033_pages_201_208.pdf)

Manninen, T., Pihlaja, P. & Huhma, H. 2001. U-Pb geochronology of the Peurasuvanto area, northern Finland. In: Vaasjoki, M. (ed.) Radiometric age determinations from Finnish Lapland and their bearing on the timing of Precambrian volcano-sedimentary sequences. Geological Survey of Finland, Special Paper 33, 189–200. Available at: [https://tupa.gtk.fi/julkaisu/specialpaper/sp\\_033\\_pages\\_189\\_200.pdf](https://tupa.gtk.fi/julkaisu/specialpaper/sp_033_pages_189_200.pdf)

Malvern Panalytical, 2022. ASD TerraSpec Halo Mineral Identifier. Available at: <https://www.malvernpanalytical.com/en/support/product-support/asd-range/terraspec-range/terraspec-halo-mineral-identifier>

Mineral Deposits of Exploration – MDaE. Mineral Deposits of Finland Database [Electronic resource]. Geological Survey of Finland [referred 22.3.2022].

Mutanen, T. 1997. Geology and ore petrology of the Akanvaara and Koitelainen mafic layered intrusions and the Keivitsa-Satovaara layered complex, northern Finland. Geological Survey of Finland, Bulletin 395, 233 p. Available at: [https://tupa.gtk.fi/julkaisu/bulletin/bt\\_395.pdf](https://tupa.gtk.fi/julkaisu/bulletin/bt_395.pdf)

Neal, L.C., Wilkinson, J.J., Mason, P.J. & Chang, Z. 2018. Spectral characteristics of propylitic alteration minerals as a vectoring tool for porphyry copper deposits. Journal of Geochemical Exploration 184, 179–198.

Niiranen, T., Lahti I., Nykänen, V., Karinen, T. 2014. Central Lapland Greenstone Belt 3D modeling project final report. Geological Survey of Finland, Report of Investigation 209, 78 p. Available at: [https://tupa.gtk.fi/julkaisu/tutkimusraportti/tr\\_209.pdf](https://tupa.gtk.fi/julkaisu/tutkimusraportti/tr_209.pdf)

Ojala, J. & Vuollo, J. 2019. Hyperspektriskannauspilotointi 2018. Geologian tutkimuskeskus, Unpublished report. 29 p. (in Finnish).

Olympus, 2022. The Vanta Seies, Handheld X-ray Fluorescence (XRF) Analyzer. Available at: [https://www.olympus-ims.com/en/landing/the-vanta-series/?apd=1&adid=vanta&acid=xrfgle&campaignid=957075597&adgroupid=53098050888&keyword=olympus%20vanta%20xrf&gclid=Cj0KCQiAsdKbBhDHARIsANJ6-jciKOTx-d3OCjprdu6X0IQs4KoGYXe\\_kGnv88XrUZXsiKtky2RjUMAAAlymEALw\\_wcB](https://www.olympus-ims.com/en/landing/the-vanta-series/?apd=1&adid=vanta&acid=xrfgle&campaignid=957075597&adgroupid=53098050888&keyword=olympus%20vanta%20xrf&gclid=Cj0KCQiAsdKbBhDHARIsANJ6-jciKOTx-d3OCjprdu6X0IQs4KoGYXe_kGnv88XrUZXsiKtky2RjUMAAAlymEALw_wcB)

Pulkkinen, E., Hulkki, H., Keinänen, V. & Salmirinne, H. 2007. Kultatutkimukset Sodankylän kunnassa Kirakka-aavalla vuosina 2001–2005. Geological Survey of Finland, archive report M19/3723/2007/10/62. 11 p. (in Finnish, with an English abstract). Available at: [https://tupa.gtk.fi/raportti/arkisto/m19\\_3723\\_2007\\_10\\_62.pdf](https://tupa.gtk.fi/raportti/arkisto/m19_3723_2007_10_62.pdf)

December 8, 2022

Rastas, P., Huhma, H., Hanski, E., Lehtonen, M. I., Härkönen, I., Kortelainen, V., Mänttari, I. & Paakkola, J. 2001. U-Pb isotopic studies on the Kittilä greenstone area, central Lapland, Finland. In: Vaasjoki, M. (ed.) Radiometric age determinations from Finnish Lapland and their bearing on the timing of Precambrian volcano-sedimentary sequences. Geological Survey of Finland. Special Paper 33, 95–141. Available at: [https://tupa.gtk.fi/julkaisu/specialpaper/sp\\_033.pdf](https://tupa.gtk.fi/julkaisu/specialpaper/sp_033.pdf)

Roache, T.J., Walshe, J.L., Huntington, J.F., Quigley, M.A., Yang, K., Bil, B.W., Blake, K.L. & Hyvärinen, T. 2011. Epidote-clinozoisite as a hyperspectral tool in exploration for Archean gold. Australian Journal of Earth Sciences 58, 813–822.

Räsänen, J. 2005. SANI-hankkeessa vuosina 2002–2004 tehdyt geologiset tutkimukset. Geological Survey of Finland, archive report, K21.42/2004/4. 26 p. (In Finnish, with an English abstract). Available at: [https://tupa.gtk.fi/raportti/arkisto/k21\\_42\\_2004\\_4.pdf](https://tupa.gtk.fi/raportti/arkisto/k21_42_2004_4.pdf)

Räsänen, J. & Huhma, H. 2001. U-Pb datings in the Sodankylä schist area, central Finnish Lapland. In: Vaasjoki, M. (Ed.), Radiometric age determinations from Finnish Lapland and their bearing on the timing of Precambrian volcano-sedimentary sequences. Geological Survey of Finland, Special Paper 33, 153–188. Available at: [https://tupa.gtk.fi/julkaisu/specialpaper/sp\\_033.pdf](https://tupa.gtk.fi/julkaisu/specialpaper/sp_033.pdf)

SatisGeo 2022. KT – 6 Kappameter. Available at: <https://satisgeo.com/susceptibility-meters/kt-6-kappameter/>

Schodlok, M.C., Whitbourn, L., Huntington, J., Mason, P., Green, A., Berman, M., Coward, D., Connor, P., Wright, W., Jolivet, M. & Martinez, R. 2016. Hylogger-3, a visible to shortwave and thermal infrared reflectance spectrometer system for drill core logging: functional description. Australian Journal of Earth Sciences 63(8), 929–940.

Shanks, W. & Thurston, R. 2012. Volcanogenic massive sulfide occurrence model: U.S. Geological Survey Scientific Investigations Report 2010–5070–C, 345 p. Available at: <https://doi.org/10.3133/sir20105070C>

Strand, K. & Köykkä, J. 2012. Early Paleoproterozoic rift volcanism in the eastern Fennoscandian Shield related to the breakup of the Kenorland supercontinent. Precambrian Research 214–215, 95–105. Available at: <https://doi.org/10.1016/j.precamres.2012.02.011>

TerraCore, 2021. GTK 2021 Hyperspectral Core Imaging Data Acquisition Report. Summary report for the hyperspectral data acquisition campaign at GTK's Rovaniemi Core Storage. TerraCore. Unpublished report. 12 p.

Torppa, A. 2021. MLA-measurements of HypeLAP Samples. Geological Survey of Finland, Unpublished report. 4 p.

Torppa, J., Haavikko, S., Korhonen, M., Köykkä, J., Laakso, K., Middleton, M., Nykänen, V., Rauhala, J., Torppa, A. & Törmänen, T. 2022. Self-organizing maps in analyzing hyperspectral drill core imaging data (oral presentation, abstract).

December 8, 2022

Tyrväinen A., 1983. Sodankylän ja Sattasen kartta-alueiden kallioperä (in Finnish). Summary: Pre-Quaternary rocks of the Sodankylä and Sattanen map-sheet areas. Suomen geologinen kartta 1:100 000: kallioperäkarttojen selitykset lehdet 3713, 3714. Espoo: Geological Survey of Finland 59. Available at: [https://tupa.gtk.fi/kartta/kallioperakartta100/kps\\_3713\\_3714.pdf](https://tupa.gtk.fi/kartta/kallioperakartta100/kps_3713_3714.pdf)

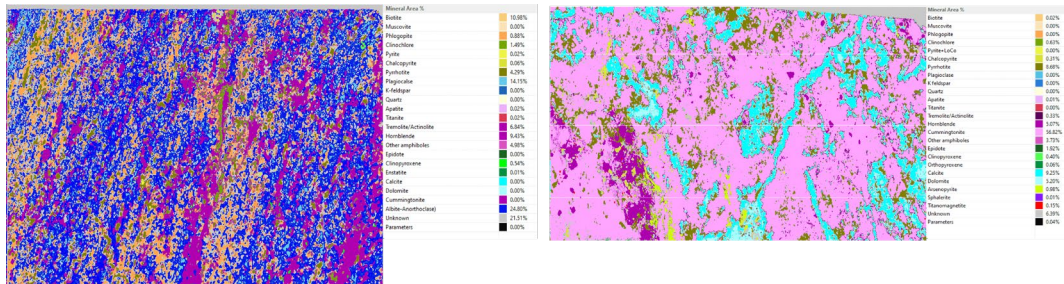
The Mineral Liberation Analysis (MLA) results of the project.

	Kirakka- K1516.11.10-13.18	Kirakka- K1516.25.09-25.96	Kirakka- K1516.27.04-28.03	Kirakka- K1516.31.00-32.00	Kirakka- K1516.33.05-34.02	Kirakka- K1516.40.19-40.25	Kirakka- K1516.49.07-50.03	Kirakka- K1516.68.06-69.04	Ruossela R208.36.00-36.07	Ruossela R208.42.05-43.11	Ruossela R208.45.05-46.05	Ruossela R208.45.05-63.10	Ruossela R208.65.00-66.07	Ruossela R208.71.00-71.08	Hirvilanmaa H155.51.05-52.00	Hirvilanmaa H155.63.00-63.05	Hirvilanmaa H155.63.05-64.00	Hirvilanmaa H155.68.35-68.40	Hirvilanmaa H155.73.05-74.00	Hirvilanmaa H155.86.40-86.45	Pahtavauma Pv-12.104.66-104	Pahtavauma Pv-12.141.11-141	Pahtavauma Pv-12.156.89-156	Pahtavauma Pv-12.169.00-169	Pahtavauma Pv-13.9.08-9.14	Pahtavauma Pv-13.53.53-53.67	Pahtavauma Pv-33.58.09-58.10	Pahtavauma Pv-33.58.09-58.10	Pahtavauma Pv-33.81.95-82.00		
PTS rock name (modified)	Tremolite-biotite rock	Biotite schist	Mica schist	Mica schist, crb- to-plagi vein	Mica schist	Carbonate- amphibole schist	Biotite-chlorite schist	Biotite schist	Amphibolite	Amphibolite	Amphibolite intermediate volcanic or metasediment?	Phyllite	Phyllite/Biotite sericite schist	Phyllite	Mafic volcanic	Talc-chlorite schist	Talc-crb rock, tic chlo-crb rock	Ch-Chlo-talc material	Crb-qz vein	Qz-vein, f.g. crb- plagi vein	Ch-plagi-qz vein	Mafic metavolcanic	Amphibole- carbonate rock	Amphibole overgrowth	Mafic volcanic	Amphibole-talc carbonate rock	Schist or mylonite	Tremolite carbonate rock	Tremolite carbonate rock	Mafic volcanic	
Mineral	23 XMOD - Wt%	28 XMOD - Wt%	25 XMOD - Wt%	26 XMOD - Wt%	27 XMOD - Wt%	28 XMOD - Wt%	29 XMOD - Wt%	30 XMOD - Wt%	31 XMOD - Wt%	32 XMOD - Wt%	33 XMOD - Wt%	34 XMOD - Wt%	35 XMOD - Wt%	36 XMOD - Wt%	37 XMOD - Wt%	38 XMOD - Wt%	39 XMOD - Wt%	40 XMOD - Wt%	41 XMOD - Wt%	42 XMOD - Wt%	43 XMOD - Wt%	44 XMOD - Wt%	45 XMOD - Wt%	46 XMOD - Wt%	47 XMOD - Wt%	48 XMOD - Wt%	49 XMOD - Wt%	50 XMOD - Wt%	51 XMOD - Wt%	52 XMOD - Wt%	
Actinolite-tremolite	29.1	3.6	0.0	0.1	0.0	26.1	0.0	0.0	1.4	5.5	13.5	2.4	0.0	26.9	1.3	0.4	0.8	3.8	1.1	0.3	2.4	0.1	0.9	1.5	0.1	37.8	0.1	0.3	0.3	2.0	
Hornblende	41.1	7.5	0.1	0.6	0.1	5.8	0.1	0.2	50.8	11.4	8.8	1.7	0.4	1.5	0.9	6.9	0.5	0.6	3.2	1.2	0.4	2.6	39.8	46.8	14.0	50.4	2.1	11.1	11.1	51.4	
Cummingtonite	0.1	0.0	0.0	0.0	0.0	4.5	0.0	0.0	2.0	0.0	0.0	0.0	0.0	0.0	0.0	0.6	0.1	1.0	1.4	0.1	0.0	25.2	59.7	3.0	13.9	0.1	0.0	38.3	38.3	0.0	
Almandine	0.0	0.0	0.0	0.1	0.0	0.0	0.0	0.0	0.0	0.0	0.0	0.0	0.0	0.0	0.0	0.0	0.0	0.0	0.0	0.0	0.0	0.0	2.2	0.0	0.0	0.0	1.6	0.0	0.0	0.0	
Albite	4.3	33.5	38.8	33.5	34.5	0.0	5.5	36.8	6.8	0.2	3.5	48.5	2.1	0.6	8.7	23.2	8.2	5.4	1.9	6.8	6.7	17.3	4.5	0.0	1.2	6.6	0.2	1.6	0.1	0.1	14.1
Ilmenite	0.1	0.0	0.0	0.0	0.0	0.0	0.0	0.0	0.2	0.8	0.0	0.0	0.0	0.4	0.0	0.0	0.0	0.1	0.0	0.0	0.1	0.2	0.1	1.0	0.9	0.0	1.2	0.3	0.2	0.2	1.1
Epazite	0.0	0.1	0.2	0.3	0.2	0.2	0.2	0.2	0.6	0.7	0.7	0.2	0.1	0.1	0.1	0.5	0.0	0.1	0.0	0.0	0.0	0.3	0.0	0.2	0.6	0.3	0.3	0.0	0.0	0.0	0.8
Arsenopyrite	0.0	0.0	0.0	0.0	0.0	0.0	0.0	0.0	0.0	0.0	0.0	0.0	0.0	0.0	0.0	0.0	0.0	0.0	0.0	0.0	0.0	0.0	0.0	0.0	0.0	0.0	0.0	0.0	0.1	0.1	0.0
Androsite	0.1	0.2	0.0	0.0	0.0	0.1	0.0	0.3	0.3	0.0	0.0	0.0	0.0	0.1	0.0	0.2	0.0	0.1	0.0	0.1	0.1	1.0	0.2	0.9	0.2	0.2	3.0	3.0	3.0	0.2	
Grossular	0.0	0.1	0.0	0.0	0.0	0.0	0.0	0.0	0.1	0.0	0.1	0.0	0.0	0.0	0.0	0.0	0.0	0.0	0.0	0.0	0.0	0.0	0.0	0.0	0.3	0.5	0.0	0.2	0.0	0.0	0.2
Biotite	20.0	35.2	15.3	24.8	16.0	49.2	16.9	16.4	0.6	5.5	9.2	0.1	0.3	0.0	0.3	4.4	0.0	0.0	0.0	0.0	0.0	0.2	1.2	0.2	11.7	1.9	27.7	0.2	0.2	2.6	
Calcite	0.0	5.9	0.0	1.7	0.0	0.3	0.0	0.1	0.5	0.3	0.0	0.8	0.0	0.3	0.2	2.4	0.0	0.0	4.8	0.0	0.0	0.1	13.5	0.8	13.5	0.8	4.4	32.1	32.1	0.8	
Oxide-ankerite	0.0	0.9	0.0	4.8	0.0	11.8	0.0	0.2	0.3	0.0	0.2	0.0	0.2	0.2	0.2	8.7	0.1	0.7	26.7	5.5	65.5	0.1	2.1	1.8	0.7	1.6	1.7	0.3	0.1	0.6	
Magnetite	0.0	0.0	0.0	0.0	0.0	0.0	0.0	0.0	0.0	0.0	0.0	0.0	0.0	0.0	0.0	1.0	0.0	42.0	10.1	3.0	0.0	0.0	0.0	0.0	0.0	0.0	0.0	0.0	0.0	0.0	
Chalcopyrite	0.0	0.0	0.0	0.0	0.0	0.0	0.0	0.0	0.8	0.1	0.1	0.1	0.1	0.1	0.0	0.0	0.0	0.0	0.0	0.0	0.0	1.1	0.9	0.0	0.0	0.1	0.9	0.0	3.7	3.7	0.0
Chromite	0.0	0.0	0.0	0.0	0.0	0.0	0.0	0.0	0.0	0.0	0.0	0.0	0.0	0.0	0.0	0.5	0.0	0.0	0.0	0.0	0.0	0.0	0.0	0.0	0.0	0.0	0.0	0.0	0.0	0.0	
Clinoclase	0.4	0.0	0.0	0.4	0.0	0.1	0.0	0.5	0.9	2.3	0.0	1.6	0.0	1.7	0.3	50.5	26.3	17.6	2.0	2.1	0.4	0.2	0.0	3.7	0.3	5.8	0.9	0.0	0.0	0.1	
Cordierite	0.0	0.0	0.1	0.1	0.1	0.0	0.1	0.0	0.0	0.0	0.0	0.0	0.1	0.0	0.1	0.0	0.0	0.0	0.0	0.0	0.0	0.0	0.1	0.0	0.0	0.0	0.4	0.0	0.0	0.0	
Dioptase-Hedenbergite	0.0	0.1	0.0	0.0	0.0	0.1	0.0	0.0	0.0	13.2	0.1	0.1	0.0	24.8	0.1	0.0	0.0	0.2	1.2	0.1	0.0	0.2	0.0	0.0	0.1	0.0	0.1	0.4	0.6	0.6	0.0
Epizite	0.0	0.1	0.0	0.0	0.0	0.0	0.0	2.5	0.1	0.0	0.0	0.0	0.0	0.4	0.1	0.0	0.0	0.0	0.0	0.0	0.0	0.0	0.0	0.0	0.0	0.0	0.6	0.6	0.0	0.1	
Goethite	0.8	0.0	0.0	0.0	0.0	0.0	0.0	0.0	0.0	0.0	0.0	0.0	0.0	0.1	0.0	0.0	4.0	0.0	2.5	0.0	0.0	0.0	0.3	0.0	0.0	0.0	0.1	0.1	0.0	0.0	
Ilmenite	0.4	0.3	0.0	0.1	0.1	0.4	0.0	0.0	4.2	0.6	0.0	0.0	0.0	0.0	3.5	0.0	0.0	0.0	0.0	0.0	0.0	3.6	0.2	1.5	3.5	0.7	0.0	0.2	4.0		
K-feldspar	0.0	0.0	0.4	0.0	0.0	0.0	1.7	0.4	0.1	0.6	2.0	0.1	34.8	0.3	5.1	0.1	0.0	0.0	0.0	0.0	0.0	0.0	0.0	0.0	0.0	0.0	0.0	0.0	0.0	0.0	
Muscovite	0.1	0.3	3.8	2.3	2.9	0.0	23.5	3.9	0.4	0.2	3.9	0.2	13.1	0.7	4.6	0.2	0.0	0.0	0.0	0.0	0.0	0.1	0.0	0.0	0.0	0.0	0.1	0.0	0.0	0.1	
Perthandite	0.0	0.0	0.0	0.0	0.0	0.1	0.0	0.0	0.0	0.0	0.0	0.0	0.0	0.0	0.0	0.0	0.0	0.0	0.0	0.0	0.0	0.0	0.1	0.0	0.0	0.0	0.0	0.0	0.0	0.0	
Plagioclase	0.9	0.0	0.9	0.0	0.1	0.0	0.3	0.0	0.0	0.7	0.0	12.9	0.0	4.8	0.0	0.1	0.0	4.0	0.0	0.0	0.0	0.0	0.0	0.0	0.0	0.0	0.0	0.0	0.0	0.0	
Plagioclase	1.8	7.9	19.4	7.6	21.1	0.0	19.6	18.1	26.6	38.9	40.6	2.0	0.9	1.1	25.2	20.3	0.4	0.4	0.3	0.4	3.9	24.6	0.0	22.4	30.6	0.1	10.8	0.2	0.2	20.3	
Pyrite	0.0	0.0	0.0	0.0	0.0	0.0	0.0	0.0	0.0	0.0	0.0	0.0	0.0	2.1	0.0	0.0	0.0	0.0	0.0	0.0	0.0	0.0	0.0	0.0	0.0	0.0	0.0	0.0	0.0	0.0	
Pyrrhotite	1.4	1.0	0.2	1.6	0.1	0.4	0.1	0.9	0.6	11.0	8.0	29.3	7.8	28.7	2.4	0.1	0.0	0.0	0.0	0.0	0.1	0.0	0.1	16.5	0.7	0.4	0.0	4.6	4.7	0.3	
Quartz	0.1	1.1	21.4	14.3	23.7	0.0	39.5	21.3	3.8	0.0	0.6	22.2	42.6	3.2	62.2	0.4	0.0	8.8	15.2	26.6	72.0	4.0	0.6	15.2	11.0	1.4	0.0	39.8	4.0	4.0	
Rutile	0.0	0.0	0.1	0.4	0.0	0.0	0.0	0.1	0.0	0.0	0.0	0.1	0.1	0.0	0.5	0.1	0.1	0.0	0.0	0.0	0.0	0.0	0.0	0.0	0.0	0.0	0.0	0.0	0.0	0.0	
Sphalerite	0.0	0.0	0.0	0.0	0.0	0.0	0.0	0.0	0.0	0.0	0.0	0.0	0.0	0.0	0.0	0.0	0.0	0.0	0.0	0.0	0.0	0.0	0.0	0.0	0.0	0.0	0.0	0.0	0.0	0.0	
Talc	0.0	0.0	0.0	0.0	0.0	0.3	0.0	0.0	0.0	0.0	0.0	0.0	0.0	0.0	24.4	18.8	12.5	1.3	0.9	0.2	0.0	0.0	0.0	0.0	0.0	0.0	0.0	0.0	0.0	0.0	
Titanite	0.0	0.3	0.0	0.1	0.0	0.0	0.0	0.1	6.2	5.0	0.9	0.0	0.6	0.5	0.3	0.0	0.0	0.0	0.0	0.0	0.0	0.0	0.0	0.0	0.0	0.0	0.3	0.0	0.0	0.2	
Unclassified	0.0	0.3	0.2	0.6	0.2	0.3	0.2	0.2	0.1	0.0	0.8	0.7	0.7	0.5	0.5	0.1	0.6	0.4	0.6	0.2	0.2	0.2	0.3	0.3	0.5	0.2	0.7	0.6	0.6	0.1	
Total number of measur	180736	147963	159799	152182	162957	164883	159439	177181	162185	148263	150736	167129	161281	154830	156208	192293	159116	148897	167724	150767	148934	155349	148911	159995	137683	139034	168800	122263	143993	100.0	

The Scanning Electron Microscope (SEM) results of the project.

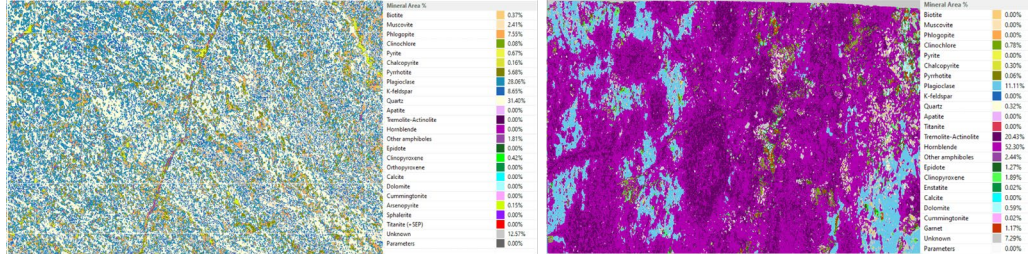
Sample 41			Sample 44		
Class	Features	% total features	Class	Features	total features
Dolomite	12361	29.6	Dolomite	30667	71.4
Chlorite	8626	20.7	Albite	8479	19.7
Quartz	8283	19.9	Quartz	1847	4.3
Talc	6900	16.5	Cu grid	623	1.4
Calcite	1428	3.4	Magnesite	470	1.1
Mg-Hornblende	728	1.7	Mg-Hornblende	382	0.9
Albite	668	1.6	Calcite	146	0.3
Cu grid	504	1.2	Talc	91	0.2
Ankerite	493	1.2	Tremolite	46	0.1
Pyrope	452	1.1	Plagioclase	40	0.1
Goethite	315	0.8	Chlorite	39	0.1
Fe-Hornblende	227	0.5	Apatite	24	0.1
Olivine	215	0.5	Diopside	24	0.1
OPX	142	0.3	Olivine	22	0.1
Fe-ox (magnetite/hematite)	131	0.3	Cl-phase	21	0.0
Tremolite	80	0.2	Pyrite	17	0.0
Diopside	25	0.1	Pyrope	10	0.0
Andradite	23	0.1	Kfsp	10	0.0
Rutile_Ti-Ox	22	0.1	Rutile_Ti-Ox	3	0.0
Magnesite	21	0.1	Fe-Hornblende	3	0.0
Actinolite	16	0.0	Sulphur	2	0.0
Fe-CPX	12	0.0	Mg Fe carb	2	0.0
Chamosite	12	0.0	Fe-ox (magnetite/hema	2	0.0
Ilmenite	8	0.0	OPX	2	0.0
Apatite	4	0.0	Metallic Fe	1	0.0
Metallic Fe	3	0.0	Fe sulphate	1	0.0
Cl-phase	2	0.0	Goethite	1	0.0
Sphene	2	0.0	Pyrrhotite	1	0.0
Fe-Ti ox	1	0.0	Gypsum	1	0.0
Almandine	1	0.0	Almandine	1	0.0
Kfsp	1	0.0	Actinolite	1	0.0
Biotite	1	0.0			
Total	41707	100		42979	100
Class	Features	% total features	Class	Features	% total features
All Features	63596	100	All Features	50660	100
Unclassified	21889	34.4	Unclassified	7681	15.2

The micro-XRF results of the project.



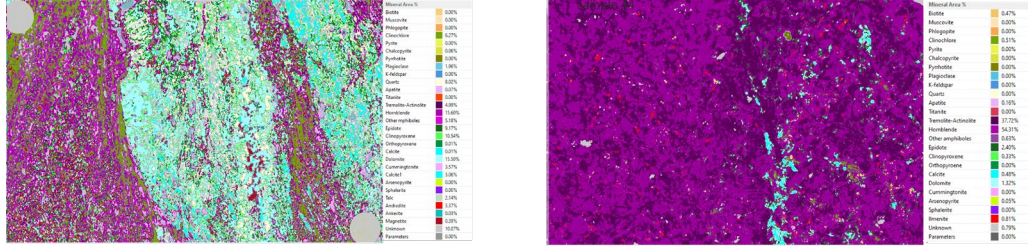
sample 33

sample 46



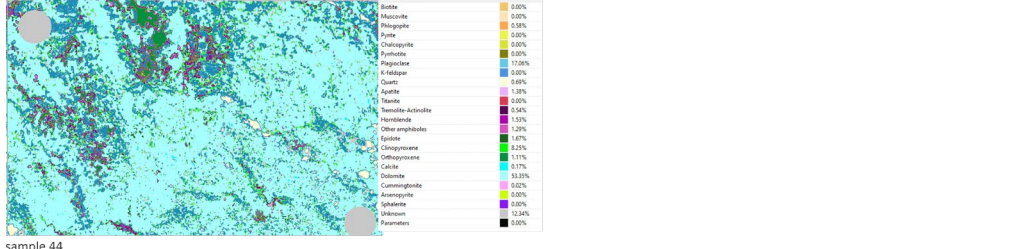
sample 35

sample 47



sample 41

sample 49



sample 44